Title: CMB as a Probe of New Physics: The Story of Cosmic Birefringence

Date: Dec 06, 2012 05:30 PM

URL: http://www.pirsa.org/12120019

Abstract: Cosmological
birefringence is a postulated rotation of the linear polarization of photons
that arises due to a Chern-Simons coupling of a new scalar field to
electromagnetism. In particular, it appears as a generic feature of simple
quintessence models for Dark Energy, and therefore, should it be detected,
could provide insight into the microphysics of cosmic acceleration. Prior work
has sought this rotation, assuming the rotation angle to be uniform across the
sky, by looking for the parity-violating TB and EB correlations in the CMB
temperature/polarization. However, if the scalar field that gives rise to
cosmological birefringence has spatial fluctuations, then the rotation angle
may vary across the sky. In this talk, I will present the results of the first
CMB-based search for direction-dependent cosmological birefringence, using
WMAP-7 data, and report the constraint on the rotation-angle power spectrum for
all multipoles up to the resolution of the instrument. I will discuss the
implications for a specific models for rotation, and show forecasts for Planck
and future experiments. I will then conclude with a brief discussion of other
exotic physical models, such as chiral gravity, and astrophysical scenarios,
such as inhomogeneous reionization, that can be probed using the same analysis.

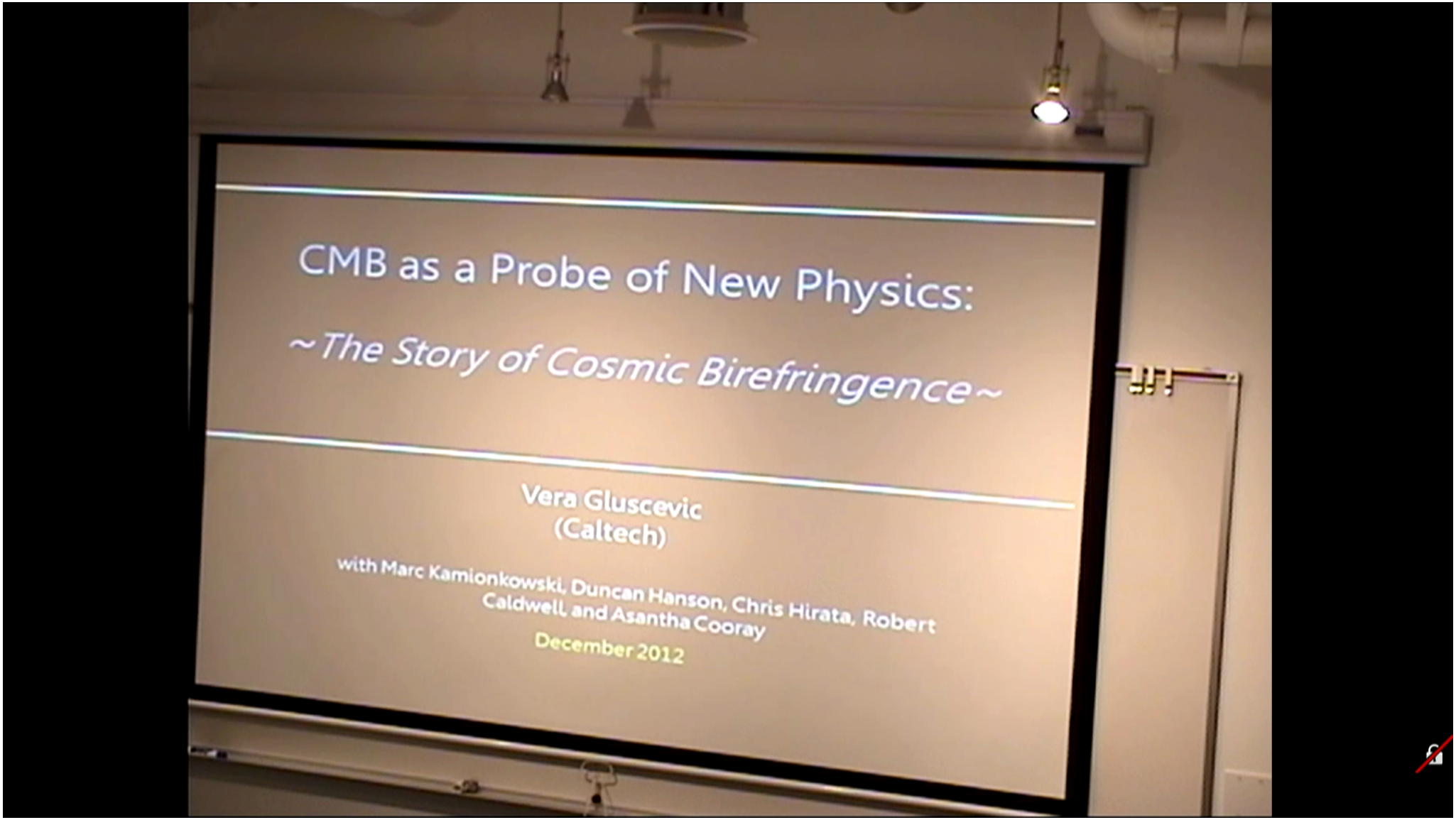
CMB as a Probe of New Physics:
~The Story of Cosmic Birefringence~
Vera Gluscevic
(Caltech)
with Marc Kamionkowski, Duncan Hanson, Chris Hirata, Robert Caldwell, and Asantha Cooray
December 2012

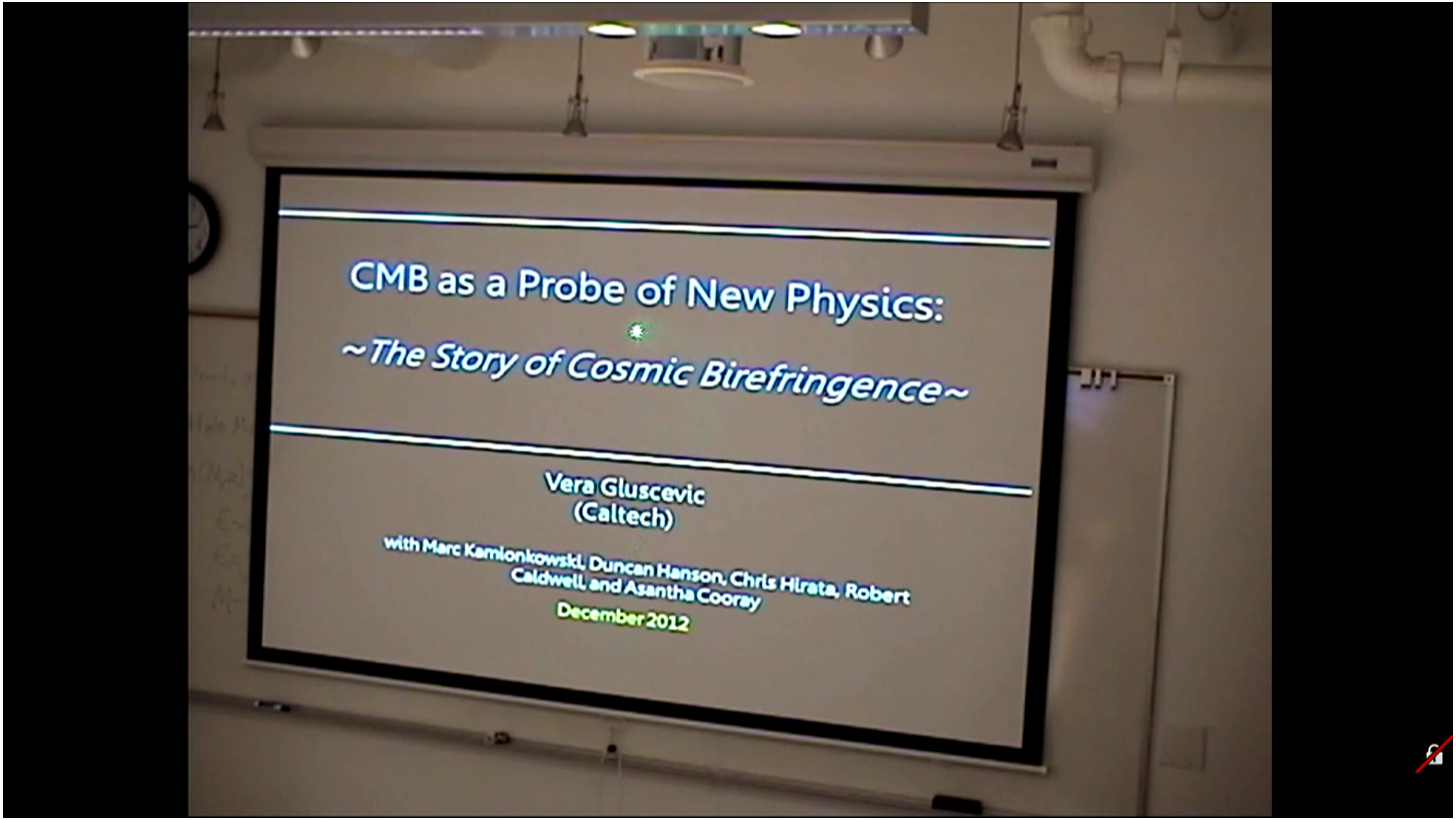
CMB as a Probe of New Physics:
~The Story of Cosmic Birefringence~
Vera Gluscevic
(Caltech)
with Marc Kamionkowski, Duncan Hanson, Chris Hirata, Robert Caldwell, and Asantha Cooray
December 2012

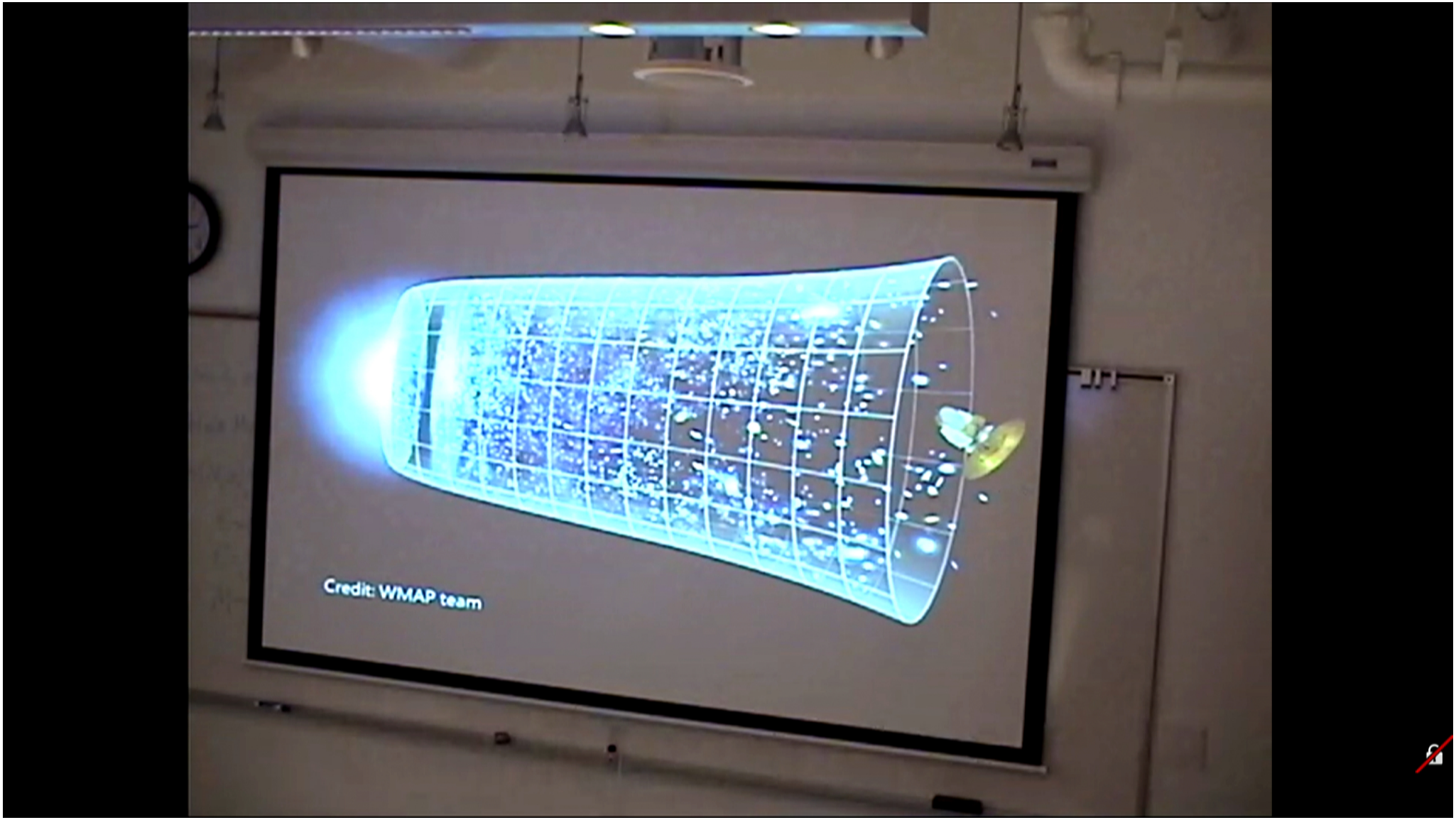
Credit: WMAP team

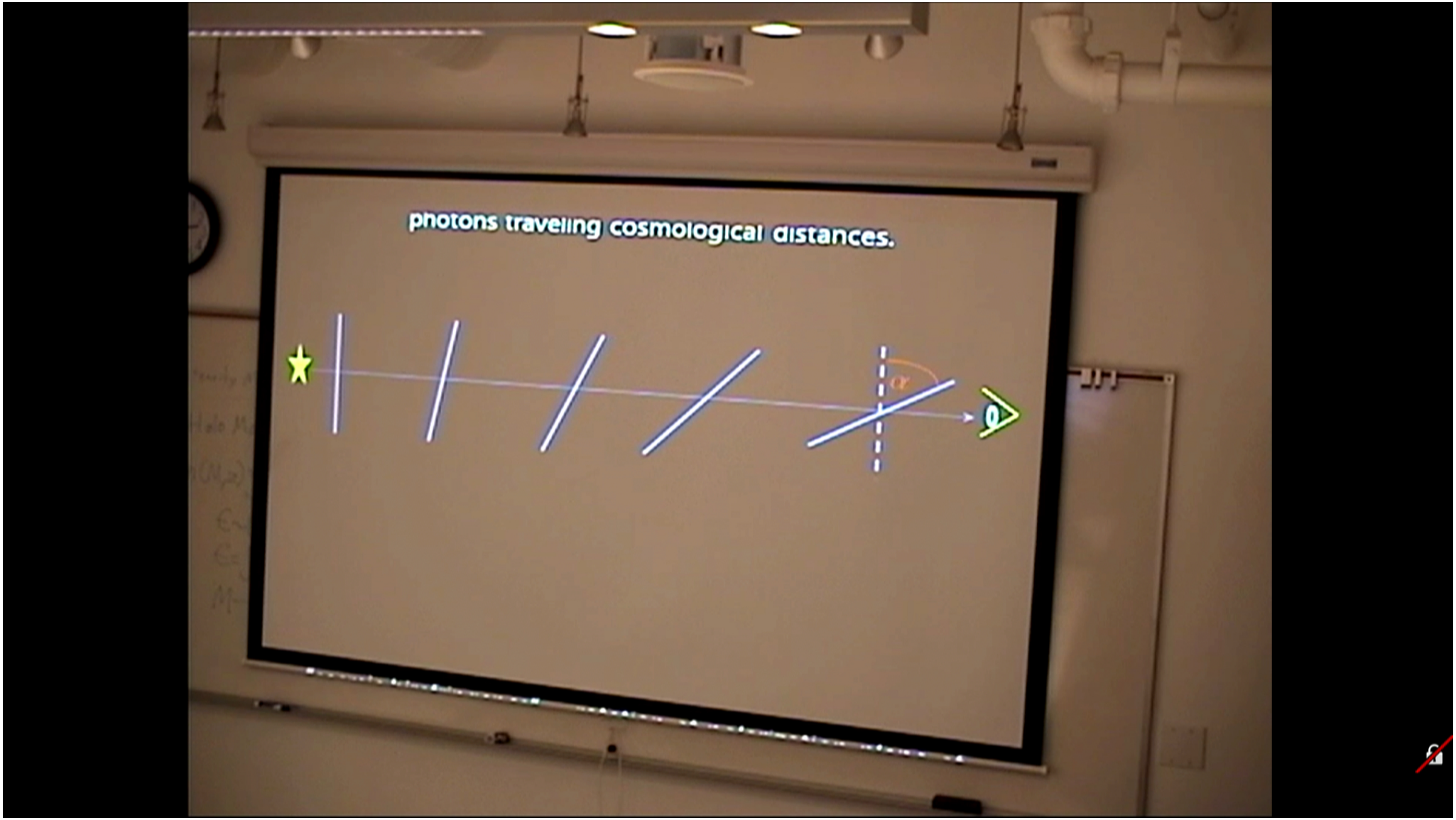
photons traveling cosmological distances.
α
O

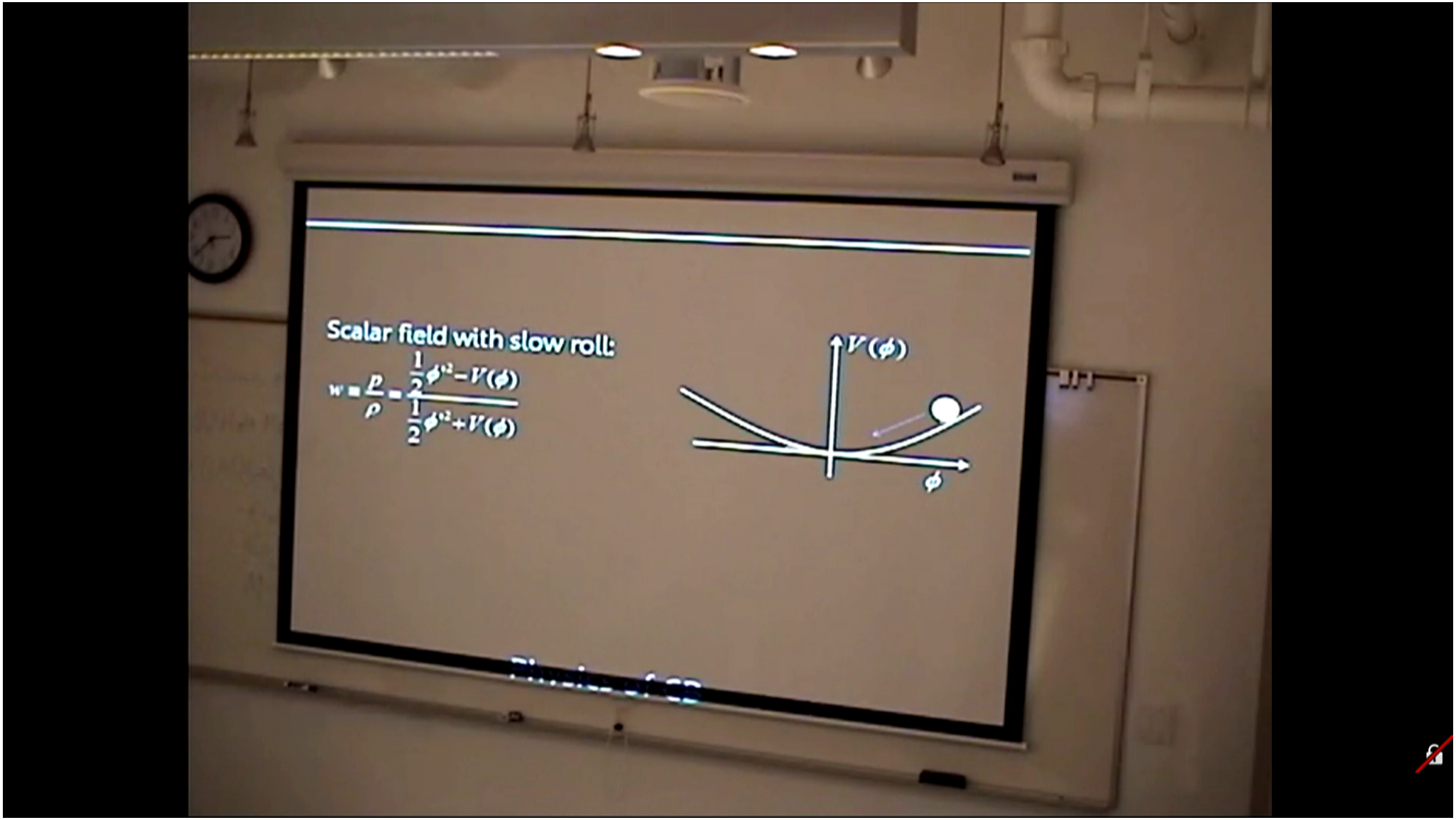
Scalar field with slow roll:
$w = \frac{p}{\rho} = \frac{\frac{1}{2}\dot{\phi}^2 - V(\phi)}{\frac{1}{2}\dot{\phi}^2 + V(\phi)}$
$V(\phi)$
ϕ

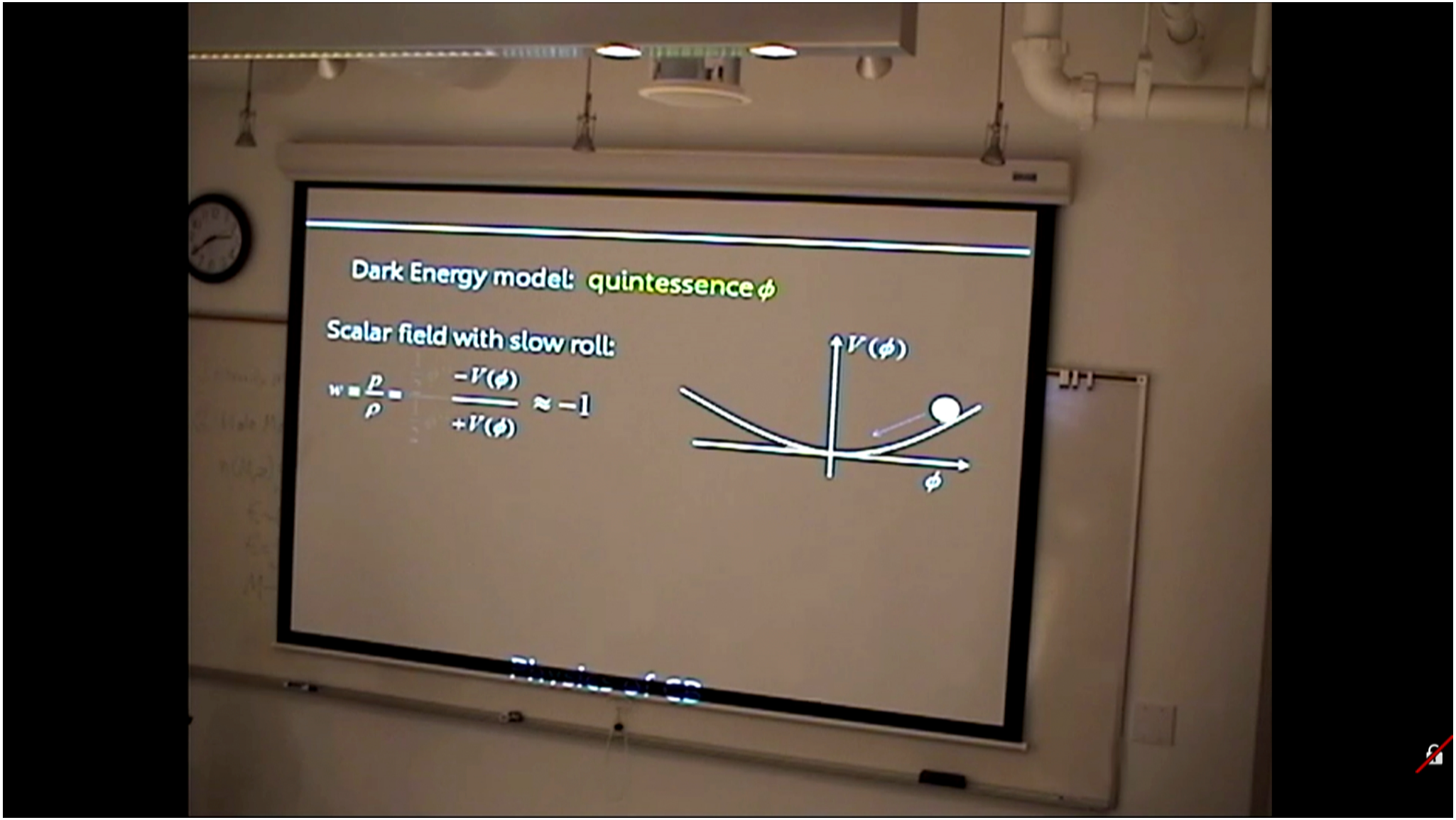
Dark Energy model: quintessence ϕ
Scalar field with slow roll:
$w = \frac{p}{\rho} = \frac{-V(\phi)}{+V(\phi)} \approx -1$
$V(\phi)$
ϕ

Dark Energy model: quintessence ϕ

Scalar field with slow roll:

$$w \equiv \frac{p}{\rho} = \frac{-V(\phi)}{+V(\phi)} \approx -1$$

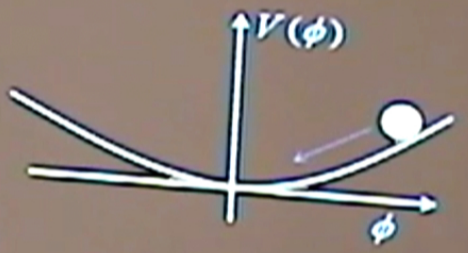

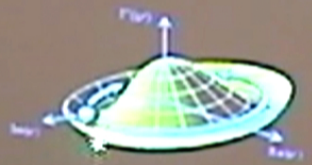

Pseudo Nambu-Goldstone Boson

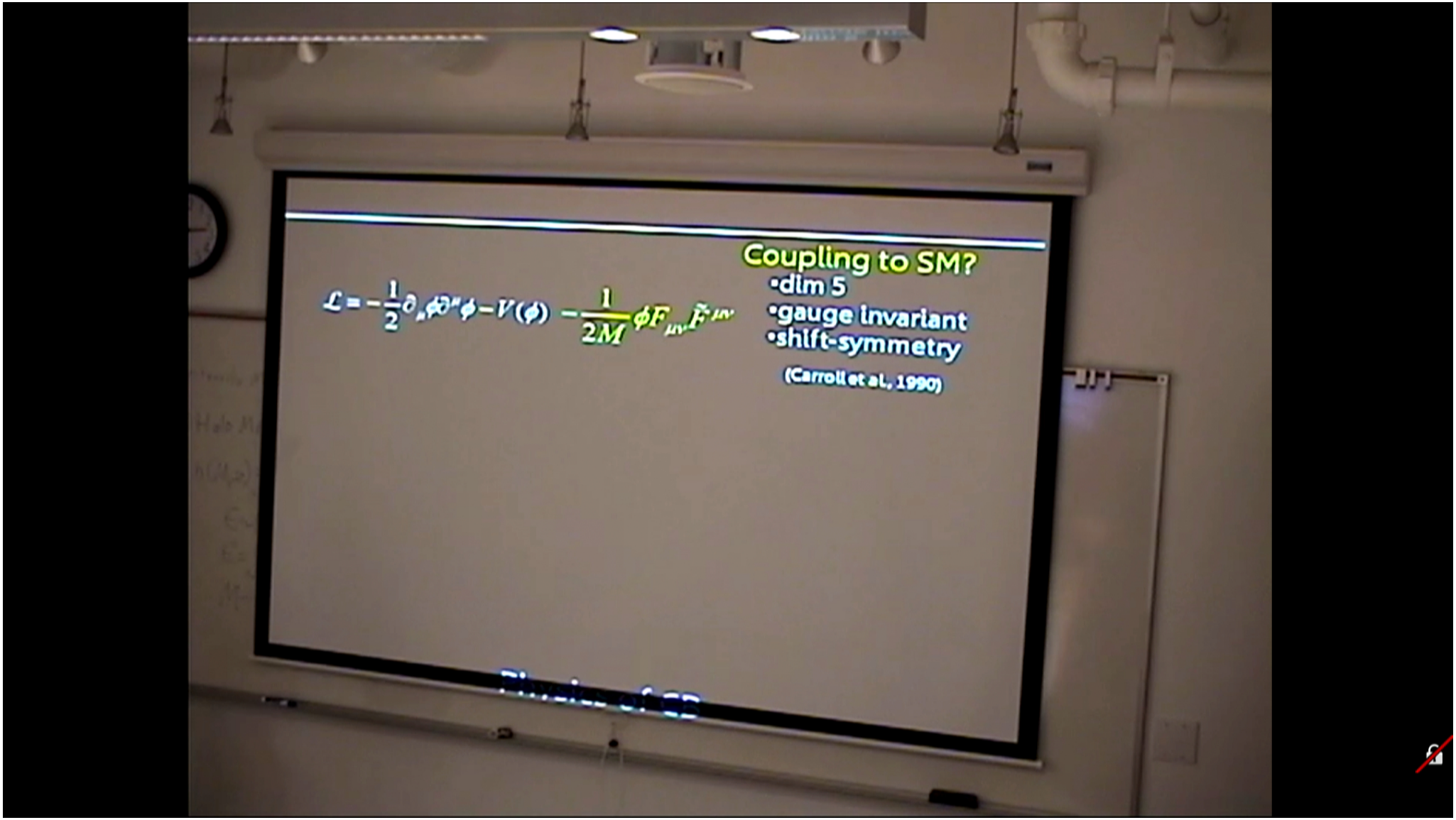
$\mathcal{L} = -\frac{1}{2}\partial_\mu\phi\partial^\mu\phi - V(\phi) - \frac{1}{2M}\phi F_{\mu\nu}\tilde{F}^{\mu\nu}$
Coupling to SM?
•dim 5
•gauge invariant
•shift-symmetry
(Carroll et al., 1990)

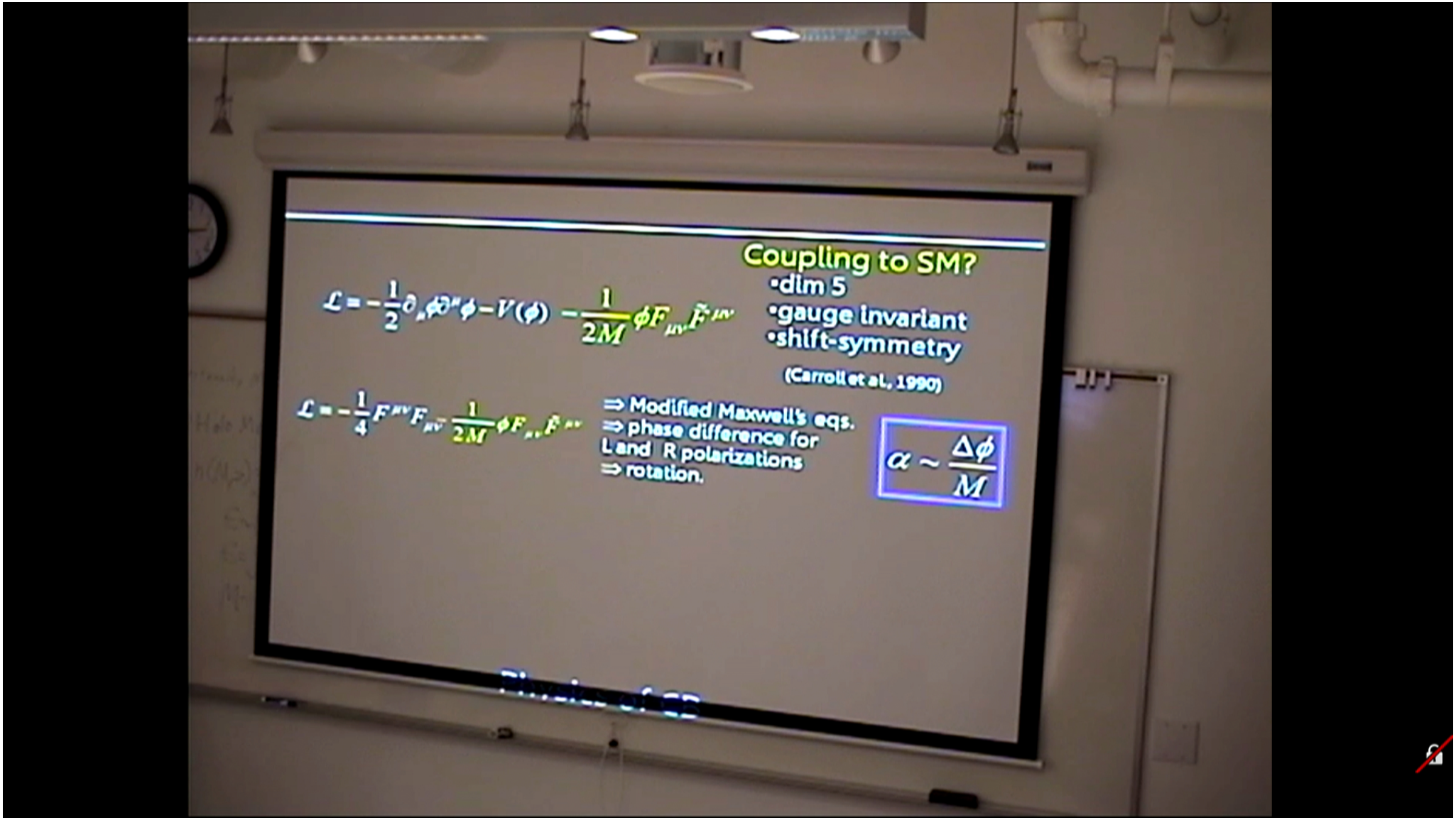
Coupling to SM?
•dim 5
•gauge invariant
•shift-symmetry
(Carroll et al., 1990)
$\mathcal{L} = -\frac{1}{2}\partial_\mu\phi\partial^\mu\phi - V(\phi) - \frac{1}{2M}\phi F_{\mu\nu}\tilde{F}^{\mu\nu}$
$\mathcal{L} = -\frac{1}{4}F^{\mu\nu}F_{\mu\nu} - \frac{1}{2M}\phi F_{\mu\nu}\tilde{F}^{\mu\nu}$
⇒ Modified Maxwell's eqs.
⇒ phase difference for L and R polarizations
⇒ rotation.
$\alpha \sim \frac{\Delta\phi}{M}$

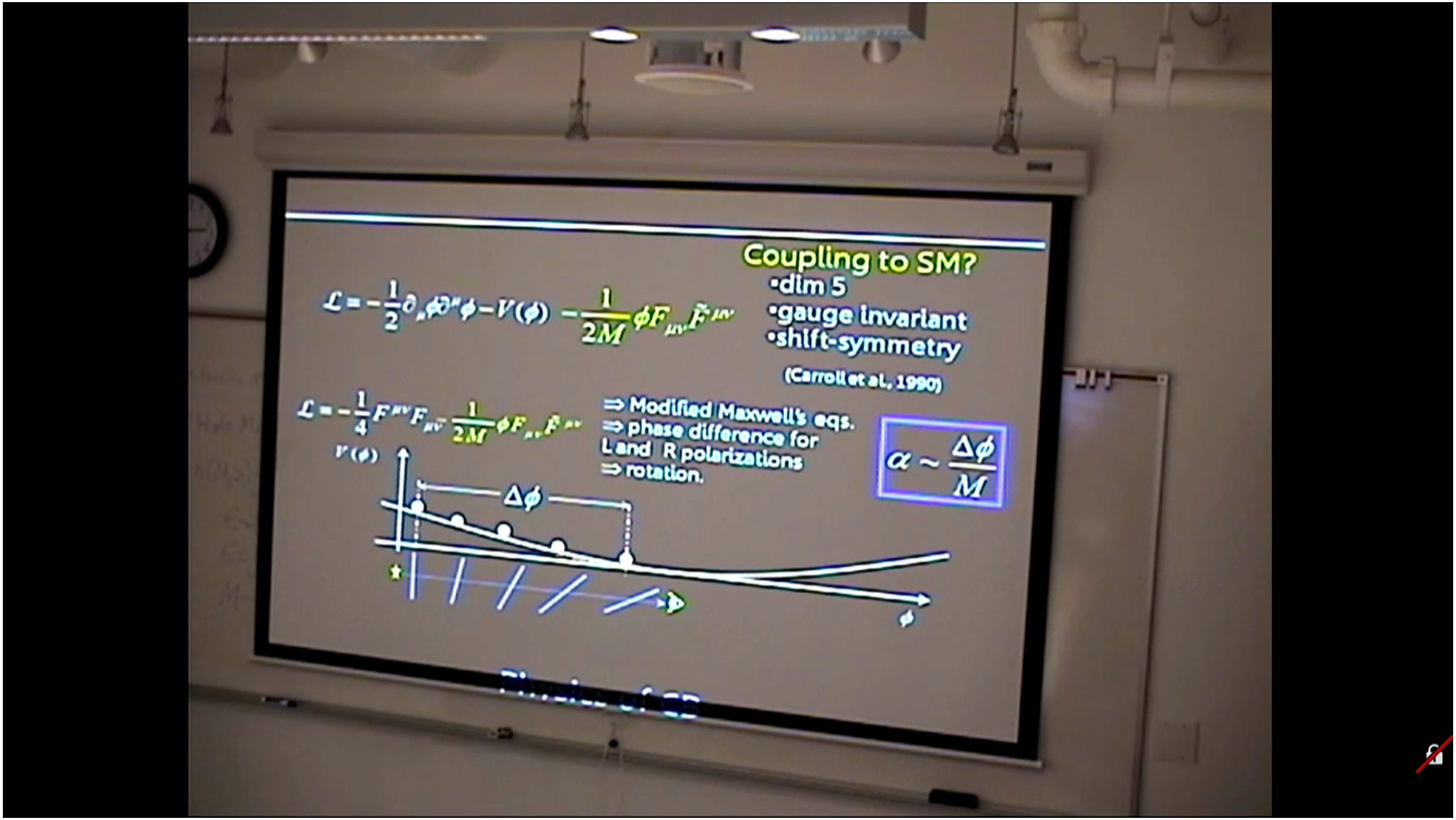
Coupling to SM?
•dim 5
•gauge invariant
•shift-symmetry
(Carroll et al., 1990)
$\mathcal{L} = -\frac{1}{2}\partial_\mu\phi\partial^\mu\phi - V(\phi) - \frac{1}{2M}\phi F_{\mu\nu}\tilde{F}^{\mu\nu}$
$\mathcal{L} = -\frac{1}{4}F^{\mu\nu}F_{\mu\nu} - \frac{1}{2M}\phi F_{\mu\nu}\tilde{F}^{\mu\nu}$
⇒ Modified Maxwell's eqs.
⇒ phase difference for L and R polarizations
⇒ rotation.
$\alpha \sim \frac{\Delta\phi}{M}$
$V(\phi)$
$\Delta\phi$
ϕ

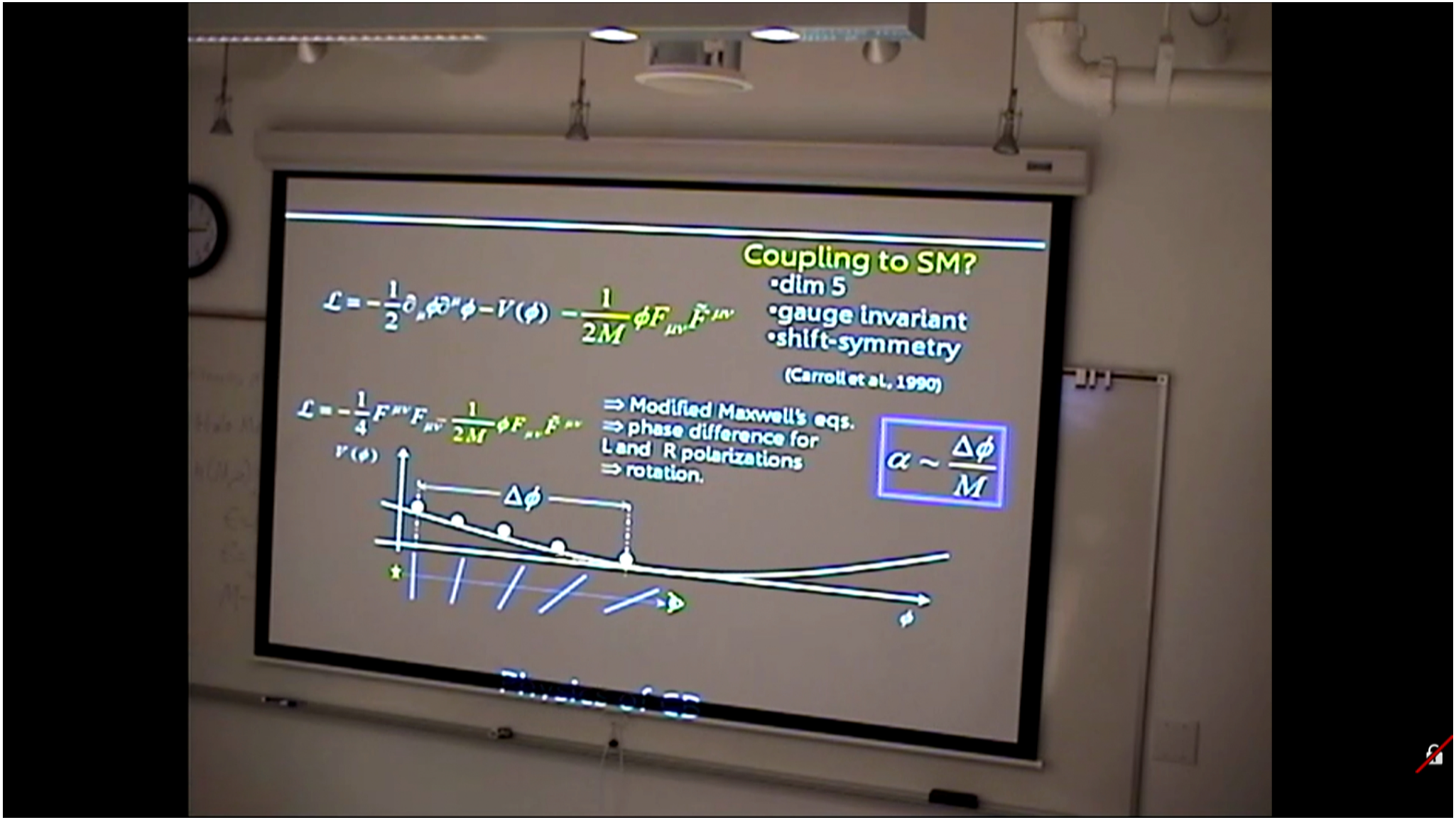
Coupling to SM?
•dim 5
•gauge invariant
•shift-symmetry
(Carroll et al., 1990)
$\mathcal{L} = -\frac{1}{2}\partial_\mu\phi\partial^\mu\phi - V(\phi) - \frac{1}{2M}\phi F_{\mu\nu}\tilde{F}^{\mu\nu}$
$\mathcal{L} = -\frac{1}{4}F^{\mu\nu}F_{\mu\nu} - \frac{1}{2M}\phi F_{\mu\nu}\tilde{F}^{\mu\nu}$
⇒ Modified Maxwell's eqs.
⇒ phase difference for L and R polarizations
⇒ rotation.
$\alpha \sim \frac{\Delta\phi}{M}$
$V(\phi)$
$\Delta\phi$
ϕ

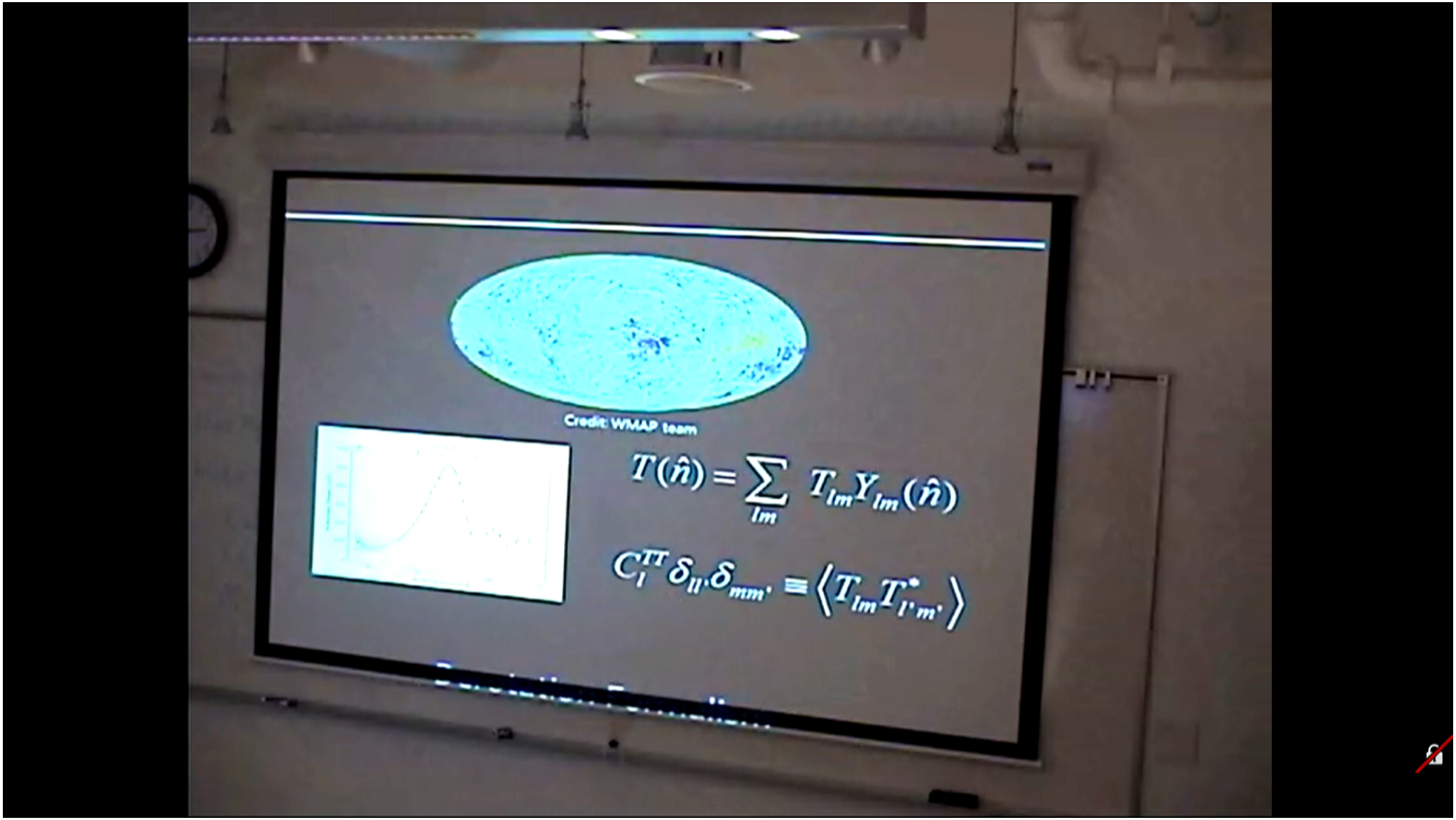
Credit: WMAP team
$T(\hat{n}) = \sum_{lm} T_{lm} Y_{lm}(\hat{n})$
$C_l^{TT} \delta_{ll'} \delta_{mm'} \equiv \langle T_{lm} T^*_{l'm'} \rangle$

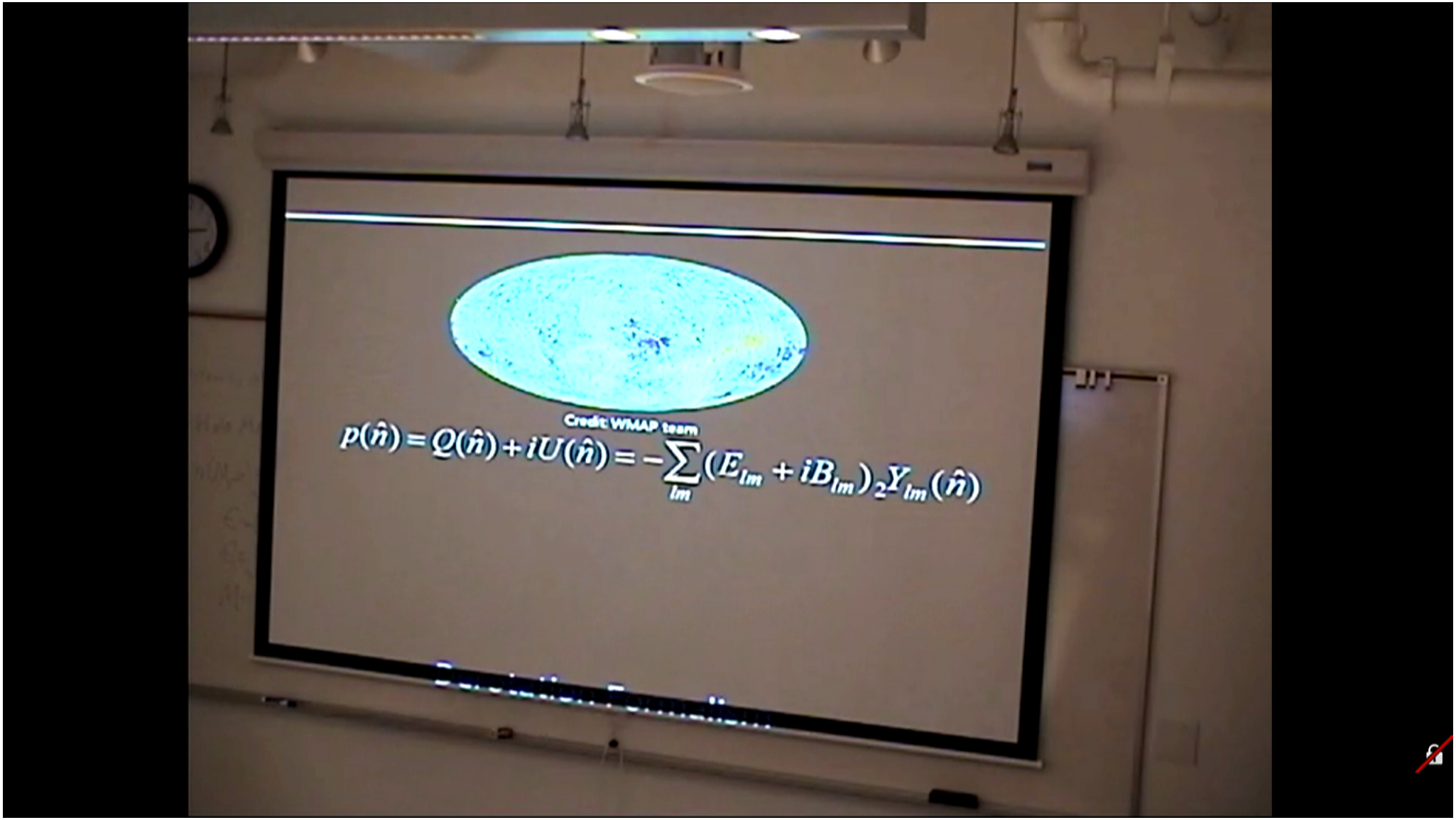
Credit: WMAP team
$p(\hat{n}) = Q(\hat{n}) + iU(\hat{n}) = -\sum_{lm}(E_{lm} + iB_{lm})\,{}_2Y_{lm}(\hat{n})$

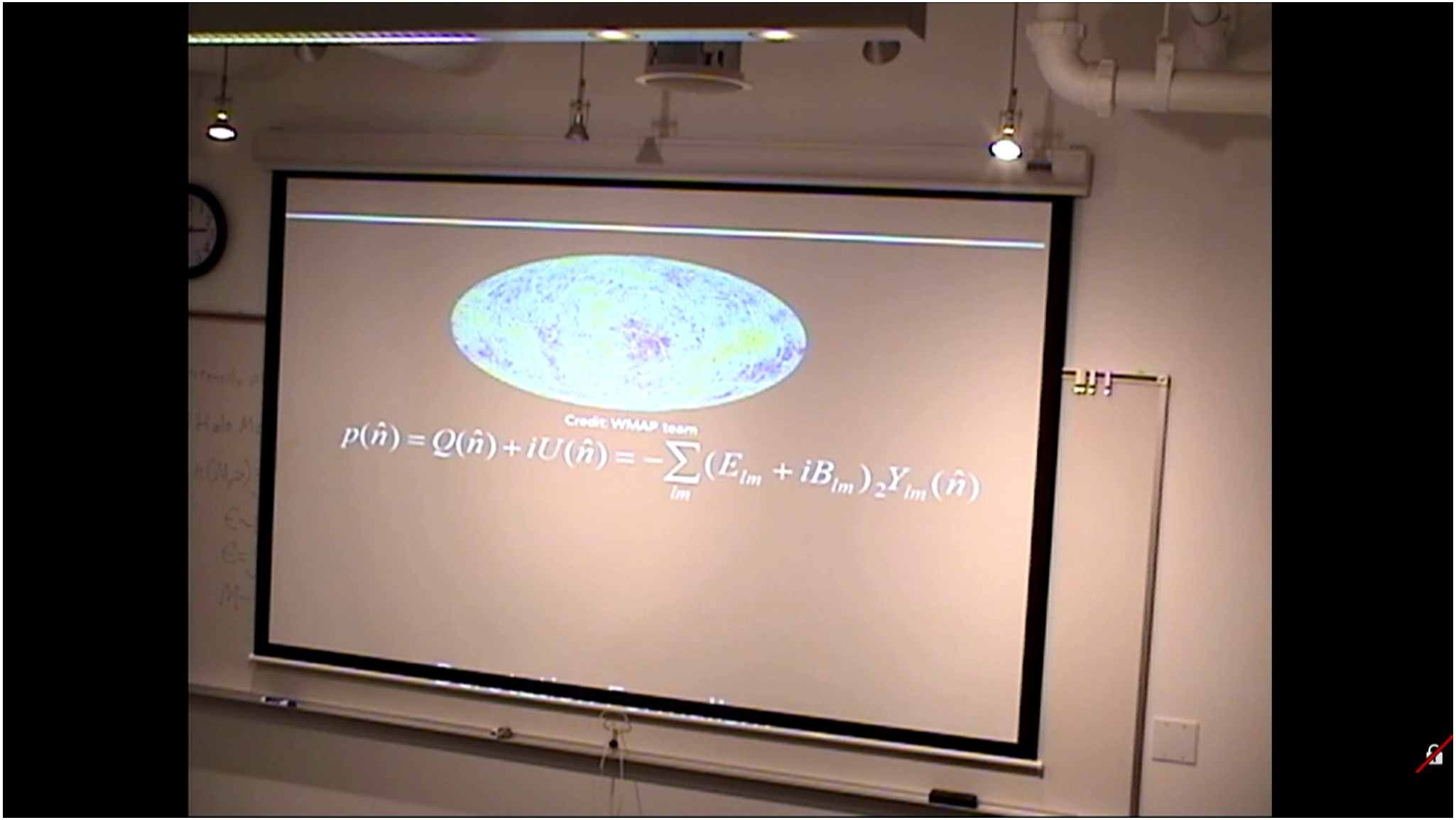
Credit: WMAP team
$p(\hat{n}) = Q(\hat{n}) + iU(\hat{n}) = -\sum_{lm}(E_{lm} + iB_{lm})\,{}_2Y_{lm}(\hat{n})$

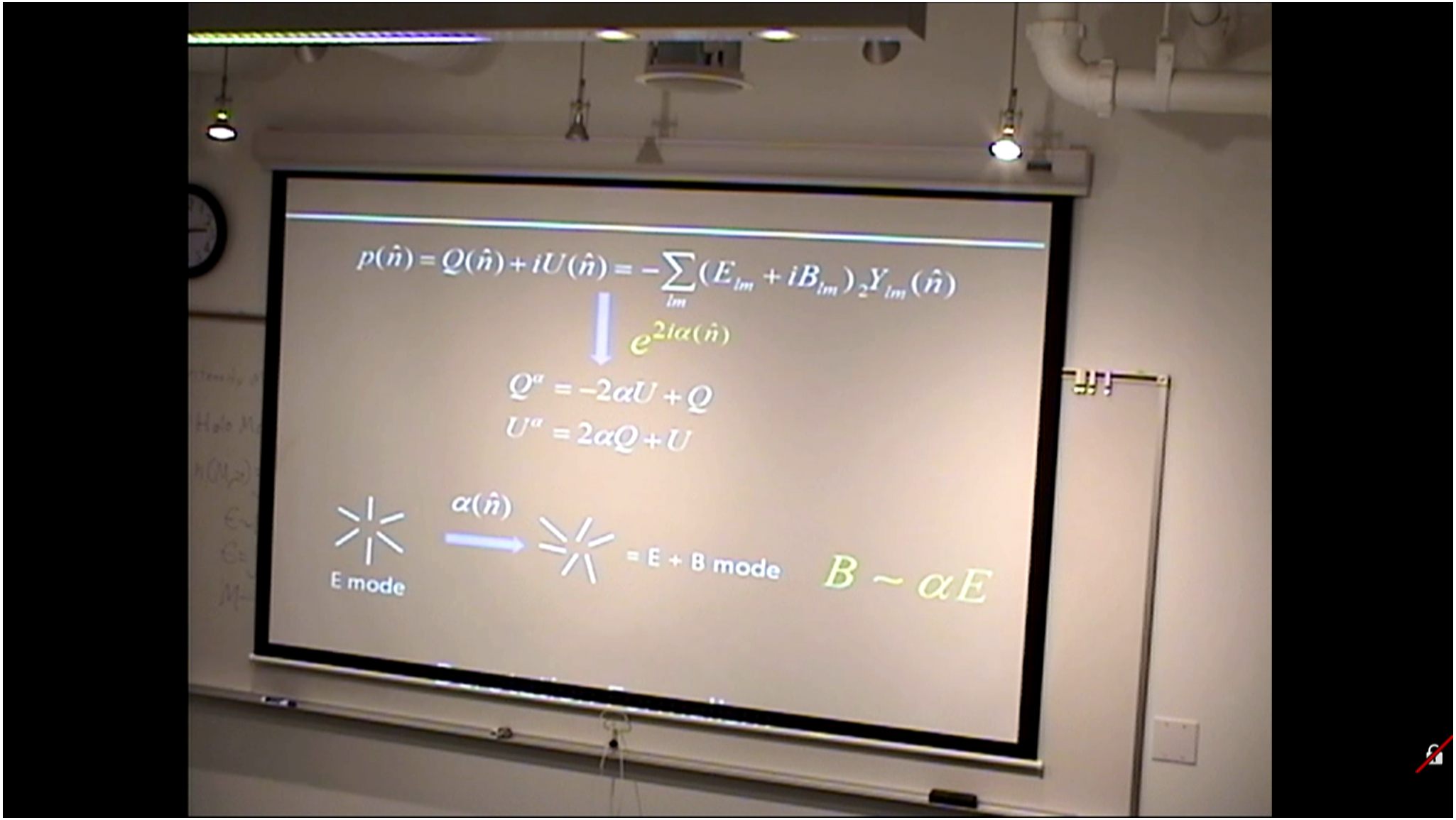
$p(\hat{n}) = Q(\hat{n}) + iU(\hat{n}) = -\sum_{lm}(E_{lm} + iB_{lm})\,{}_2Y_{lm}(\hat{n})$
$e^{2i\alpha(\hat{n})}$
$Q^{\alpha} = -2\alpha U + Q$
$U^{\alpha} = 2\alpha Q + U$
$\alpha(\hat{n})$
E mode
= E + B mode
$B \sim \alpha E$

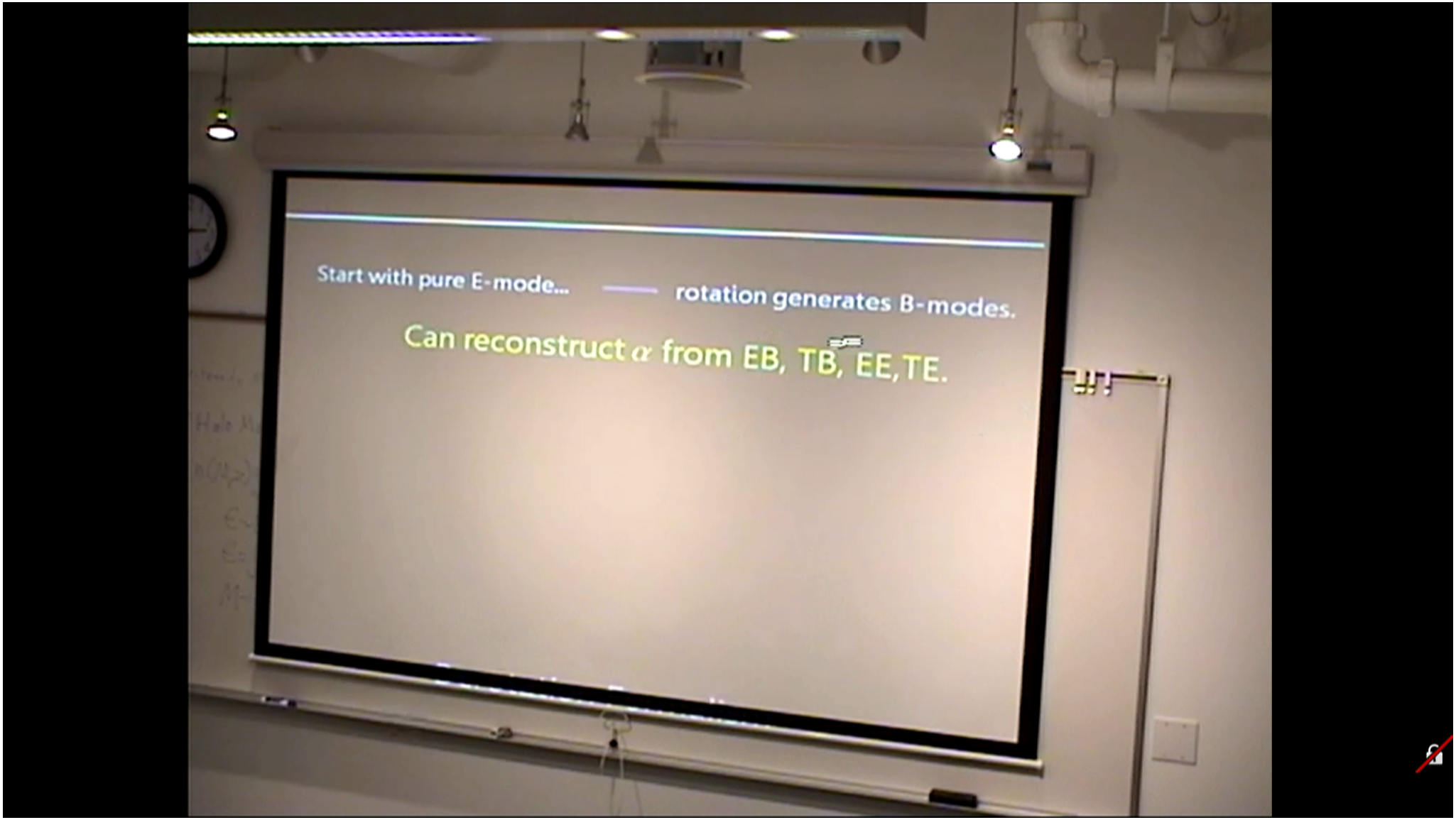
Start with pure E-mode...
rotation generates B-modes.
Can reconstruct α from EB, TB, EE, TE.

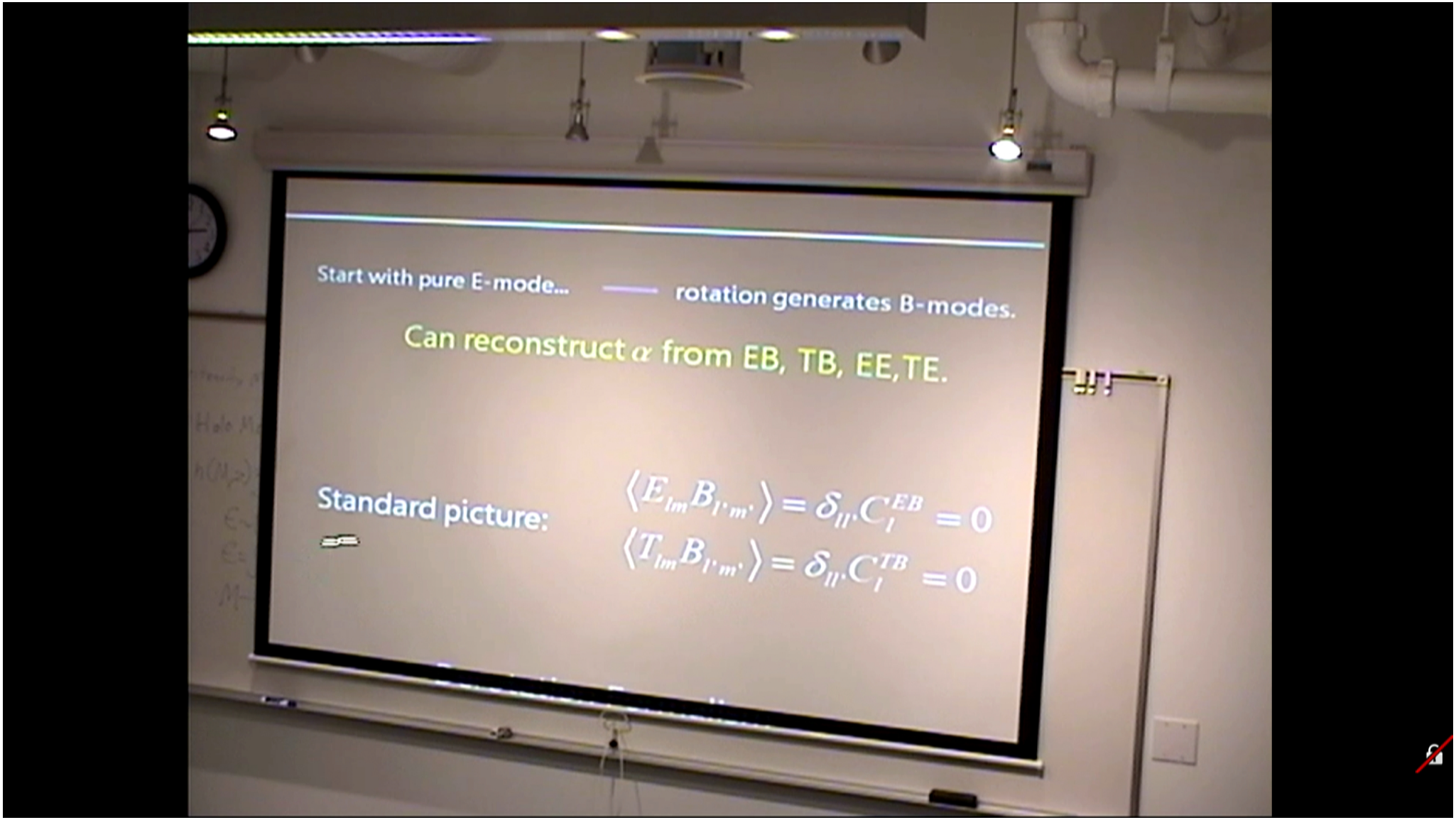
Start with pure E-mode... rotation generates B-modes.
Can reconstruct α from EB, TB, EE, TE.
Standard picture:
$\langle E_{lm} B_{l'm'} \rangle = \delta_{ll'} C_l^{EB} = 0$
$\langle T_{lm} B_{l'm'} \rangle = \delta_{ll'} C_l^{TB} = 0$

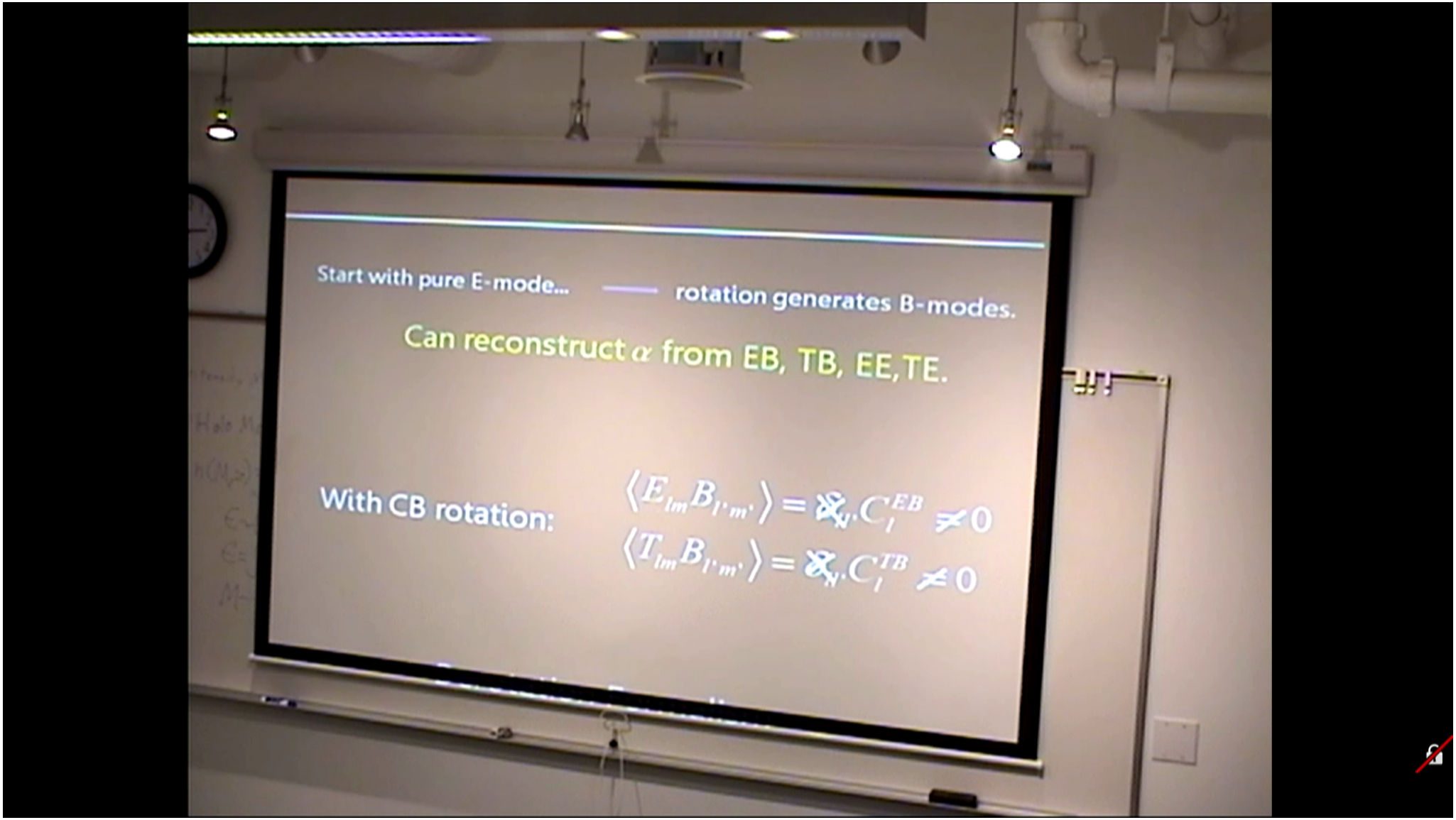
Start with pure E-mode... rotation generates B-modes.
Can reconstruct α from EB, TB, EE, TE.
With CB rotation:
$\langle E_{lm} B_{l'm'} \rangle = \alpha_{ll'} C_l^{EB} \neq 0$
$\langle T_{lm} B_{l'm'} \rangle = \alpha_{ll'} C_l^{TB} \neq 0$

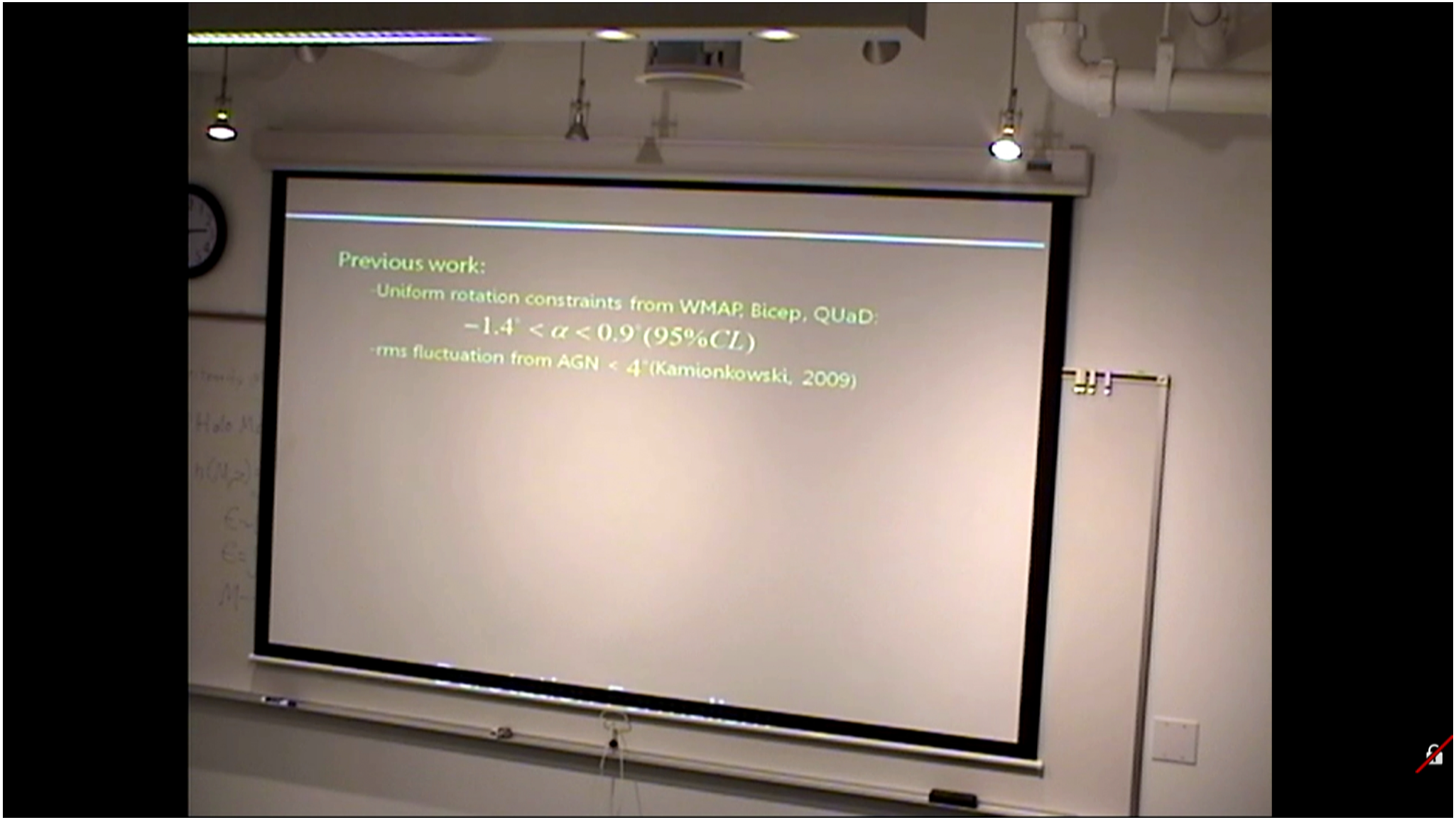
Previous work:
-Uniform rotation constraints from WMAP, Bicep, QUaD:
$-1.4^{\circ} < \alpha < 0.9^{\circ} (95\% CL)$
-rms fluctuation from AGN < 4° (Kamionkowski, 2009)

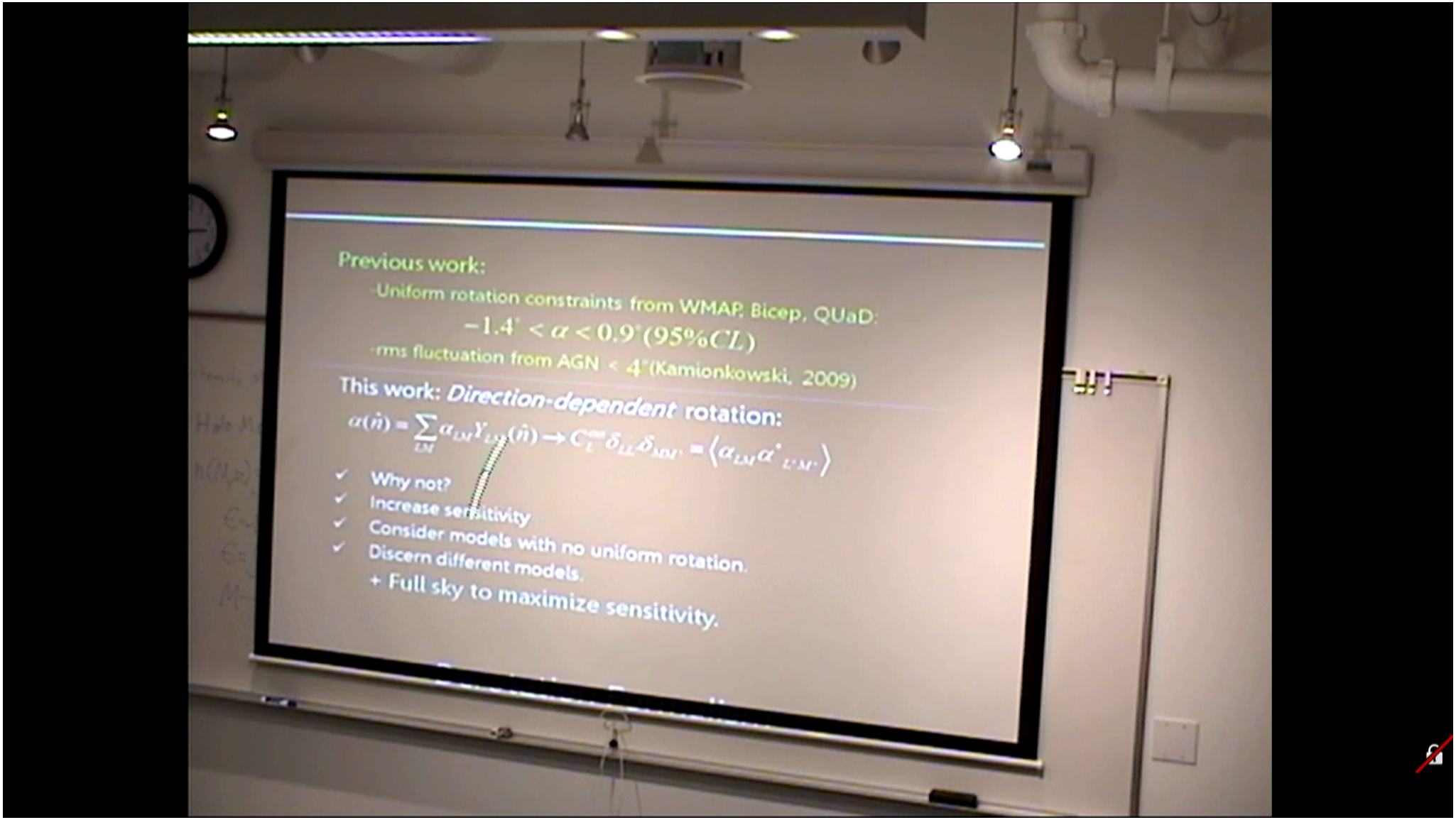
Previous work:
-Uniform rotation constraints from WMAP, Bicep, QUaD:
$-1.4^\circ < \alpha < 0.9^\circ (95\% CL)$
-rms fluctuation from AGN < 4° (Kamionkowski, 2009)
This work: *Direction-dependent* rotation:
$\alpha(\hat{n}) = \sum_{LM} \alpha_{LM} Y_{LM}(\hat{n}) \rightarrow C_L^{\alpha\alpha} \delta_{LL'} \delta_{MM'} = \langle \alpha_{LM} \alpha^*_{L'M'} \rangle$
✓ Why not?
✓ Increase sensitivity
✓ Consider models with no uniform rotation.
✓ Discern different models.
+ Full sky to maximize sensitivity.

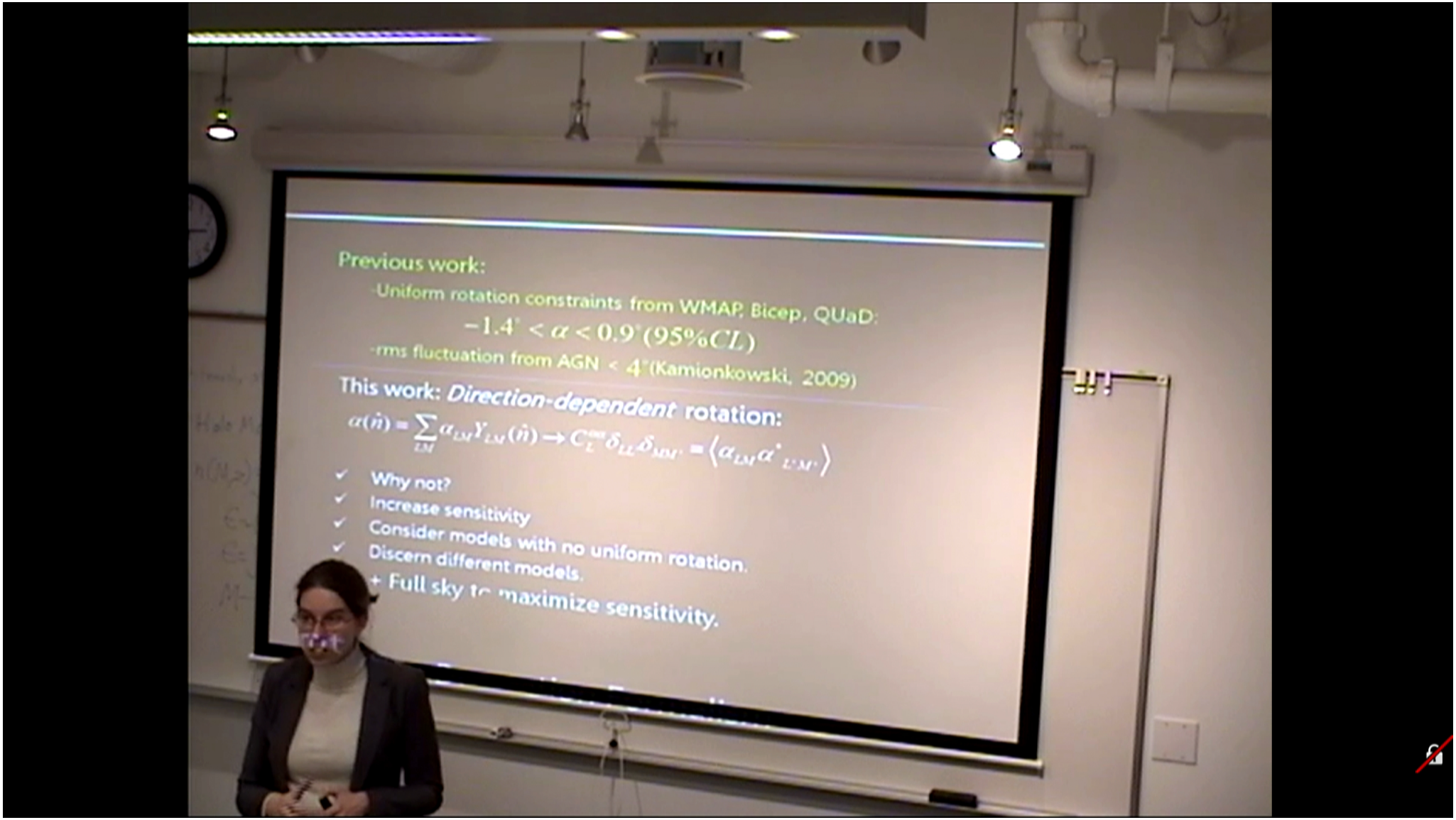
Previous work:
-Uniform rotation constraints from WMAP, Bicep, QUaD:
$-1.4^\circ < \alpha < 0.9^\circ (95\% CL)$
-rms fluctuation from AGN < 4° (Kamionkowski, 2009)
This work: *Direction-dependent* rotation:
$\alpha(\hat{n}) = \sum_{LM} \alpha_{LM} Y_{LM}(\hat{n}) \rightarrow C_L^{\alpha\alpha} \delta_{LL'} \delta_{MM'} = \langle \alpha_{LM} \alpha^*_{L'M'} \rangle$
✓ Why not?
✓ Increase sensitivity
✓ Consider models with no uniform rotation.
✓ Discern different models.
+ Full sky to maximize sensitivity.

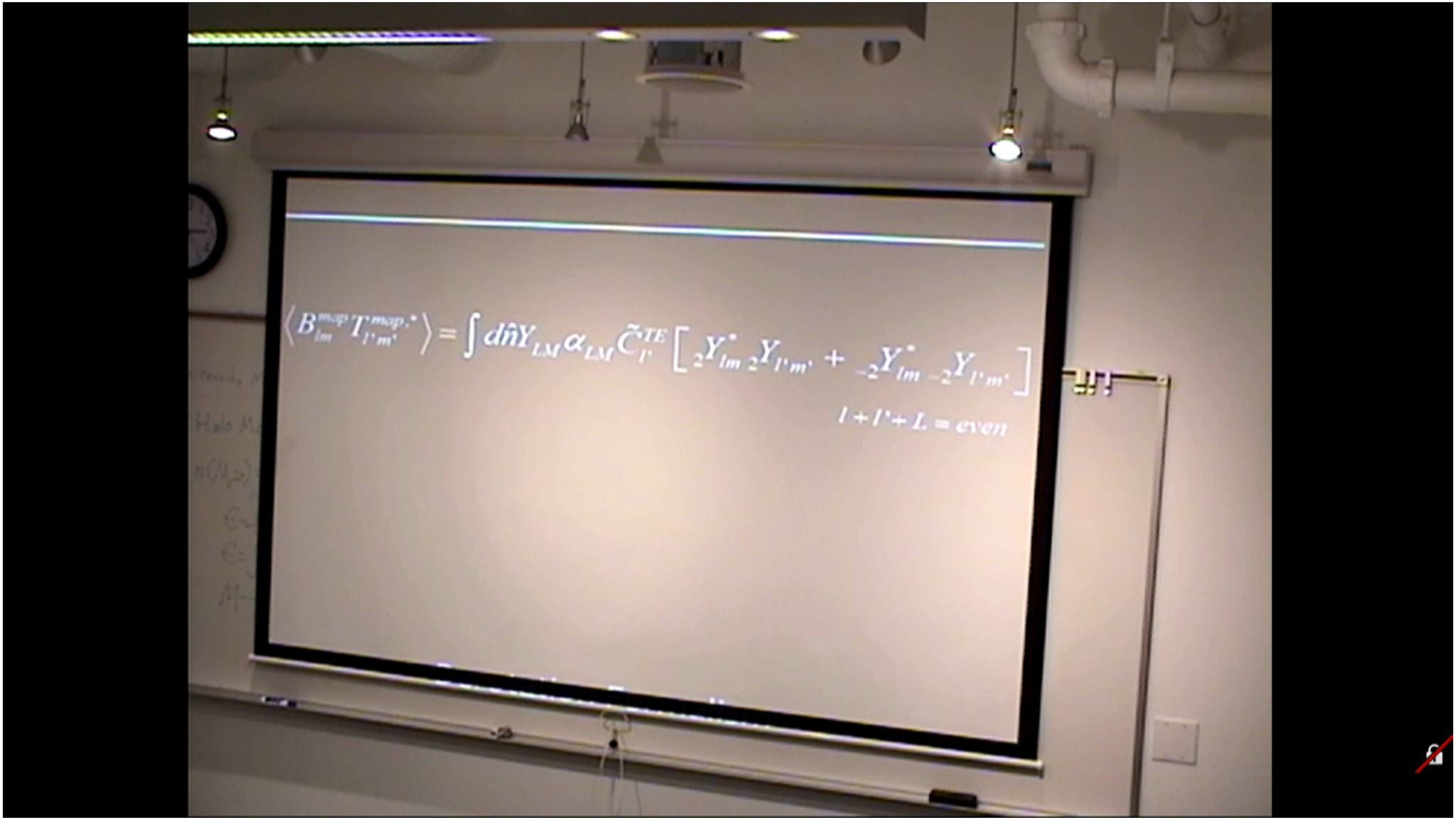
$\langle B_{lm}^{map} T_{l'm'}^{map,*} \rangle = \int d\hat{n} Y_{LM} \alpha_{LM} \tilde{C}_{l'}^{TE} \left[{}_2Y_{lm}^{*} \, {}_2Y_{l'm'} + {}_{-2}Y_{lm}^{*} \, {}_{-2}Y_{l'm'} \right]$
$l + l' + L = even$

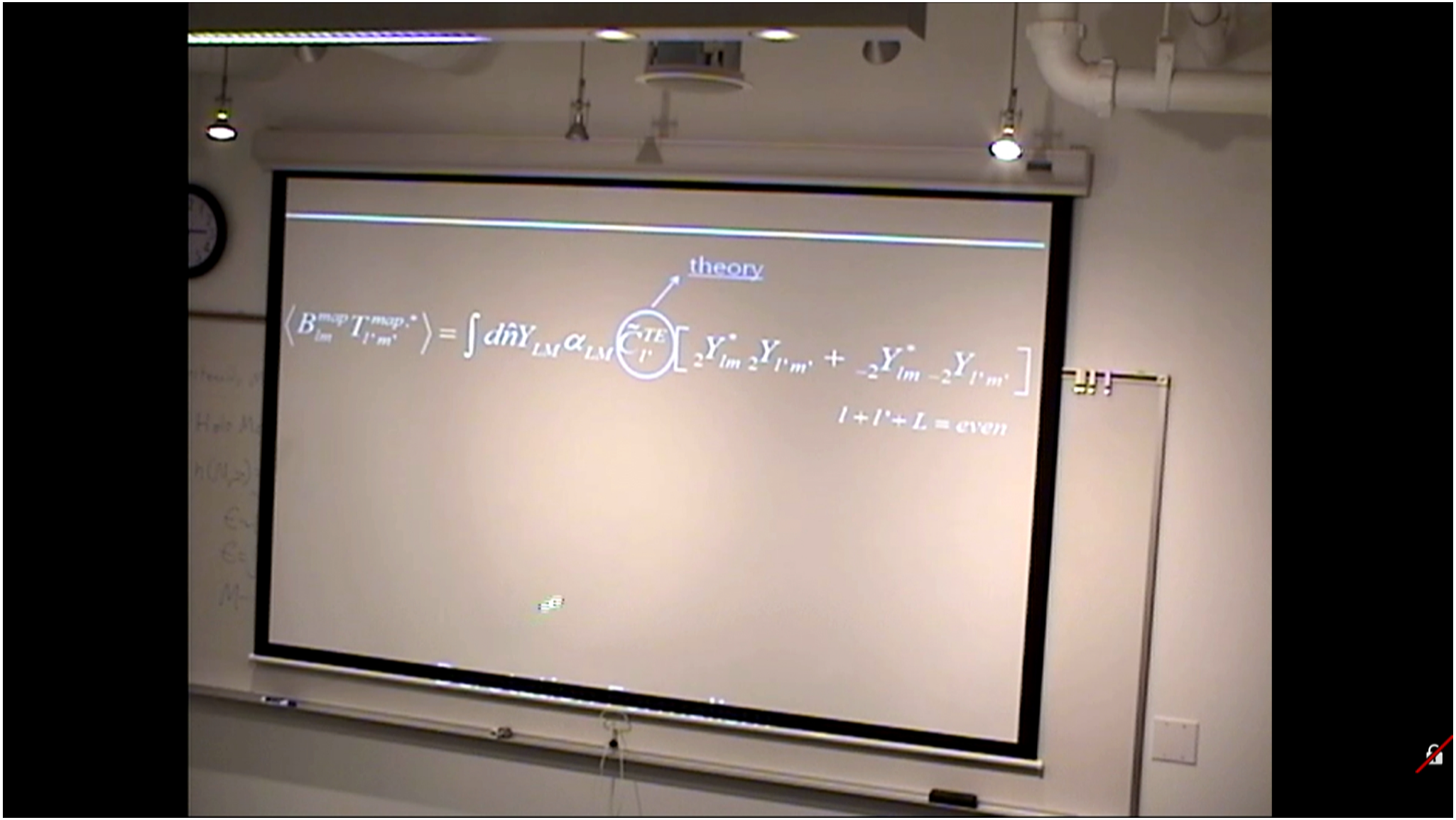
theory
$\langle B_{lm}^{map} T_{l'm'}^{map,*} \rangle = \int d\hat{n} Y_{LM} \alpha_{LM} \tilde{C}_{l'}^{TE} [{}_2Y_{lm}^* {}_2Y_{l'm'} + {}_{-2}Y_{lm}^* {}_{-2}Y_{l'm'}]$
$l + l' + L = even$

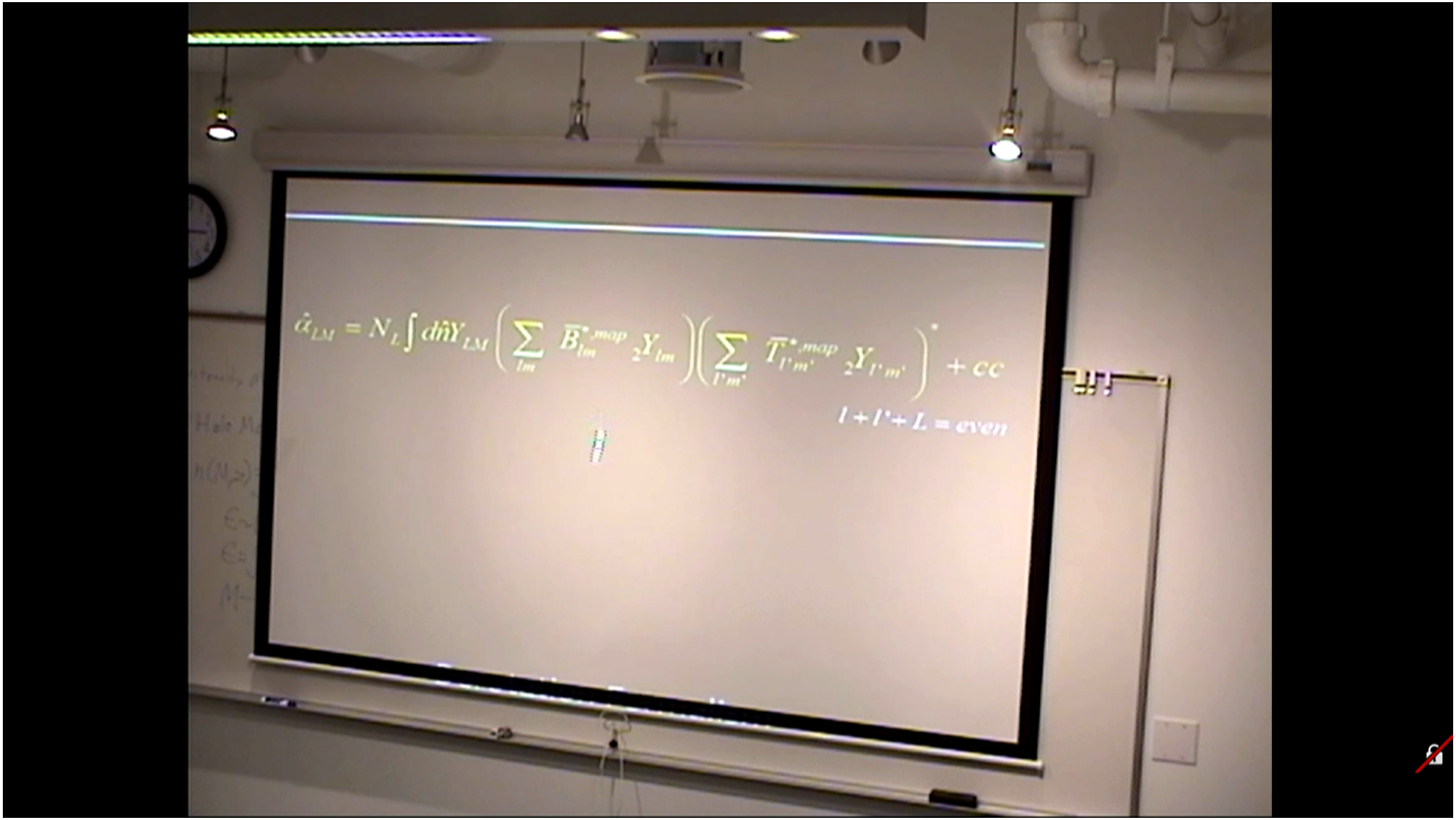
$\hat{\alpha}_{LM} = N_L \int d\hat{n} Y_{LM} \left(\sum_{lm} \overline{B}^{*map}_{lm} {}_2Y_{lm} \right) \left(\sum_{l'm'} \overline{T}^{*map}_{l'm'} {}_2Y_{l'm'} \right)^* + cc$
$l + l' + L = even$

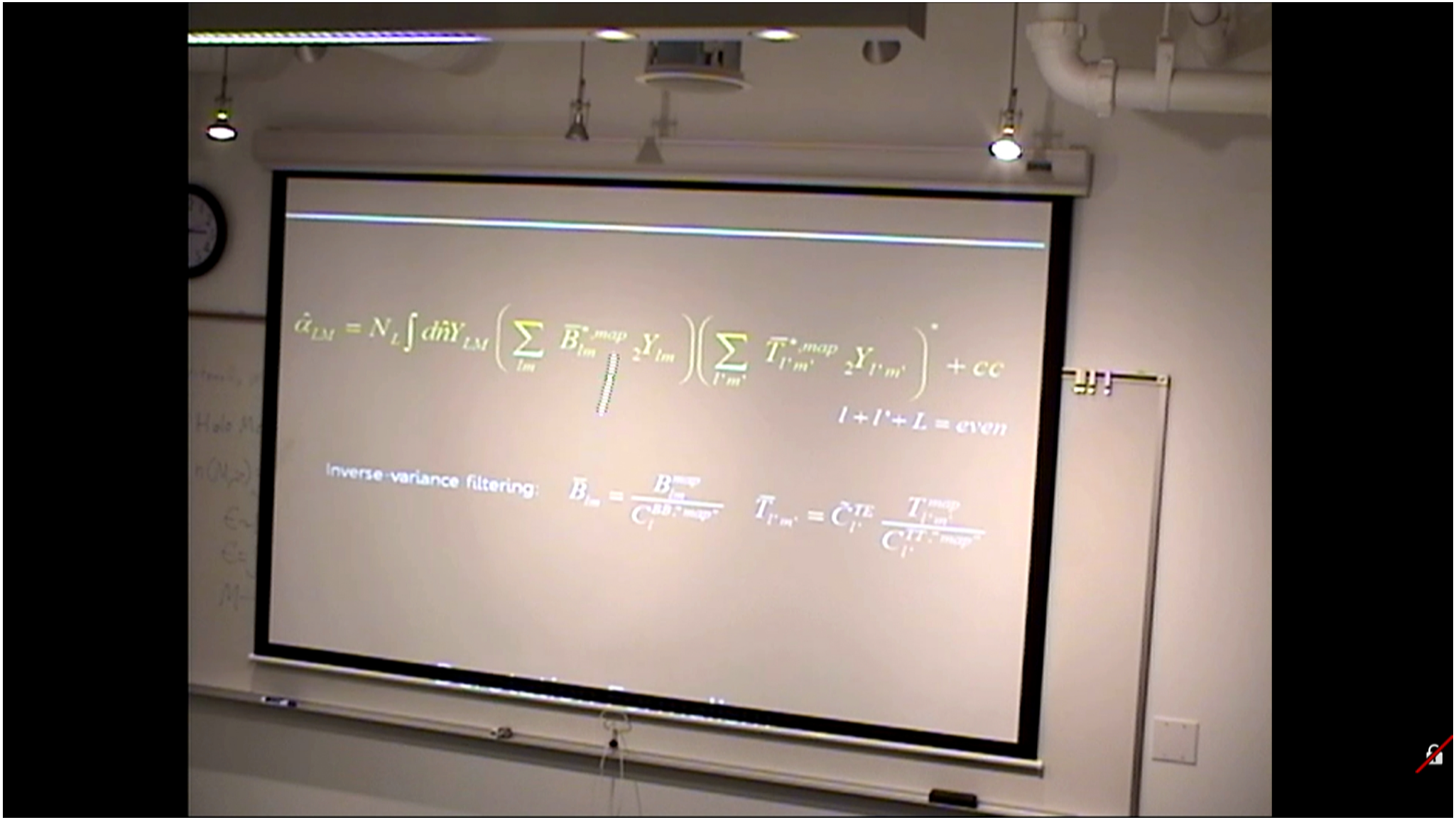
$\hat{\alpha}_{LM} = N_L \int d\hat{n} Y_{LM} \left(\sum_{lm} \bar{B}^{*\,map}_{lm} {}_2Y_{lm} \right) \left(\sum_{l'm'} \bar{T}^{*\,map}_{l'm'} {}_2Y_{l'm'} \right)^* + cc$
$l + l' + L = even$
Inverse-variance filtering: $\bar{B}_{lm} = \frac{B^{map}_{lm}}{C_l^{BB,\,map}}$ $\bar{T}_{l'm'} = \tilde{C}_{l'}^{TE} \frac{T^{map}_{l'm}}{C_{l'}^{TT,\,map}}$

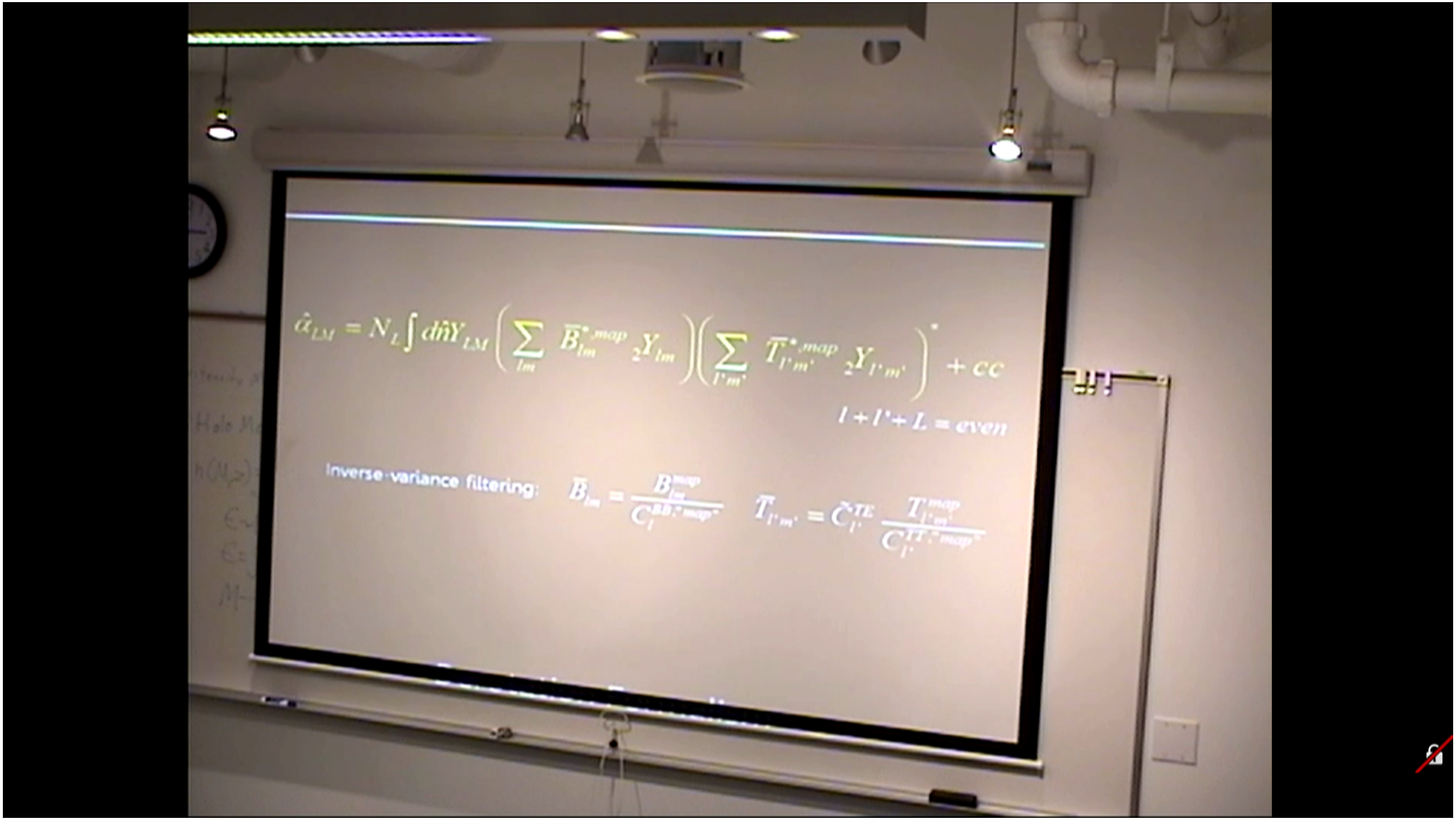
$\hat{\alpha}_{LM} = N_L \int d\hat{n} Y_{LM} \left(\sum_{lm} \bar{B}^{*map}_{lm} {}_2Y_{lm} \right) \left(\sum_{l'm'} \bar{T}^{*map}_{l'm'} {}_2Y_{l'm'} \right)^* + cc$
$l + l' + L = even$
Inverse-variance filtering:
$\bar{B}_{lm} = \frac{B^{map}_{lm}}{C^{BB,map}_l}$
$\bar{T}_{l'm'} = \tilde{C}^{TE}_{l'} \frac{T^{map}_{l'm'}}{C^{TT,map}_{l'}}$

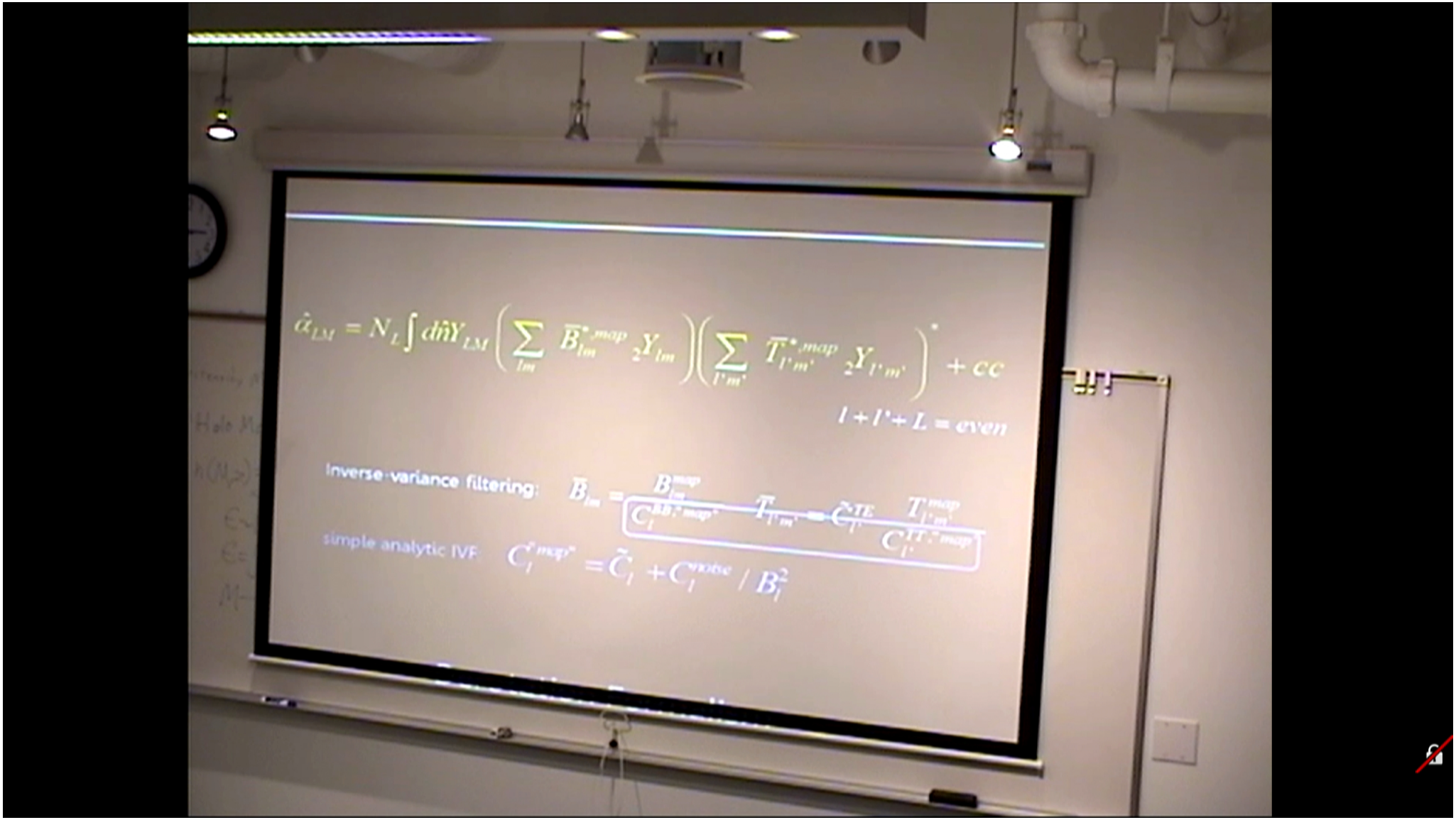
$\hat{\alpha}_{LM} = N_L \int d\hat{n} Y_{LM} \left(\sum_{lm} \bar{B}^{*map}_{lm} {}_2Y_{lm} \right) \left(\sum_{l'm'} \bar{T}^{*map}_{l'm'} {}_2Y_{l'm'} \right)^* + cc$
$l + l' + L = even$
inverse-variance filtering:
$\bar{B}_{lm} = \frac{B^{map}_{lm}}{C^{BB,*map*}_l} - \bar{T}_{l'm'} \frac{\tilde{C}^{TE}_l}{C^{TT,*map}_{l'}} T^{map}_{l'm'}$
simple analytic IVF
$C^{*map*}_l = \tilde{C}_l + C^{noise}_l / B^2_l$

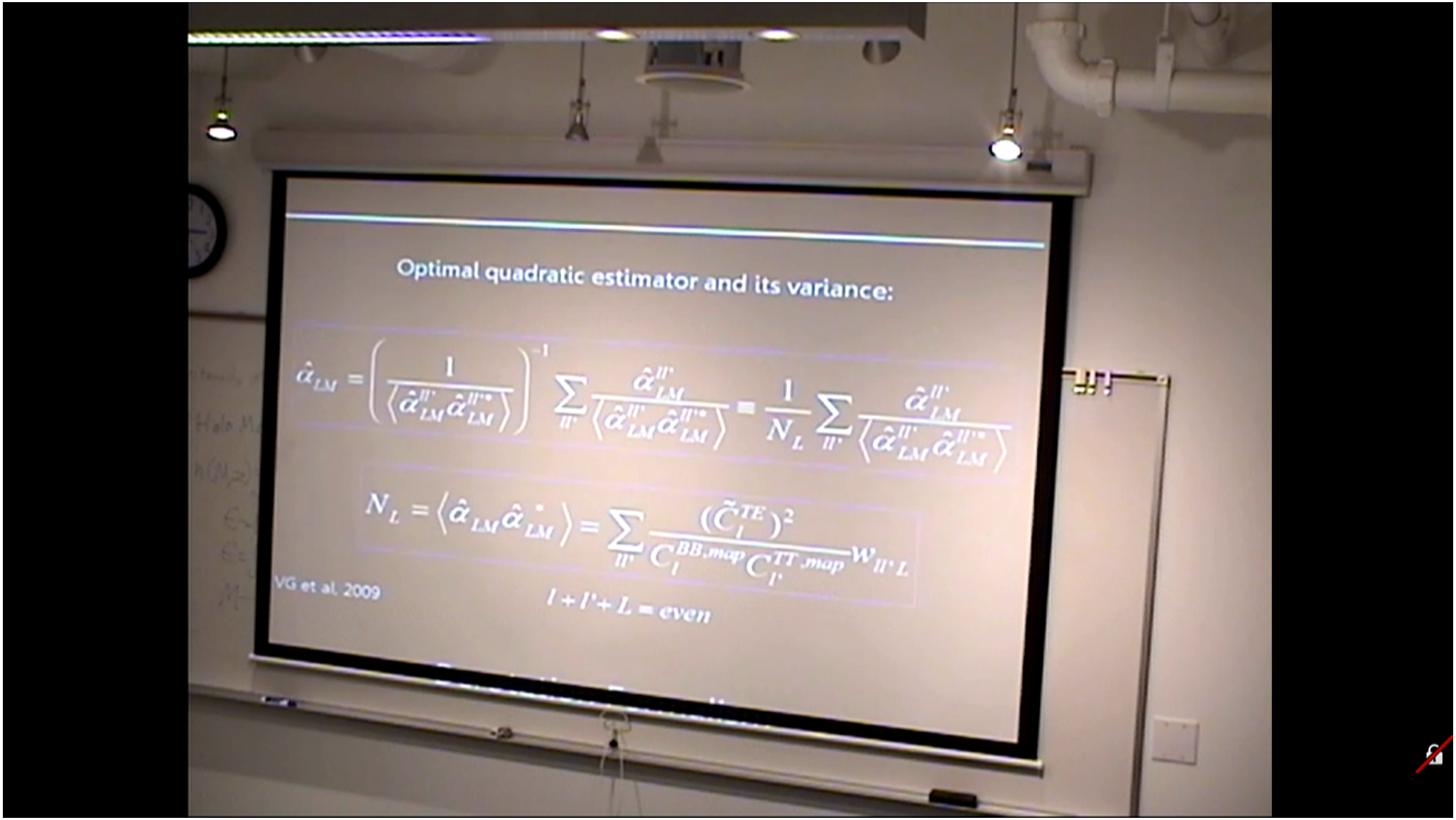
Optimal quadratic estimator and its variance:
$\hat{\alpha}_{LM} = \left(\frac{1}{\langle \hat{\alpha}^{ll'}_{LM} \hat{\alpha}^{ll'*}_{LM} \rangle} \right)^{-1} \sum_{ll'} \frac{\hat{\alpha}^{ll'}_{LM}}{\langle \hat{\alpha}^{ll'}_{LM} \hat{\alpha}^{ll'*}_{LM} \rangle} = \frac{1}{N_L} \sum_{ll'} \frac{\hat{\alpha}^{ll'}_{LM}}{\langle \hat{\alpha}^{ll'}_{LM} \hat{\alpha}^{ll'*}_{LM} \rangle}$
$N_L = \langle \hat{\alpha}_{LM} \hat{\alpha}^{*}_{LM} \rangle = \sum_{ll'} \frac{(\tilde{C}_l^{TE})^2}{C_l^{BB,map} C_{l'}^{TT,map}} W_{ll'L}$
$l + l' + L = even$
VG et al. 2009

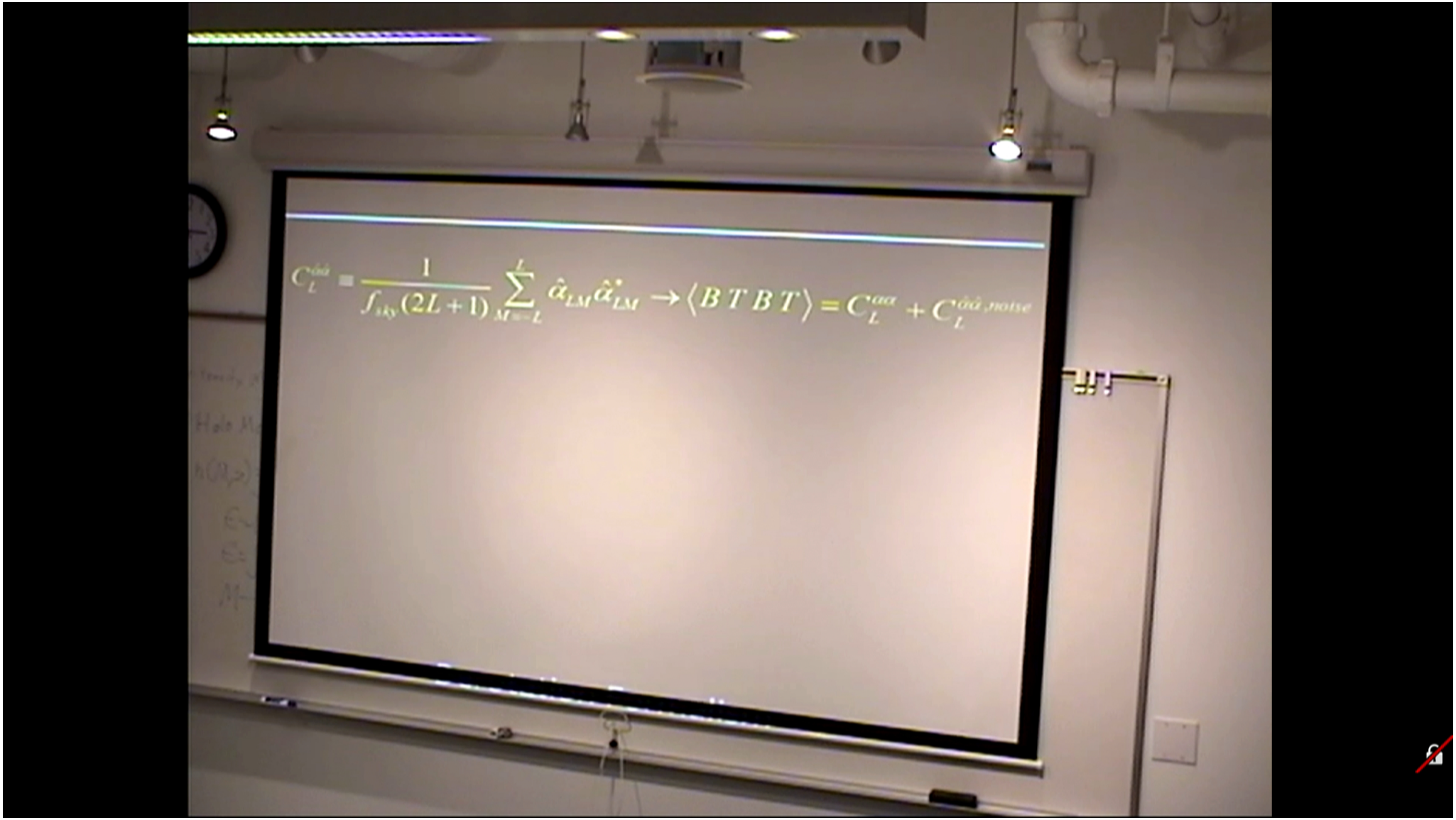
$C_L^{\hat{a}\hat{a}} \equiv \frac{1}{f_{sky}(2L+1)} \sum_{M=-L}^{L} \hat{a}_{LM} \hat{a}^*_{LM} \rightarrow \langle B\,T\,B\,T \rangle = C_L^{aa} + C_L^{\hat{a}\hat{a}\,noise}$

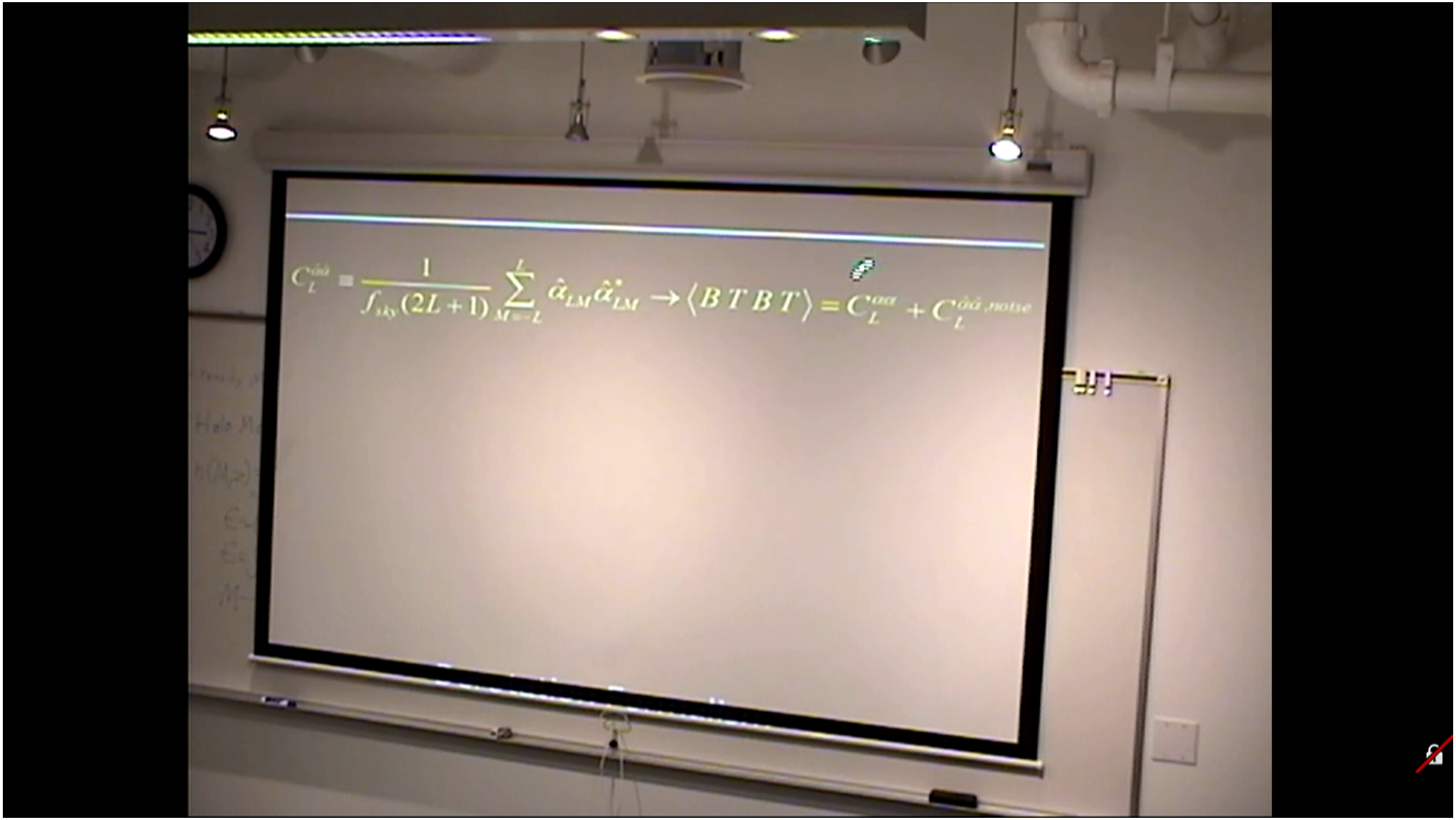
$C_L^{\hat{a}\hat{a}} \equiv \frac{1}{f_{sky}(2L+1)} \sum_{M=-L}^{L} \hat{a}_{LM} \hat{a}^*_{LM} \rightarrow \langle B\,T\,B\,T \rangle = C_L^{aa} + C_L^{\hat{a}\hat{a}\,noise}$

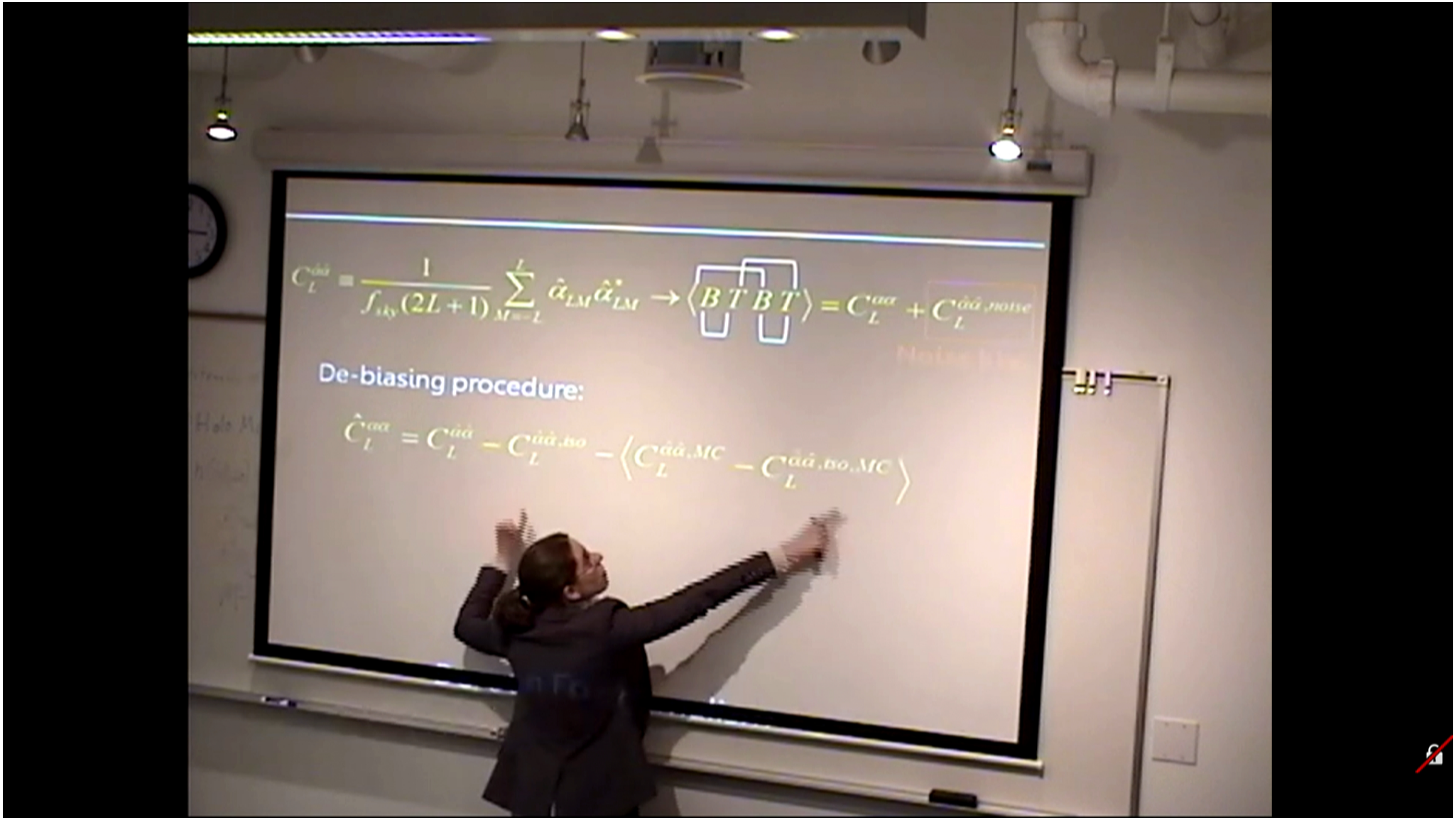
$C_L^{\hat{a}\hat{a}} \equiv \frac{1}{f_{sky}(2L+1)} \sum_{M=-L}^{L} \hat{a}_{LM} \hat{a}^*_{LM} \rightarrow \langle BTBT \rangle = C_L^{aa} + C_L^{\hat{a}\hat{a},noise}$
De-biasing procedure:
$\hat{C}_L^{aa} = C_L^{\hat{a}\hat{a}} - C_L^{\hat{a}\hat{a},BO} - \langle C_L^{\hat{a}\hat{a},MC} - C_L^{\hat{a}\hat{a},BO,MC} \rangle$

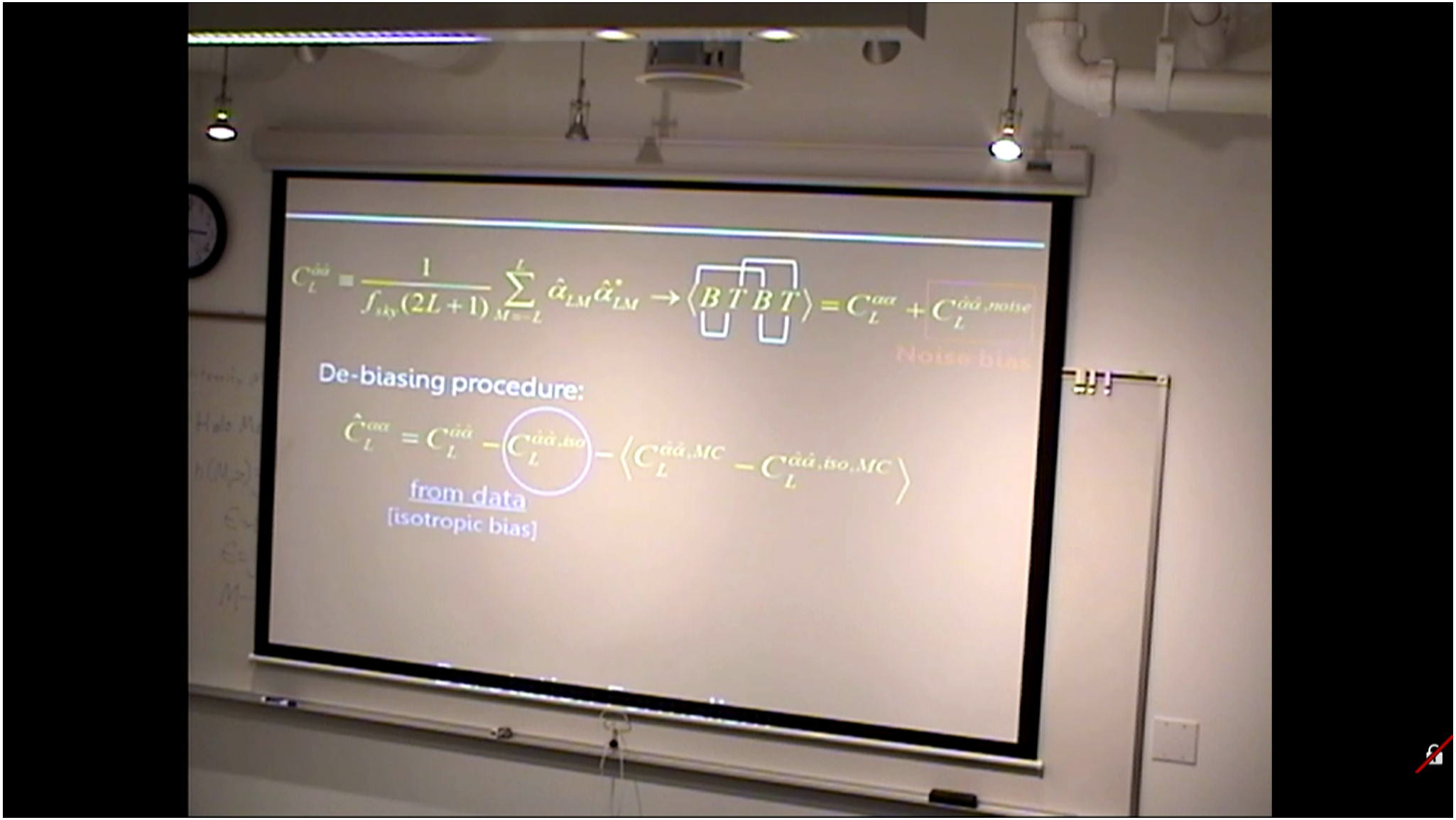
$C_L^{\hat{a}\hat{a}} \equequiv \frac{1}{f_{sky}(2L+1)} \sum_{M=-L}^{L} \hat{a}_{LM} \hat{a}^*_{LM} \rightarrow \langle BTBT \rangle = C_L^{aa} + C_L^{\hat{a}\hat{a},noise}$
Noise bias
De-biasing procedure:
$\hat{C}_L^{aa} = C_L^{\hat{a}\hat{a}} - C_L^{\hat{a}\hat{a},iso} - \langle C_L^{\hat{a}\hat{a},MC} - C_L^{\hat{a}\hat{a},iso,MC} \rangle$
from data
[isotropic bias]

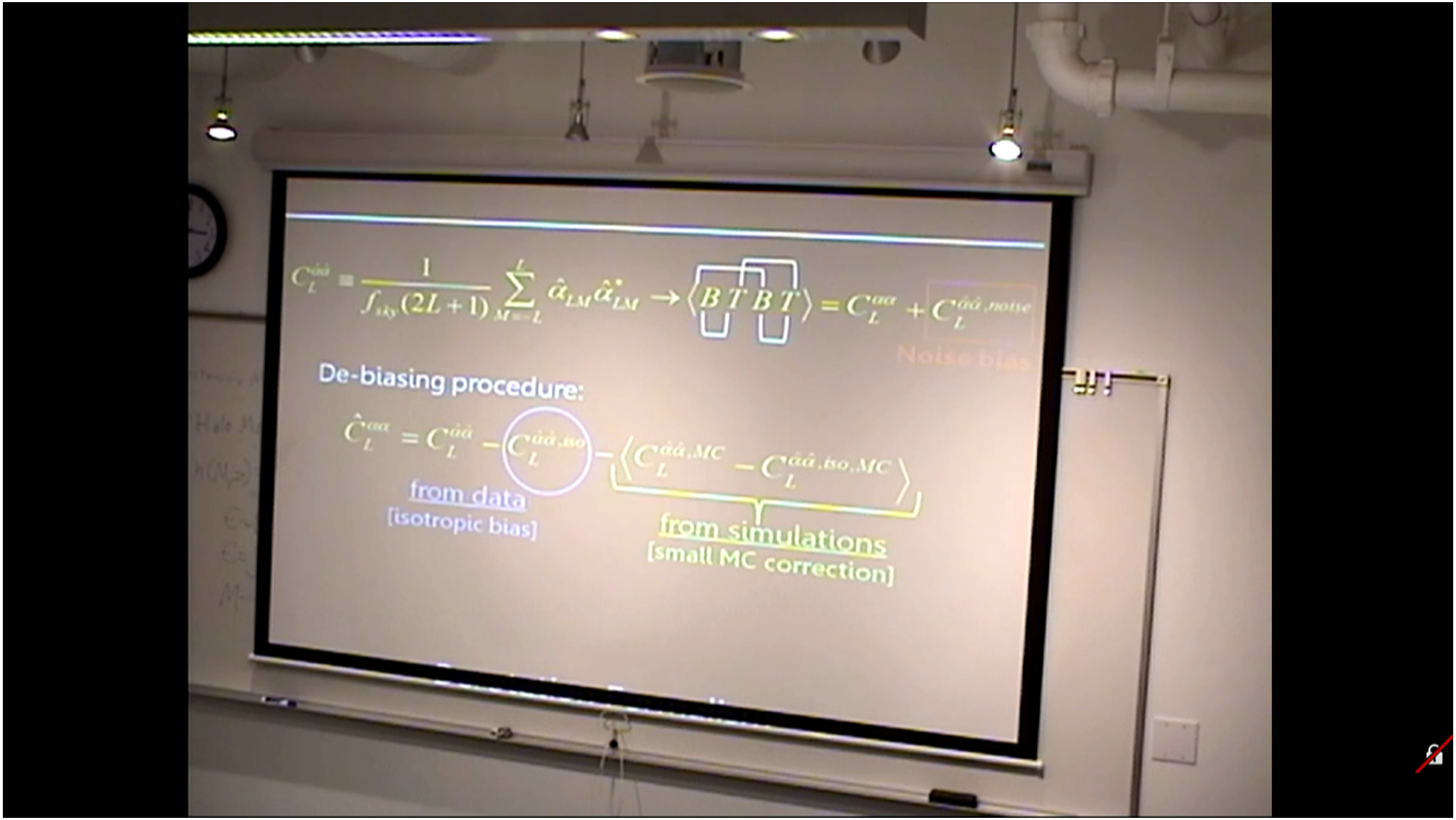
$C_L^{\hat{a}\hat{a}} \equiv \frac{1}{f_{sky}(2L+1)} \sum_{M=-L}^{L} \hat{a}_{LM} \hat{a}^*_{LM} \rightarrow \langle BTBT \rangle = C_L^{aa} + C_L^{\hat{a}\hat{a},noise}$
Noise bias
De-biasing procedure:
$\hat{C}_L^{aa} = C_L^{\hat{a}\hat{a}} - C_L^{\hat{a}\hat{a},iso} - \langle C_L^{\hat{a}\hat{a},MC} - C_L^{\hat{a}\hat{a},iso,MC} \rangle$
from data
[isotropic bias]
from simulations
[small MC correction]

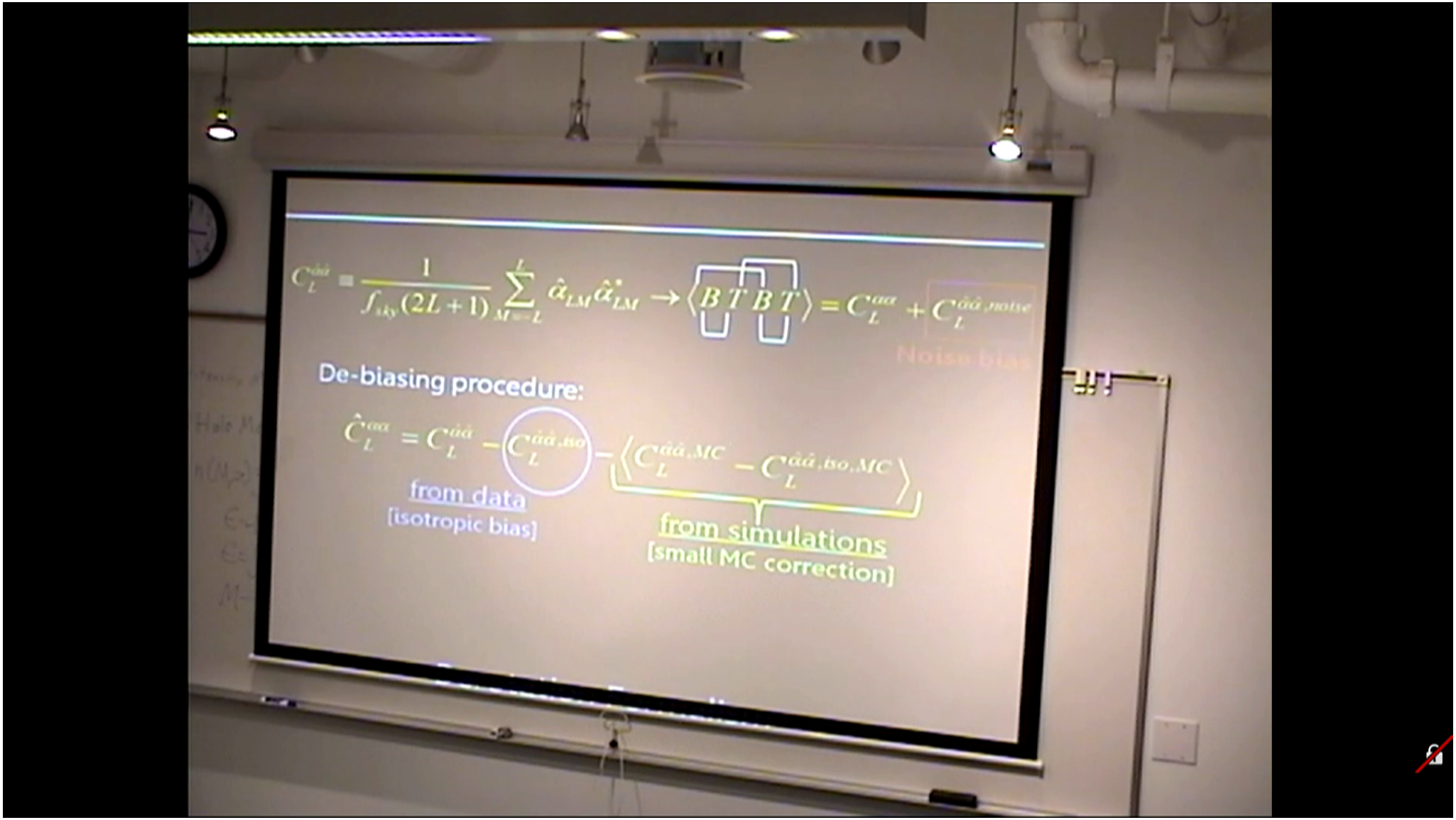
$C_L^{\hat{a}\hat{a}} = \frac{1}{f_{sky}(2L+1)} \sum_{M=-L}^{L} \hat{a}_{LM} \hat{a}^*_{LM} \rightarrow \langle BTBT \rangle = C_L^{aa} + C_L^{\hat{a}\hat{a},noise}$
Noise bias
De-biasing procedure:
$\hat{C}_L^{aa} = C_L^{\hat{a}\hat{a}} - C_L^{\hat{a}\hat{a},iso} - \langle C_L^{\hat{a}\hat{a},MC} - C_L^{\hat{a}\hat{a},iso,MC} \rangle$
from data
[isotropic bias]
from simulations
[small MC correction]

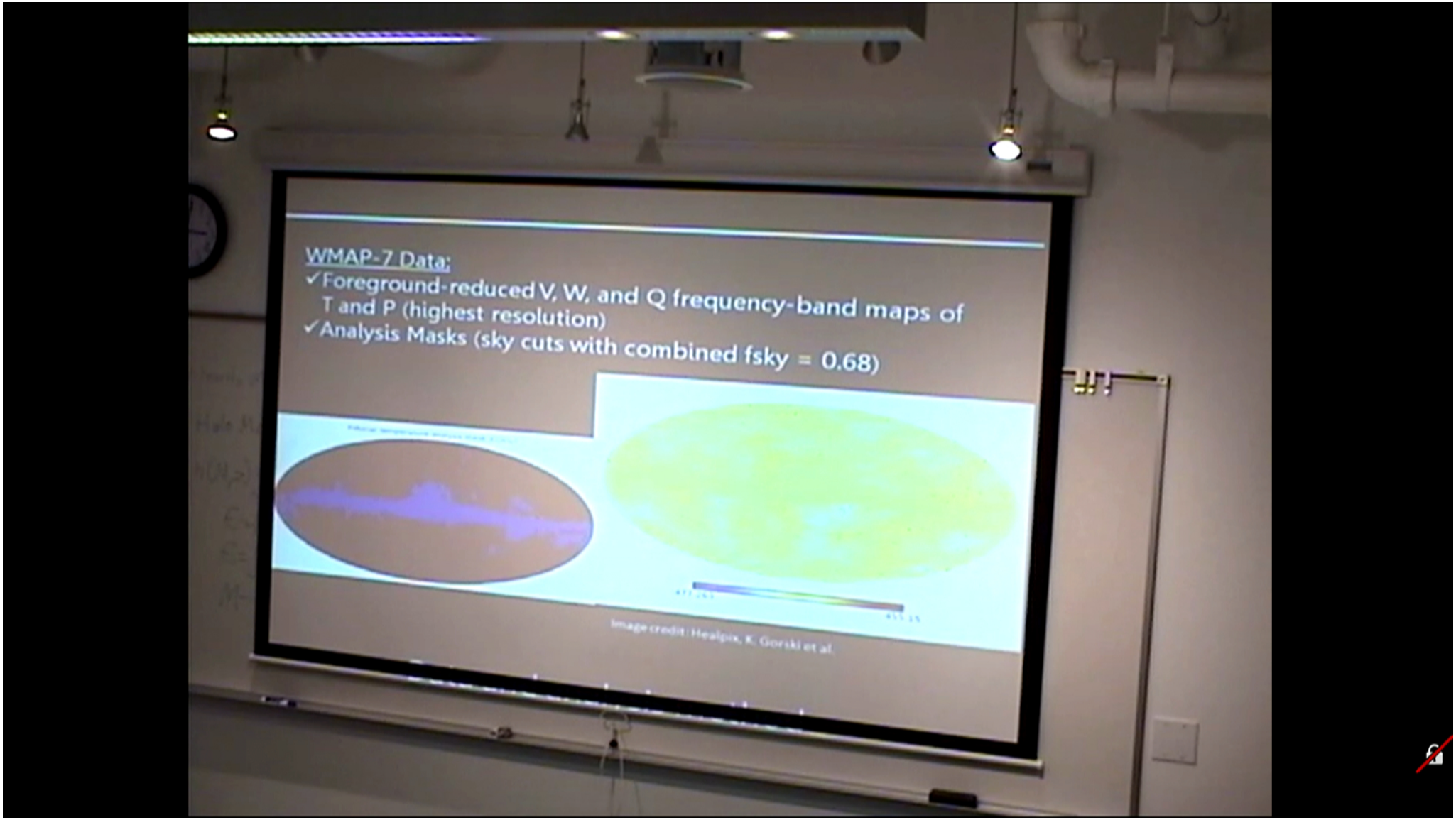
WMAP-7 Data:
✓Foreground-reduced V, W, and Q frequency-band maps of T and P (highest resolution)
✓Analysis Masks (sky cuts with combined fsky = 0.68)
Image credit: Healpix, K. Gorski et al.

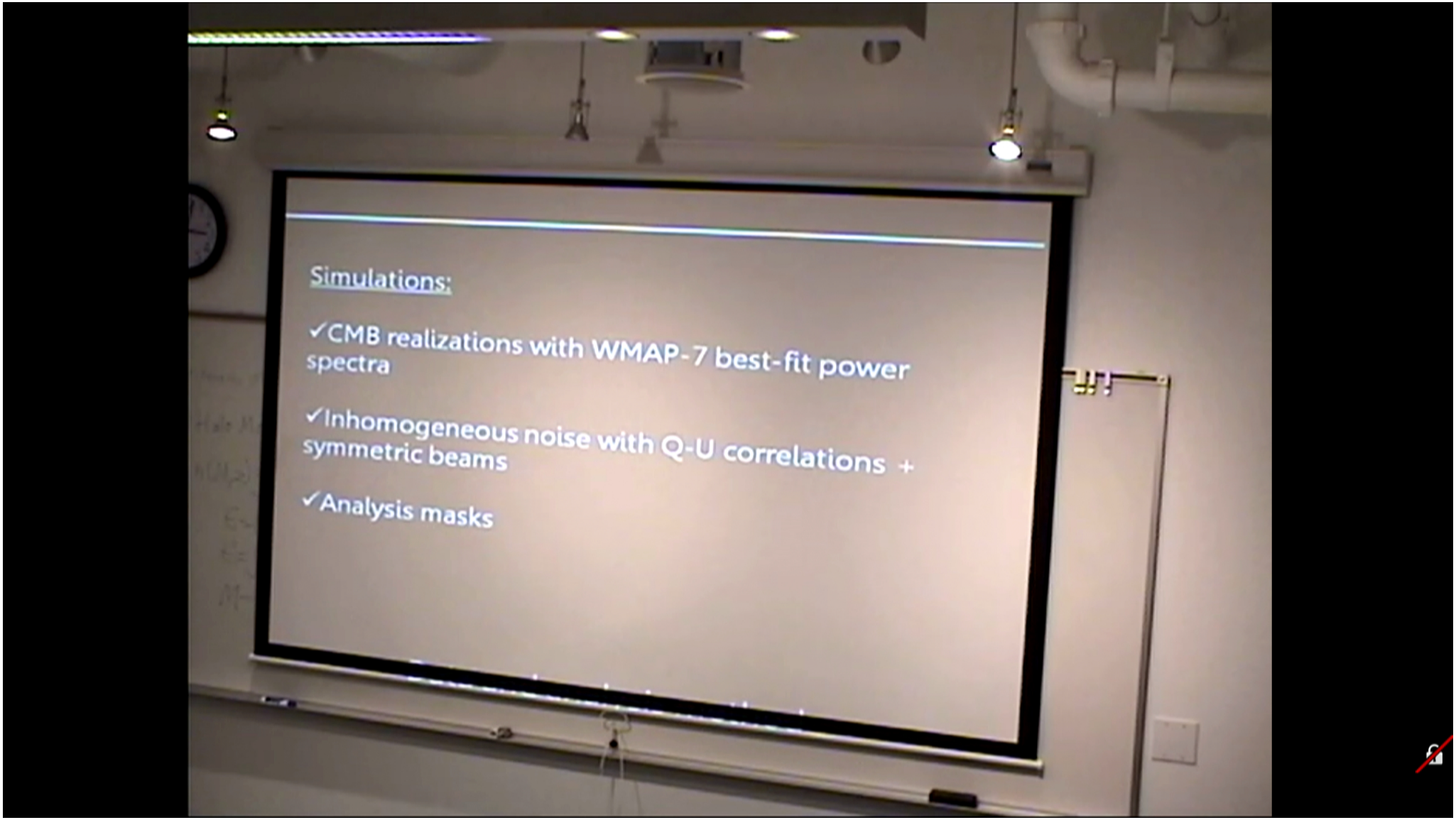
Simulations:
✓CMB realizations with WMAP-7 best-fit power spectra
✓Inhomogeneous noise with Q-U correlations + symmetric beams
✓Analysis masks

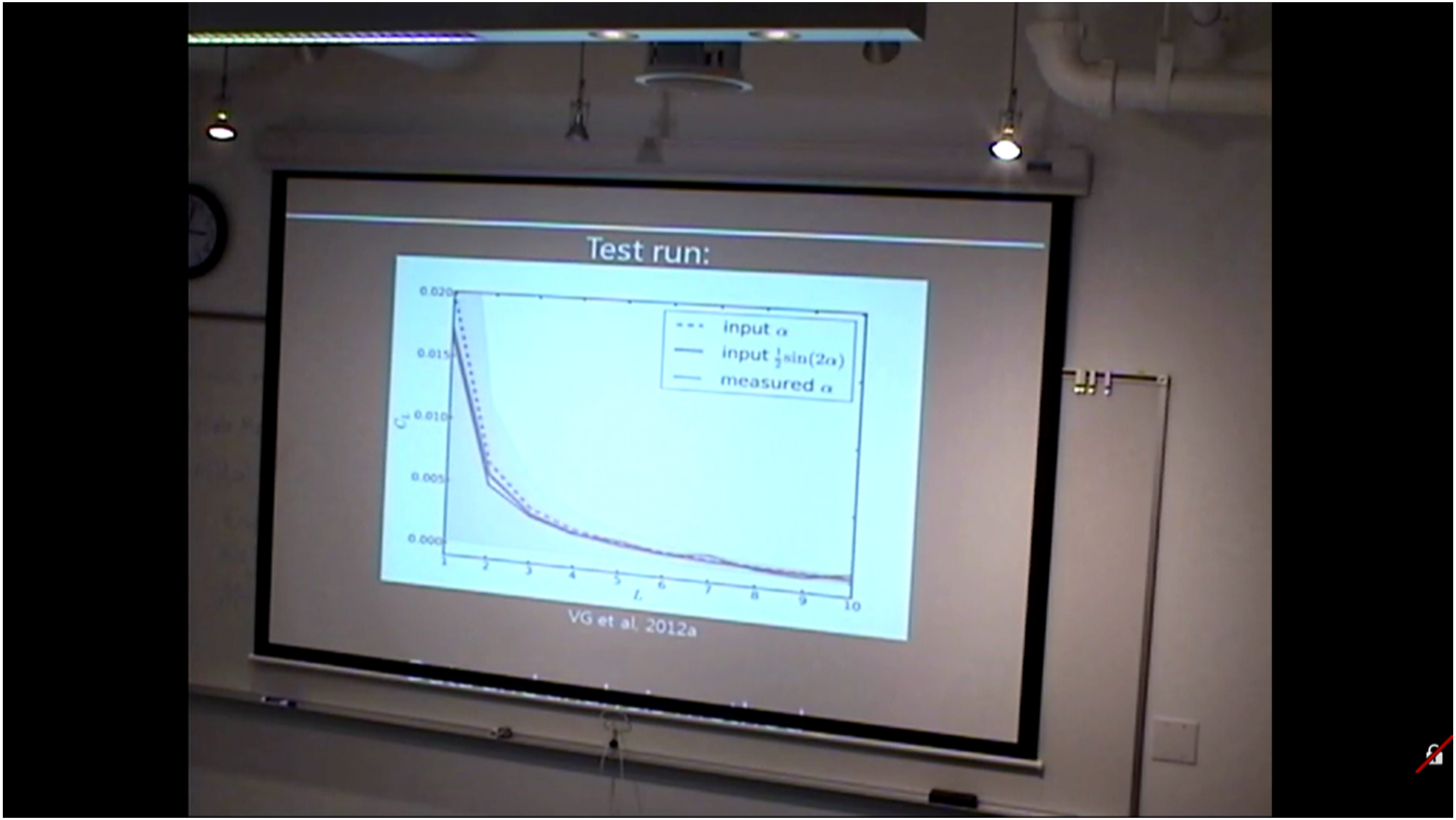
Test run:
input α
input $\frac{1}{2}\sin(2\alpha)$
measured α
C_L
L
VG et al. 2012a

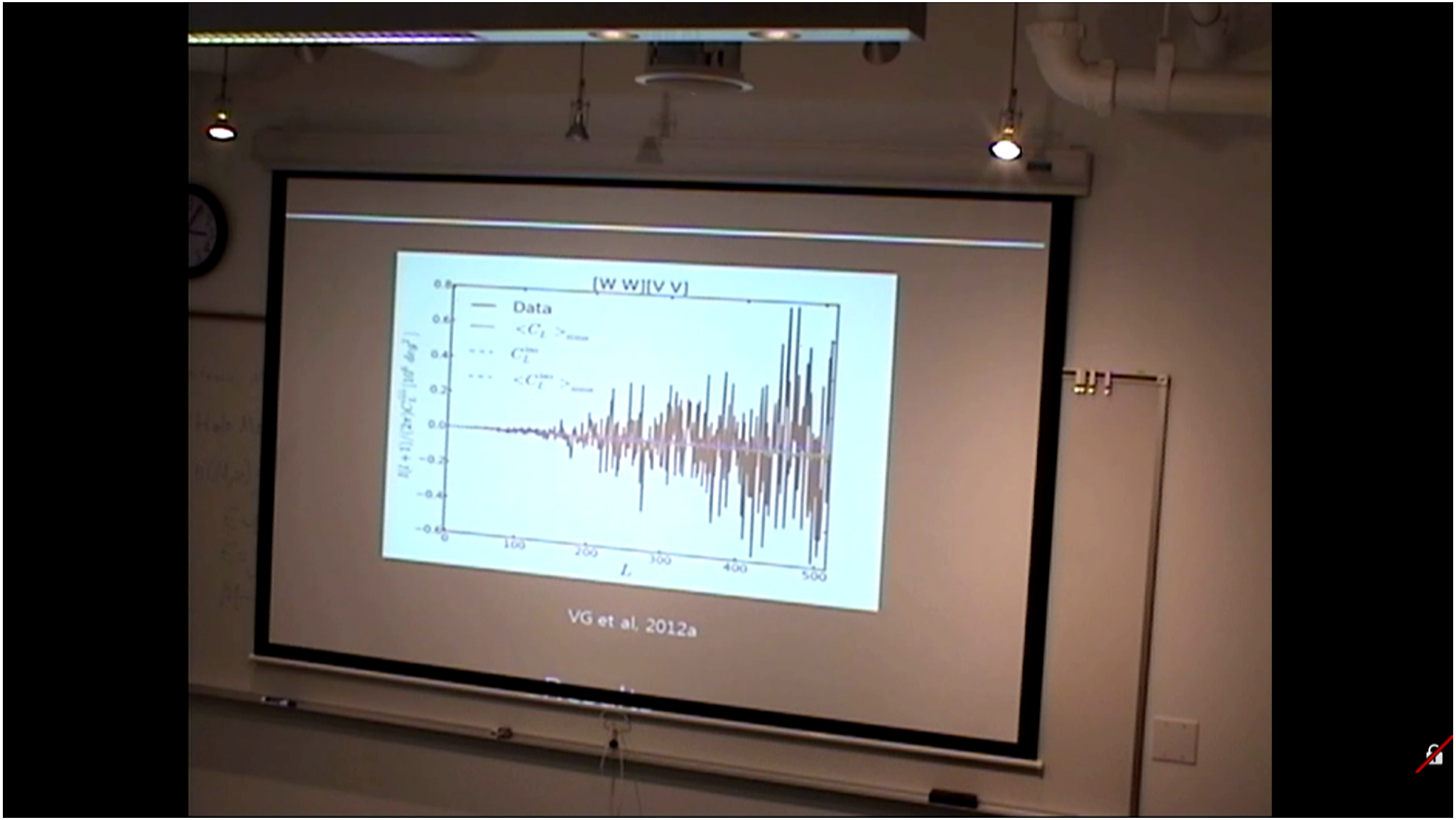
[W W][V V]
Data
VG et al. 2012a

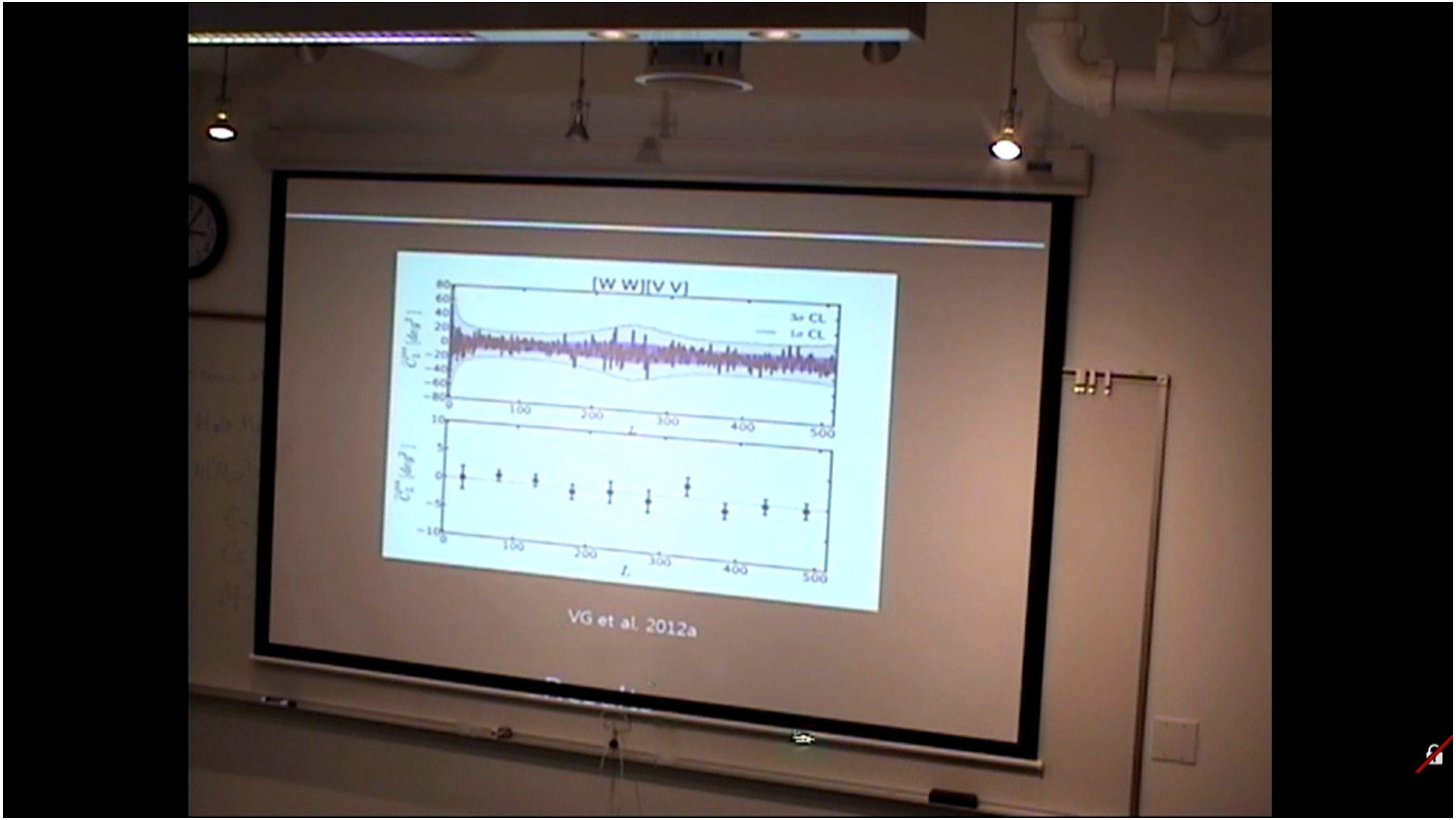
(W W)(V V)
3σ CL
1σ CL
VG et al. 2012a

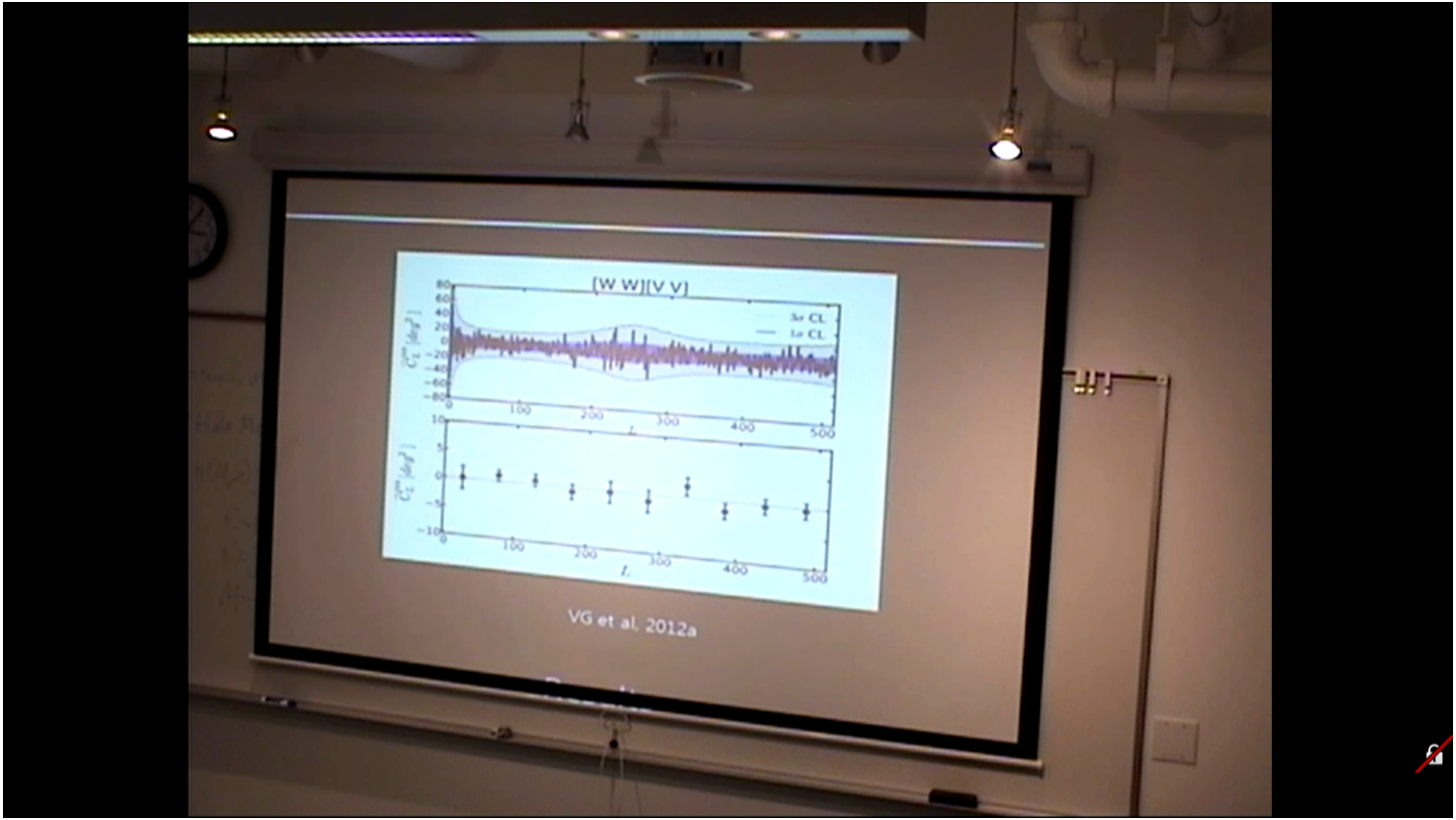
(W W)(V V)
3σ CL
1σ CL
VG et al. 2012a

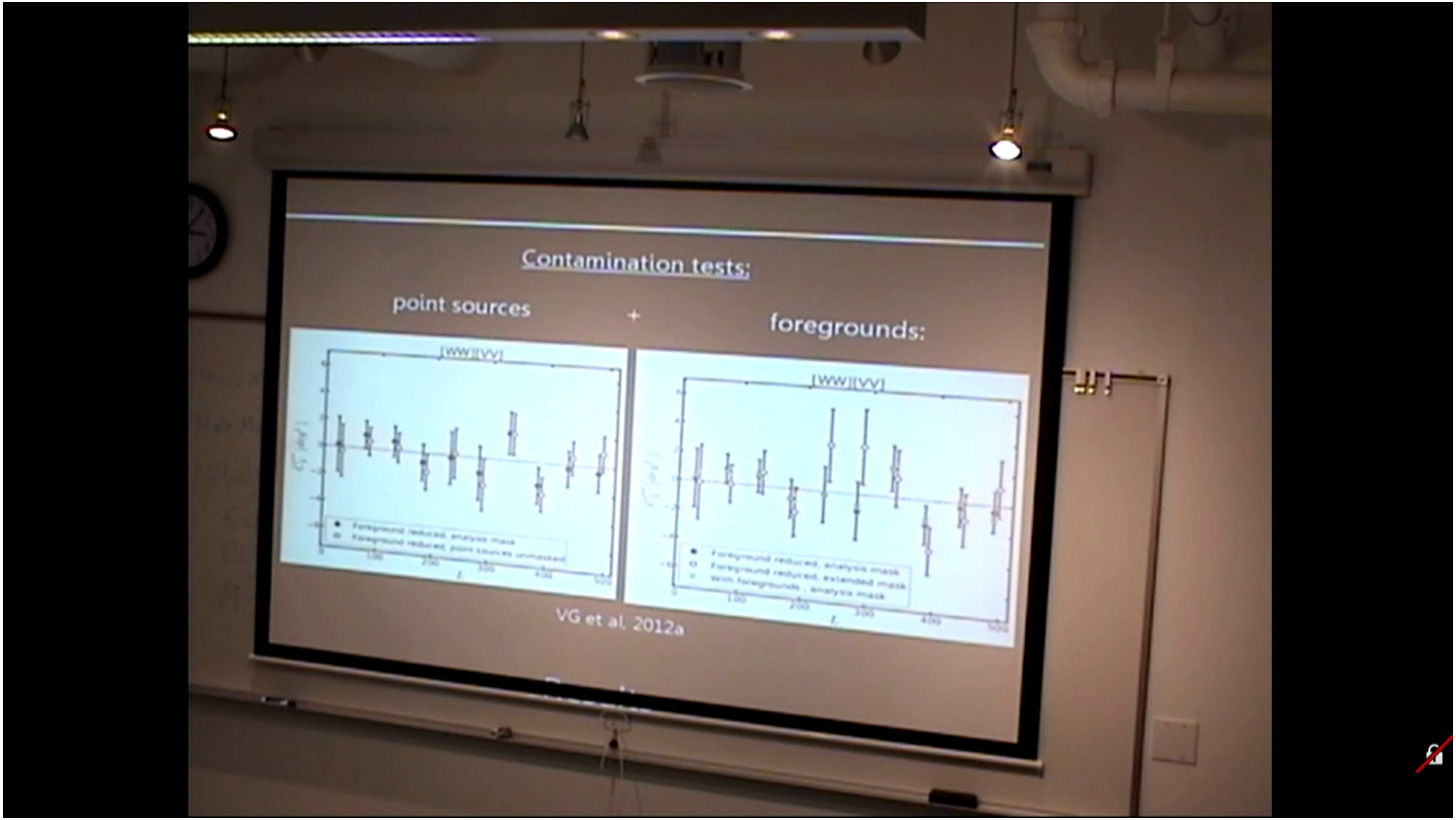
Contamination tests:
point sources
+
foregrounds:
[WW][VV]
Foreground reduced, analysis mask
Foreground reduced, point sources unmasked
[WW][VV]
Foreground reduced, analysis mask
Foreground reduced, extended mask
With foregrounds , analysis mask
VG et al. 2012a

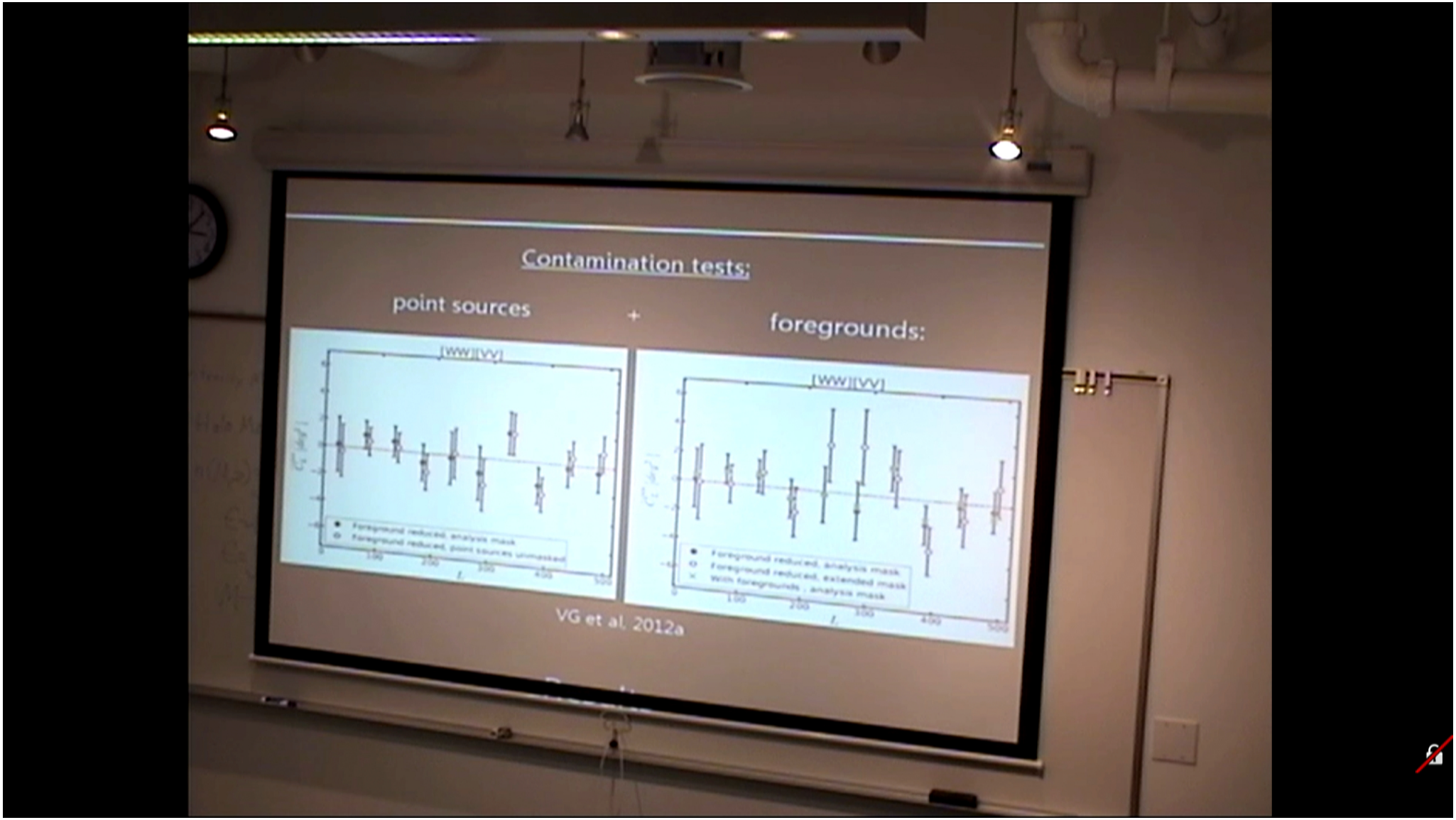
Contamination tests:
point sources
+
foregrounds:
[WW][VV]
[WW][VV]
VG et al. 2012a

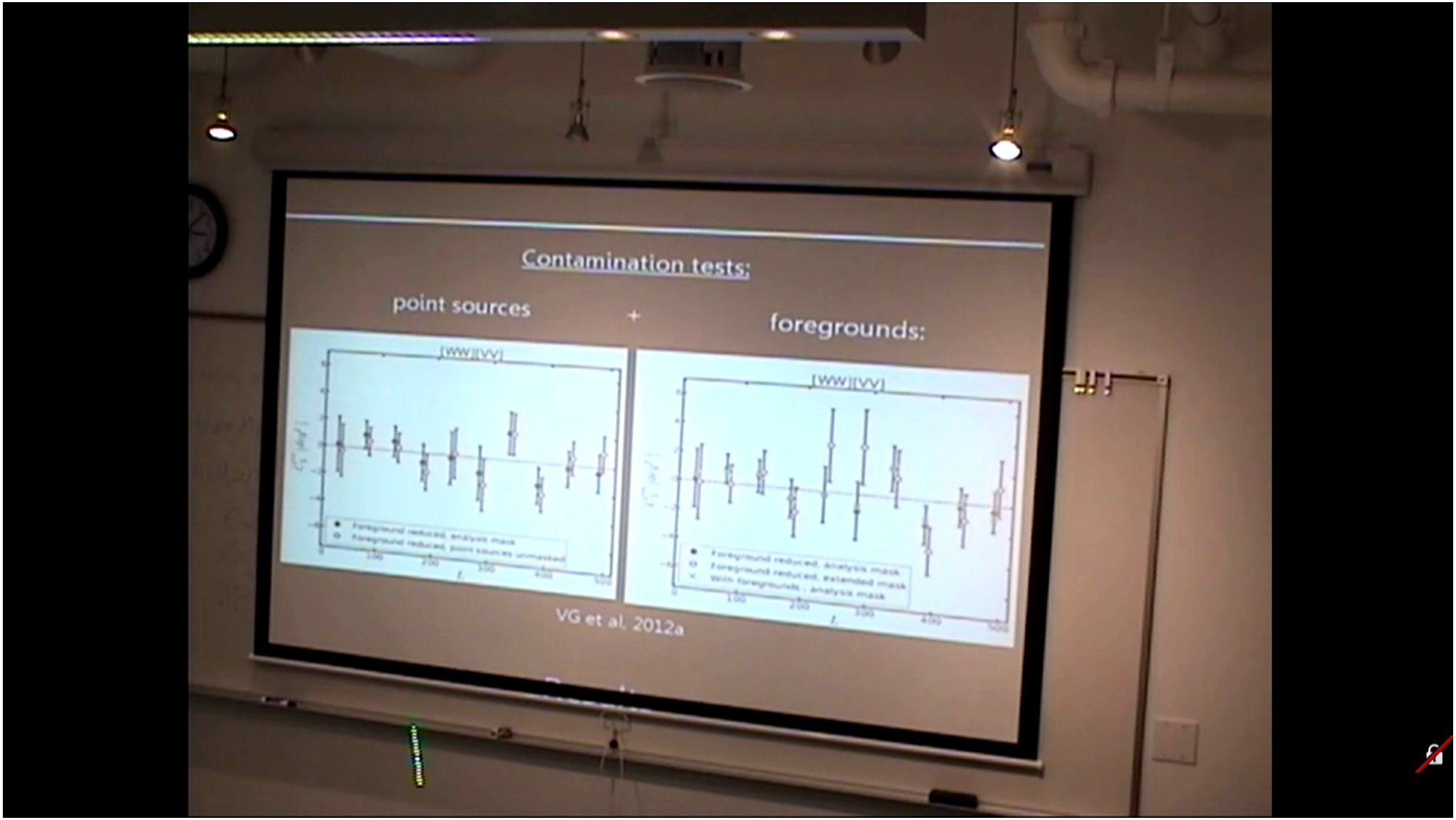
Contamination tests:
point sources
+
foregrounds:
[WW][VV]
[WW][VV]
VG et al. 2012a

Constraints on a scale-invariant power spectrum:

$$C_L^{aa,\,fiducial} = \frac{A}{L(L+1)}$$

Minimum-variance estimator for the amplitude A:

$$\sqrt{C_2^{aa}/(4\pi)} < 1^\circ$$

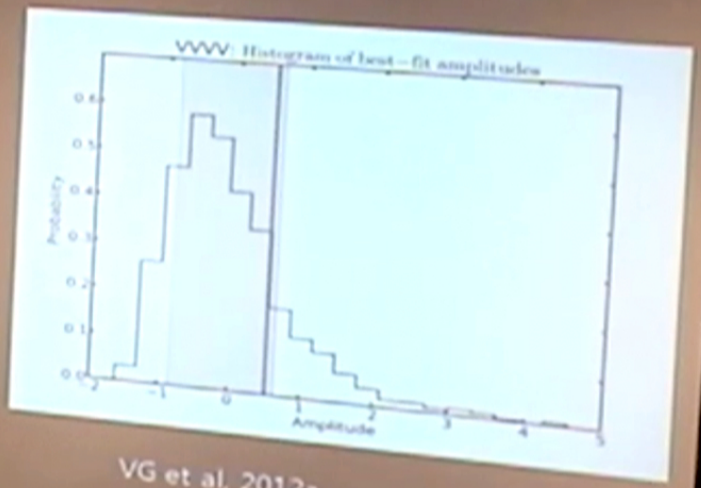

VG et al. 2012a

Constraints on a scale-invariant power spectrum:

$$C_L^{aa\ fiducial} = \frac{A}{L(L+1)}$$

Minimum-variance estimator for the amplitude A:

$$\sqrt{C_2^{aa}/(4\pi)} < 1^\circ$$

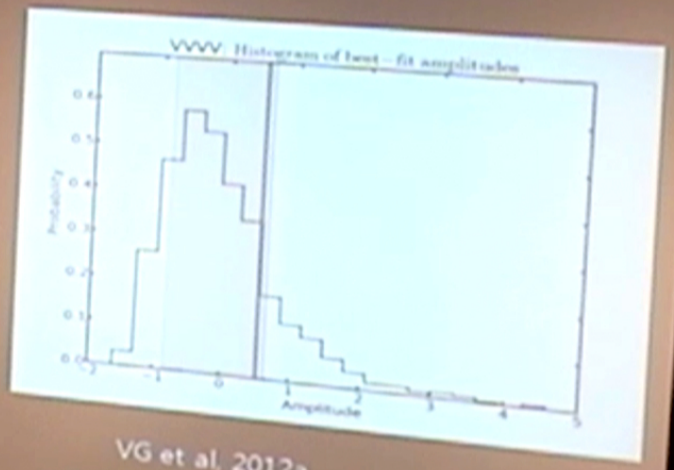

VG et al, 2012a

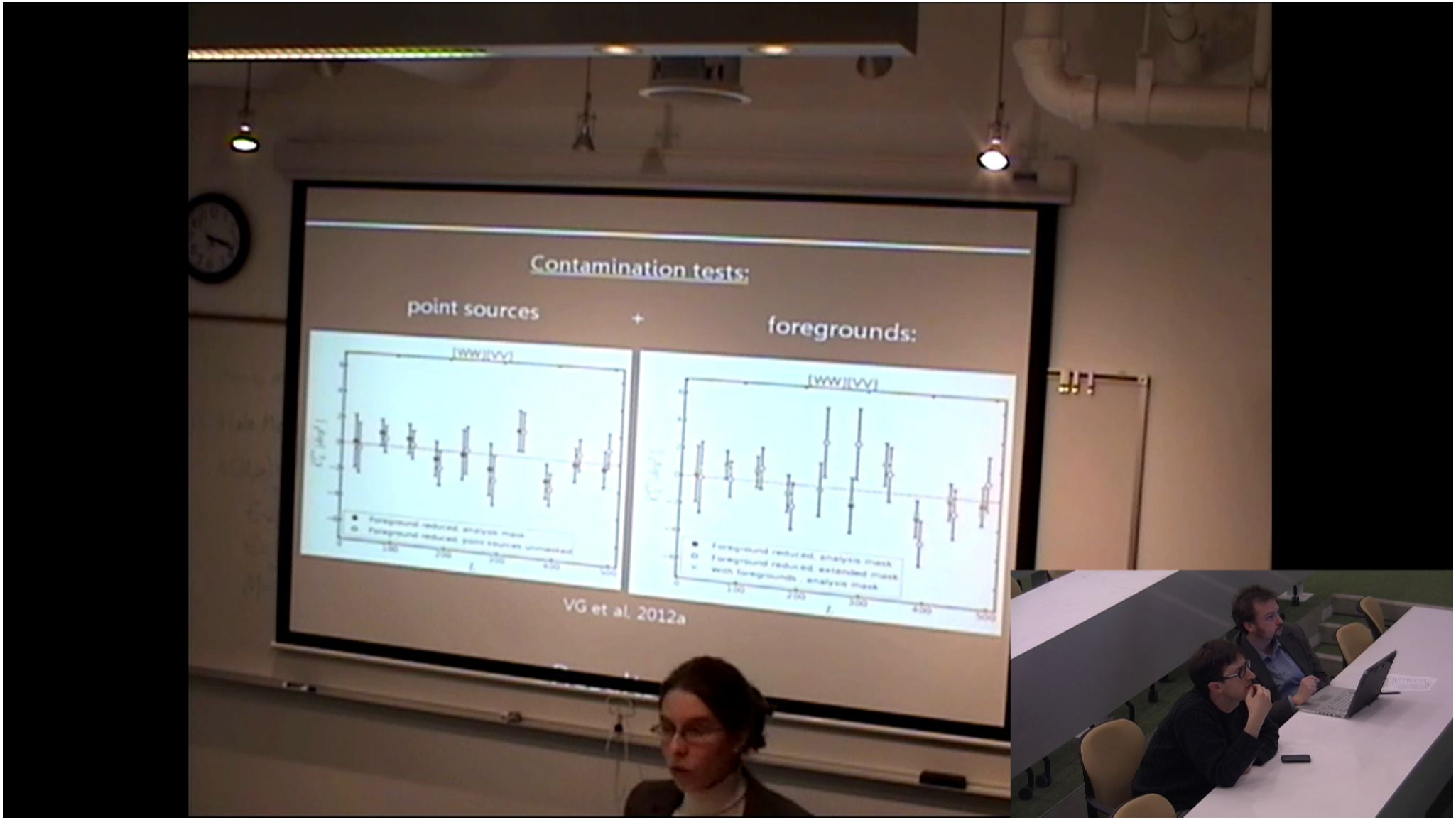
Contamination tests:
point sources
+
foregrounds:
[WW][VV]
[WW][VV]
VG et al. 2012a

Constraints on a scale-invariant power spectrum:

$$C_L^{\alpha\alpha,\,fiducial} = \frac{A}{L(L+1)}$$

Minimum-variance estimator for the amplitude A:

$$\sqrt{C_2^{\alpha\alpha}/(4\pi)} < 1^\circ$$

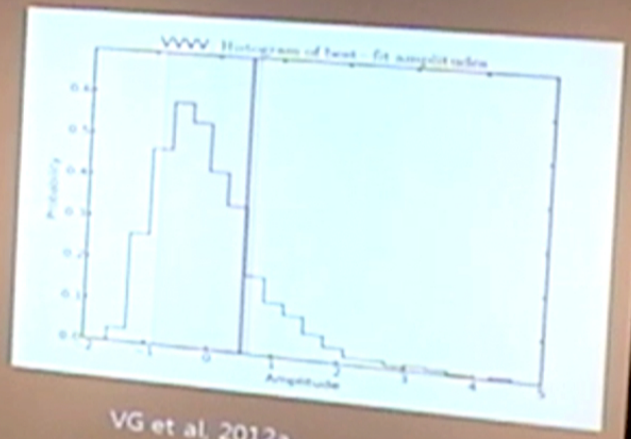

VG et al. 2012a

Constraints on a scale-invariant power spectrum:

$$C_L^{\alpha\alpha,\,fiducial} = \frac{A}{L(L+1)}$$

Minimum-variance estimator for the amplitude A:

$$\sqrt{C_2^{\alpha\alpha}/(4\pi)} < 1^\circ$$

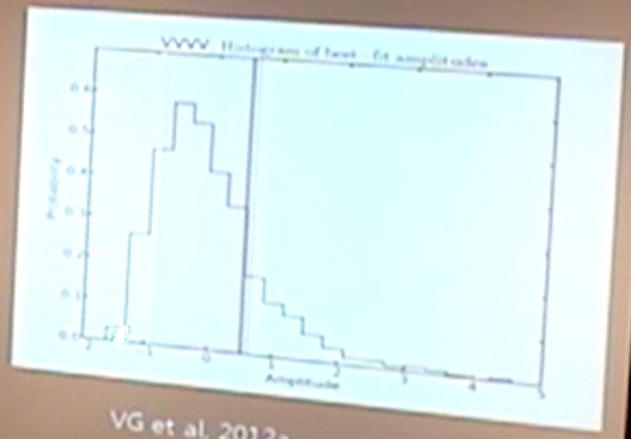

VG et al. 2012a

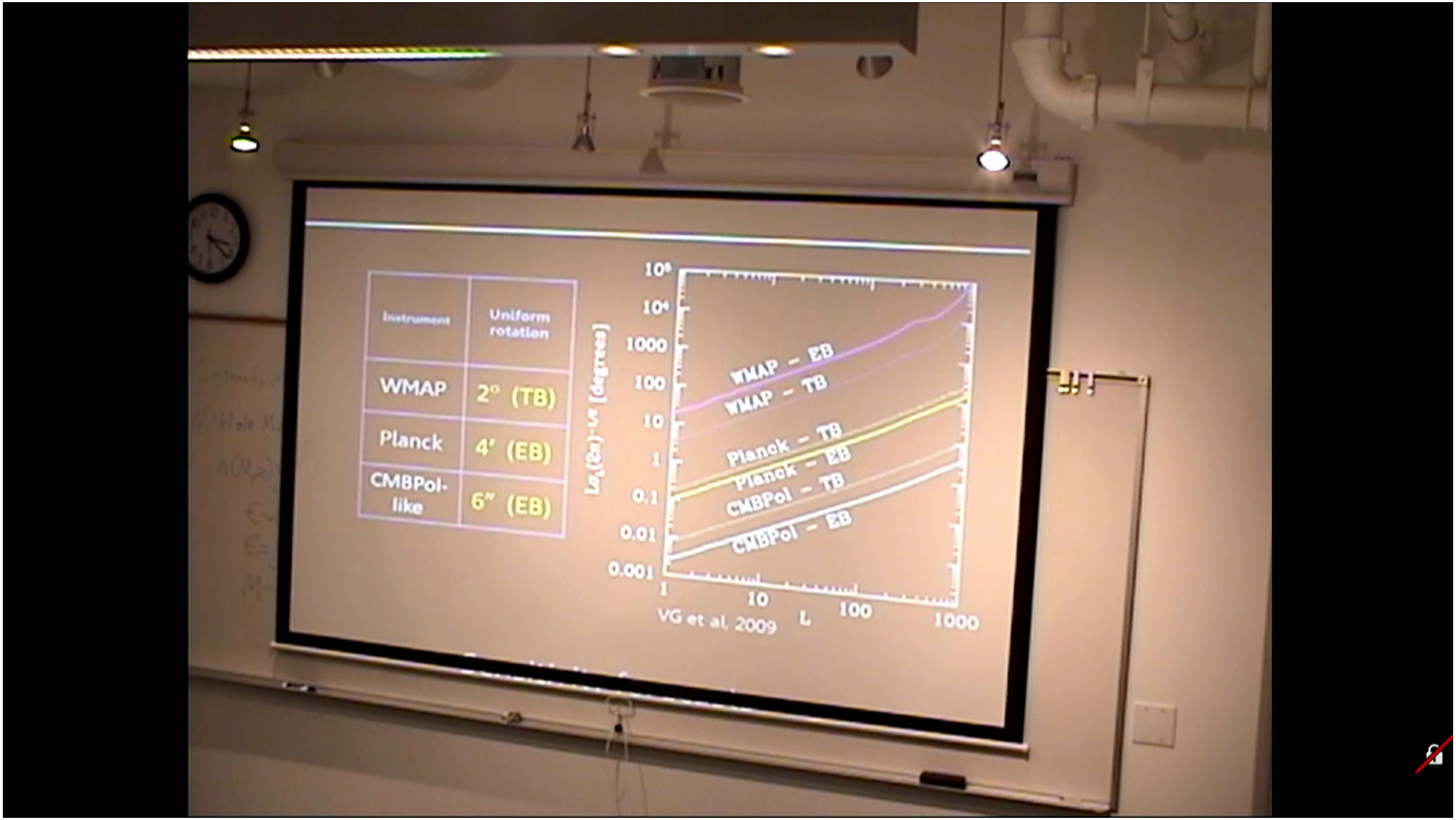
Instrument
Uniform rotation
WMAP
2° (TB)
Planck
4′ (EB)
CMBPol-like
6″ (EB)
WMAP – EB
WMAP – TB
Planck – TB
Planck – EB
CMBPol – TB
CMBPol – EB
VG et al. 2009
L

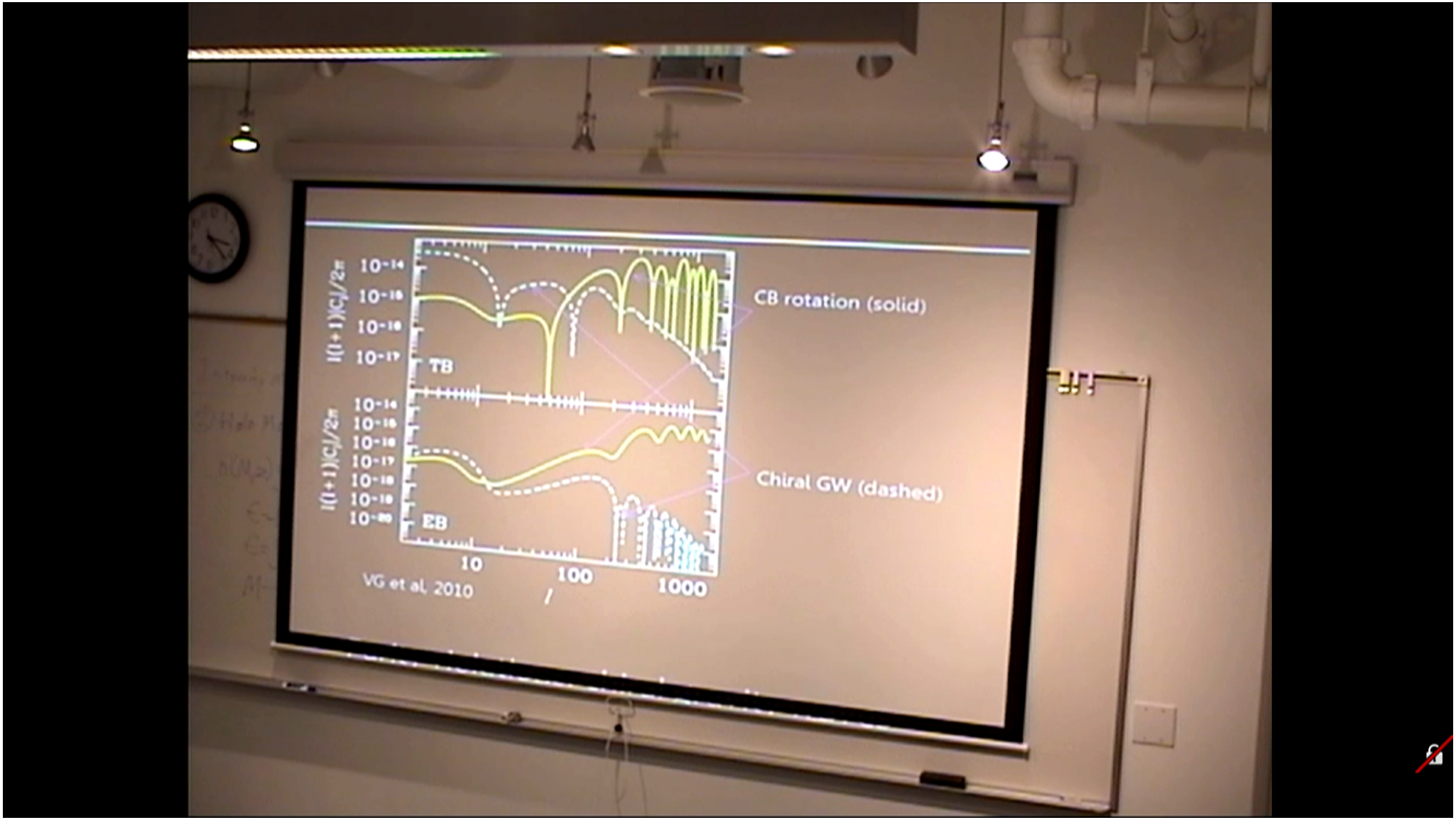
CB rotation (solid)
Chiral GW (dashed)
TB
EB
VG et al. 2010
10
100
1000
l

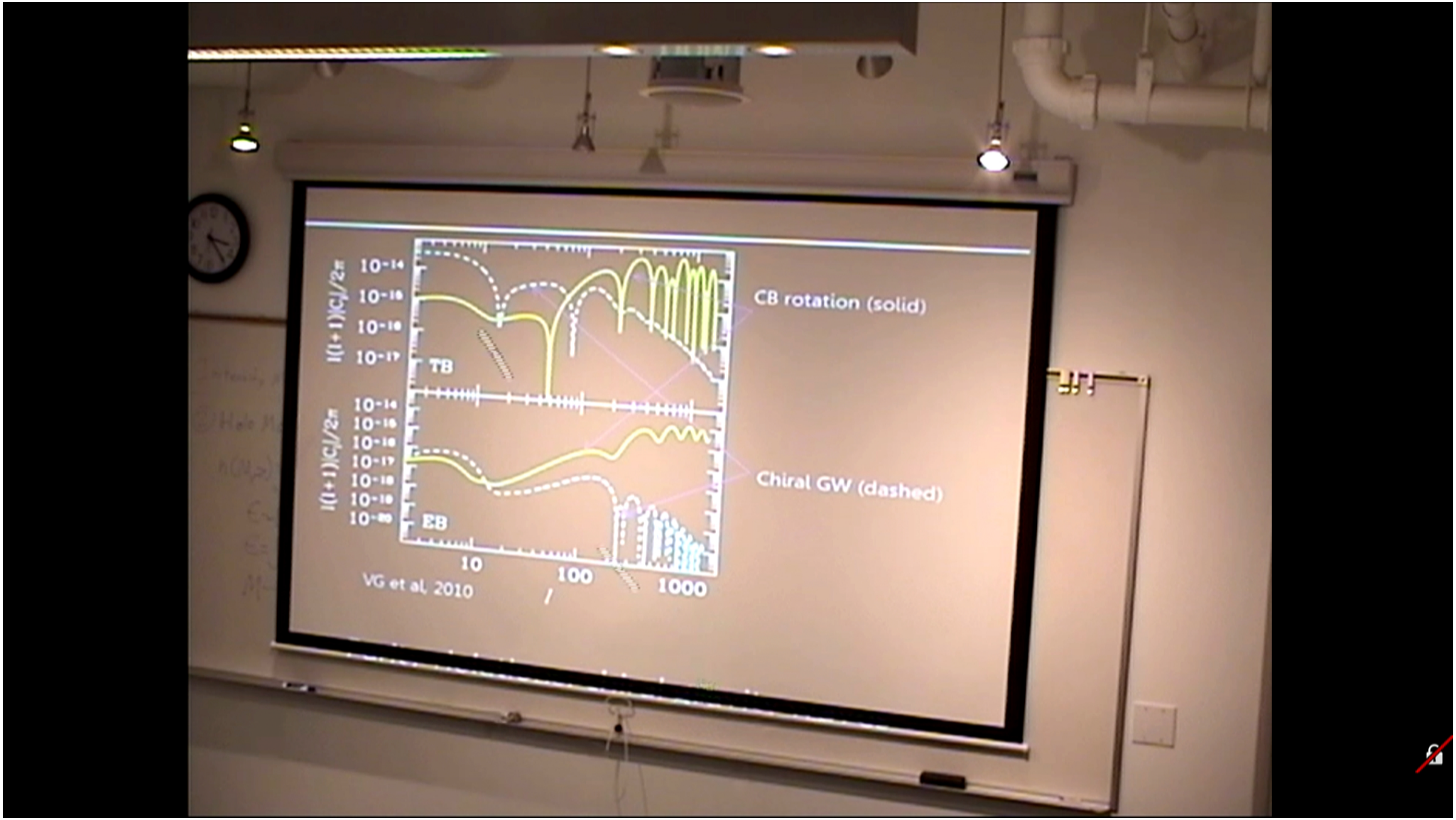
CB rotation (solid)
Chiral GW (dashed)
TB
EB
VG et al, 2010
10
100
1000
l

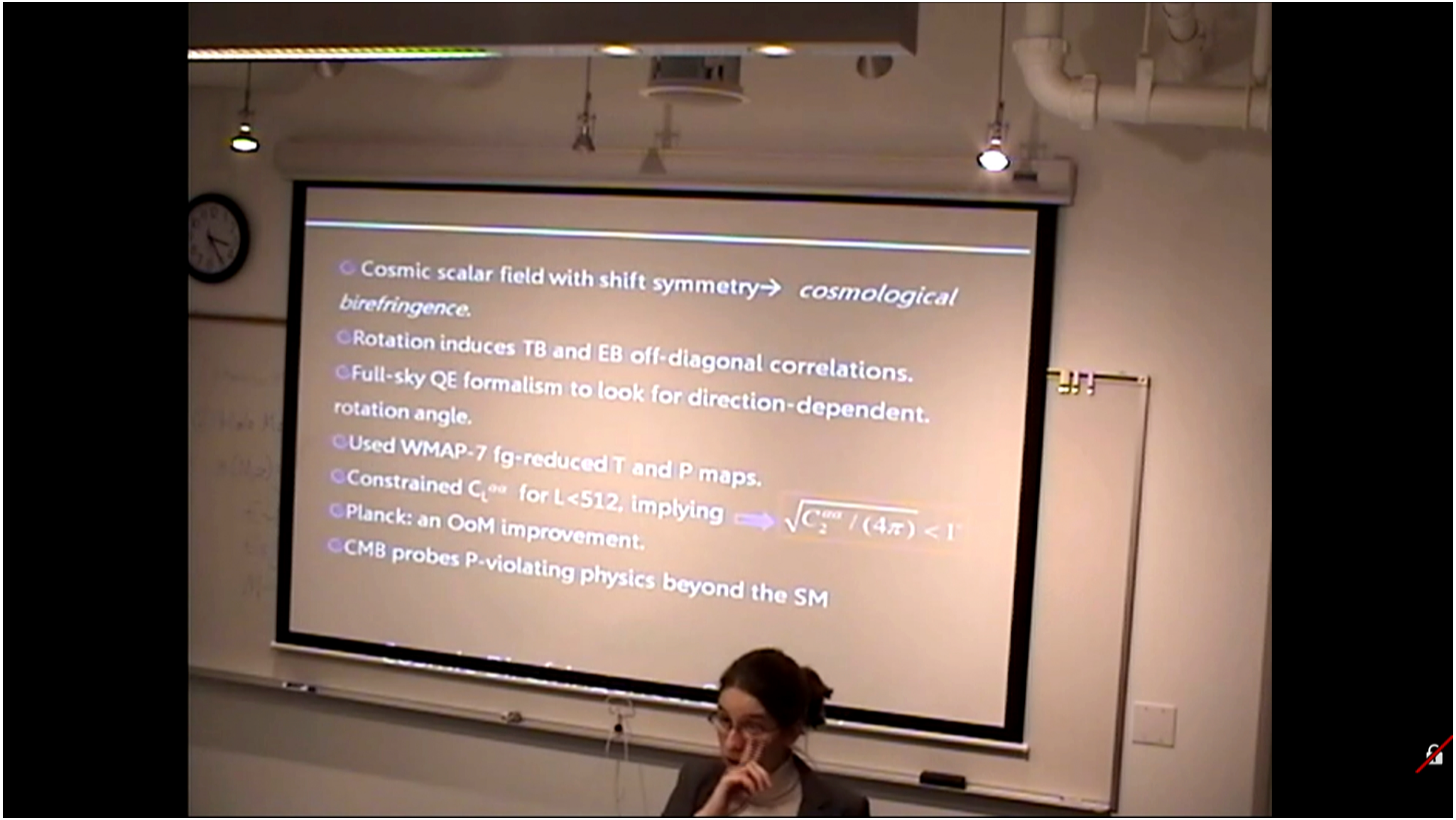
Cosmic scalar field with shift symmetry→ cosmological birefringence.
Rotation induces TB and EB off-diagonal correlations.
Full-sky QE formalism to look for direction-dependent rotation angle.
Used WMAP-7 fg-reduced T and P maps.
Constrained $C_L^{\alpha\alpha}$ for L<512, implying $\sqrt{C_2^{\alpha\alpha}/(4\pi)} < 1^\circ$
Planck: an OoM improvement.
CMB probes P-violating physics beyond the SM


Appendix:
Cosmic Reionization

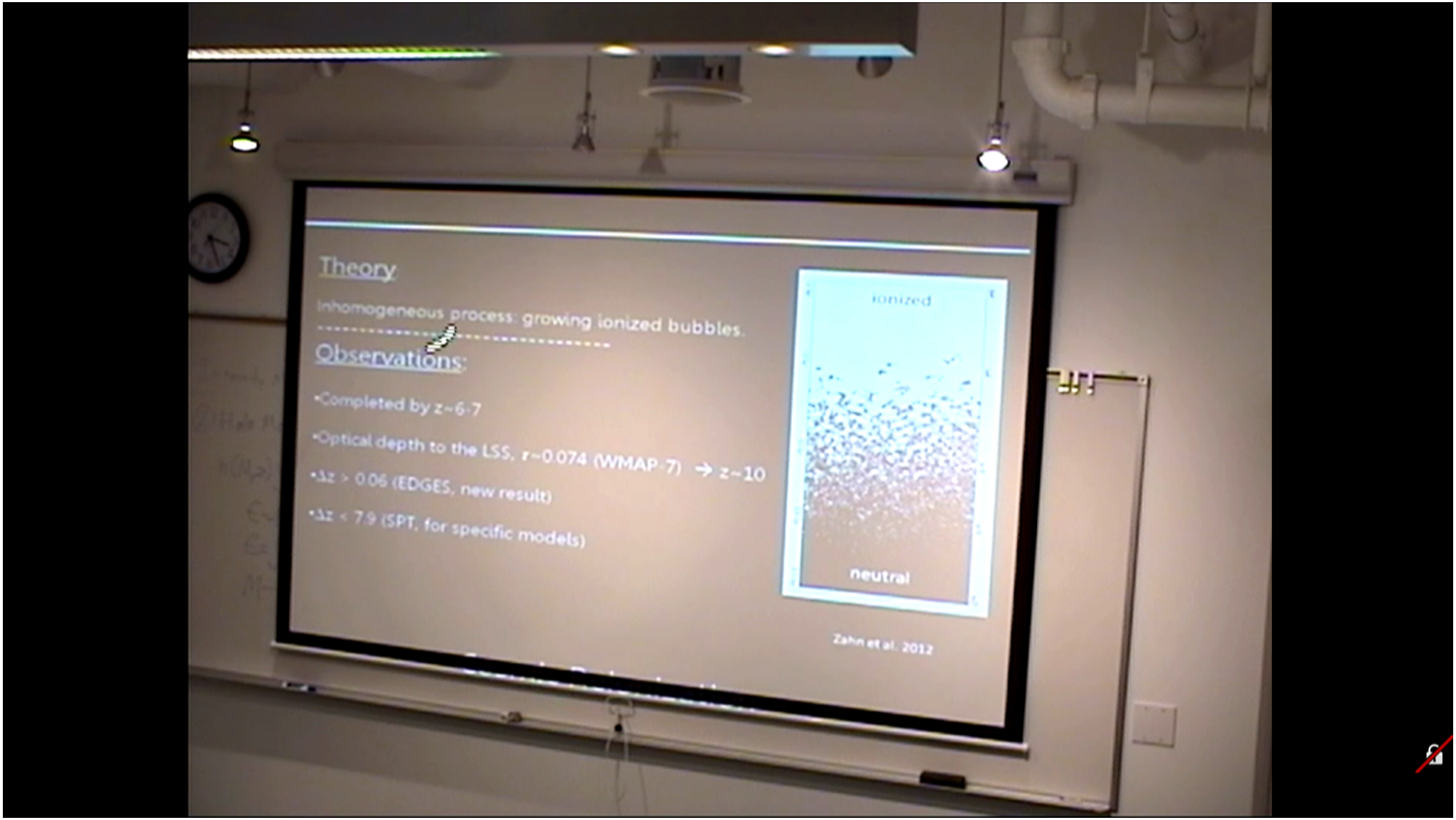
Theory
Inhomogeneous process: growing ionized bubbles.
Observations:
•Completed by z~6-7
•Optical depth to the LSS, τ~0.074 (WMAP-7) → z~10
•Δz > 0.06 (EDGES, new result)
•Δz < 7.9 (SPT, for specific models)
ionized
neutral
Zahn et al. 2012

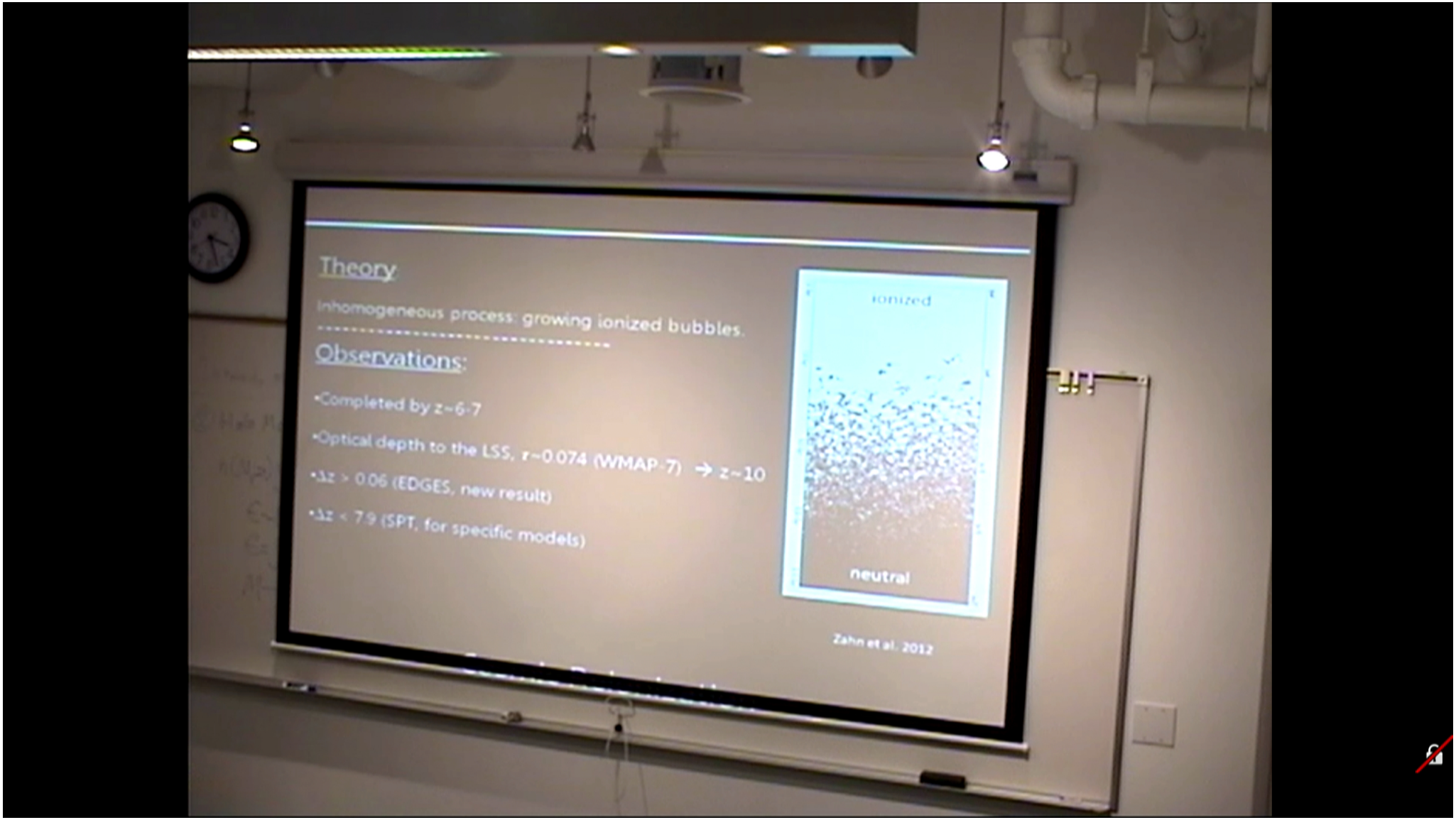
Theory
Inhomogeneous process: growing ionized bubbles.
Observations:
•Completed by z~6-7
•Optical depth to the LSS, τ~0.074 (WMAP-7) → z~10
•Δz > 0.06 (EDGES, new result)
•Δz < 7.9 (SPT, for specific models)
ionized
neutral
Zahn et al. 2012

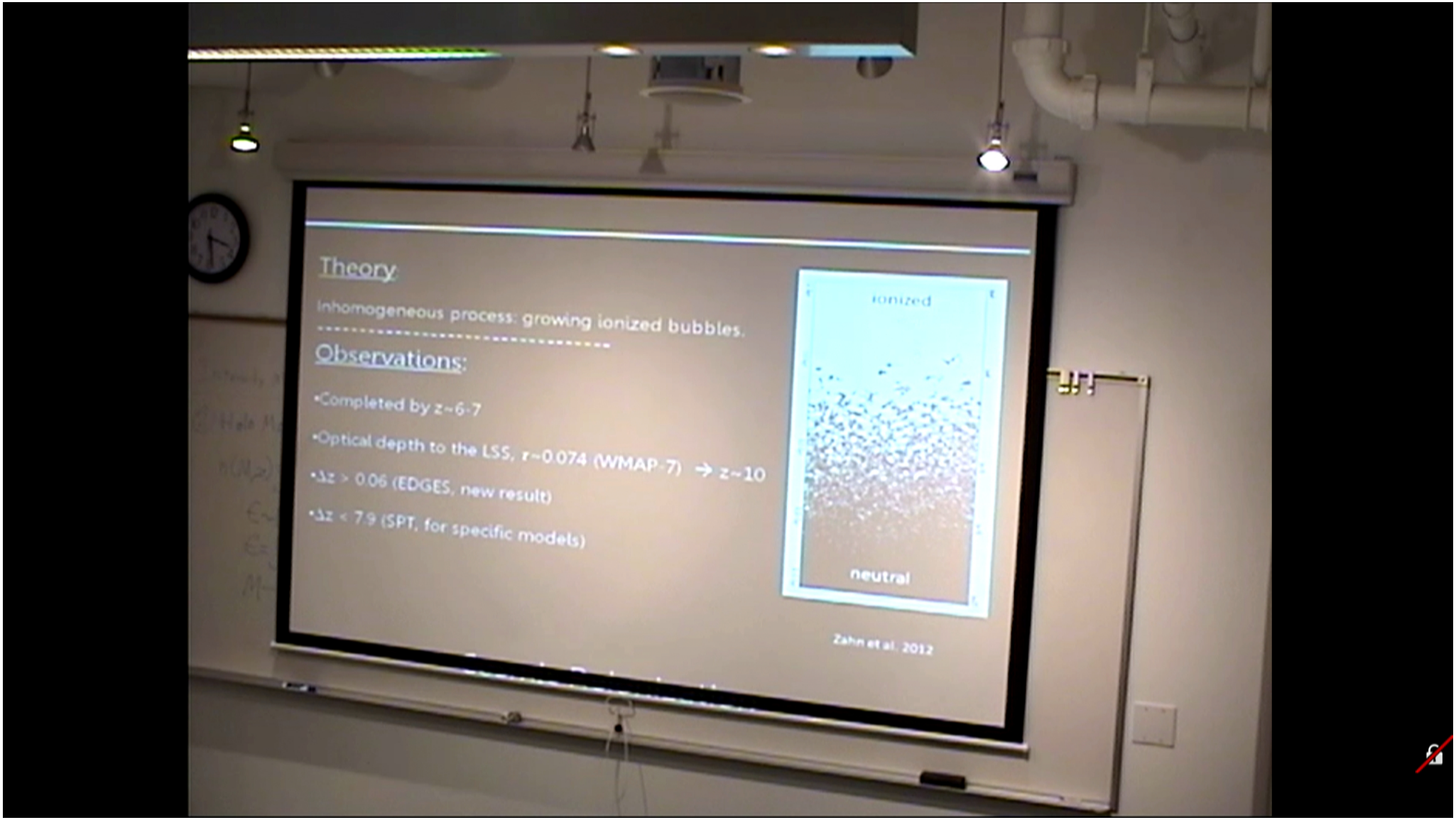
Theory:
Inhomogeneous process: growing ionized bubbles.
Observations:
•Completed by z~6-7
•Optical depth to the LSS, τ~0.074 (WMAP-7) → z~10
•Δz > 0.06 (EDGES, new result)
•Δz < 7.9 (SPT, for specific models)
ionized
neutral
Zahn et al. 2012

$$\Delta T(\hat{n}) = e^{-\tau(\hat{n})}\Delta\tilde{T}(\hat{n})$$

$$p(\hat{n}) \equiv Q(\hat{n}) + iU(\hat{n}) = e^{-\tau(\hat{n})}\tilde{p}(\hat{n})$$

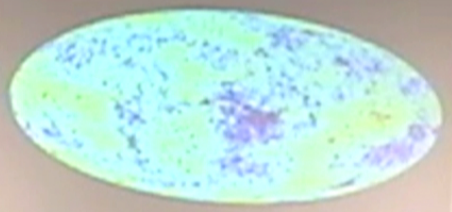

Induces off-diagonal correlations.

$$\hat{\tau}_{LM} = -iN_L \int d\hat{n} Y_{LM}(\hat{n}) \left[\sum_{lm} \bar{B}_{lm\,2} Y_{lm}(\hat{n}) \sum_{l'm'} \bar{T}_{l'm'\,2} Y^*_{l'm'}(\hat{n}) + cc \right]$$

$$l + l' + L = odd$$

Dvorkin et al. 2009; Hanson and Lewis, 2009

$$\Delta T(\hat{n}) = e^{-\tau(\hat{n})}\Delta\tilde{T}(\hat{n})$$

$$p(\hat{n}) \equiv Q(\hat{n}) + iU(\hat{n}) = e^{-\tau(\hat{n})}\tilde{p}(\hat{n})$$

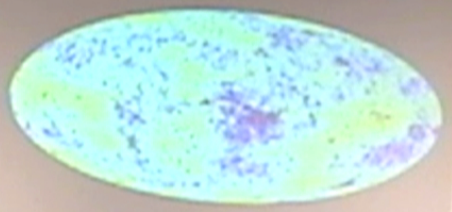

Induces off-diagonal correlations.

$$\hat{\tau}_{LM} = -iN_L \int d\hat{n} Y_{LM}(\hat{n}) \left[\sum_{lm} \bar{B}_{lm\,2} Y_{lm}(\hat{n}) \sum_{l'm'} \bar{T}_{l'm'\,2} Y^*_{l'm'}(\hat{n}) + cc \right]$$

$$l + l' = odd$$

Dvorkin et al. 2009; Hanson and Lewis, 2009

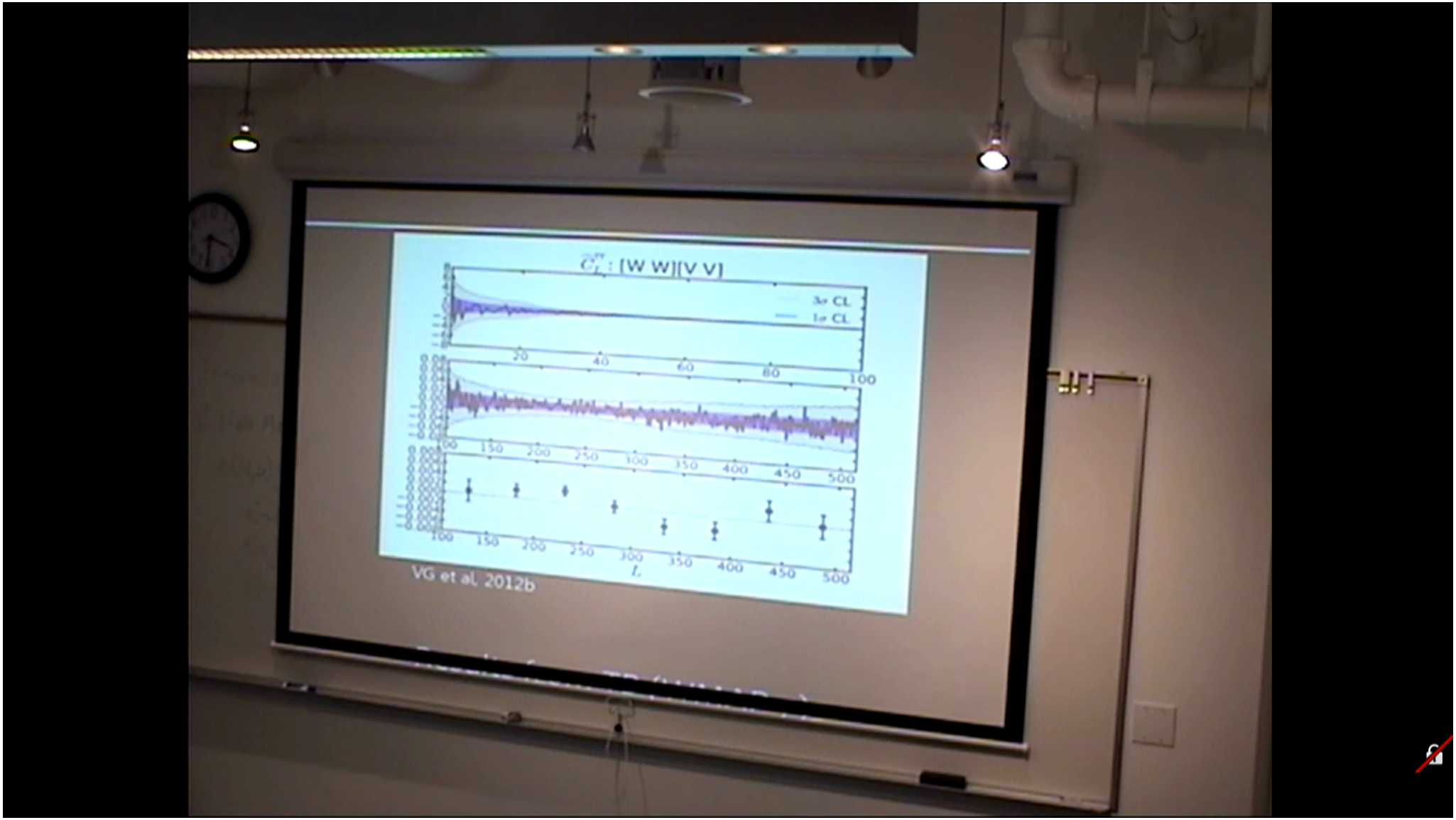
C_L^{TT} : [W W][V V]
3σ CL
1σ CL
20
40
60
80
100
100
150
200
250
300
350
400
450
500
L
VG et al. 2012b

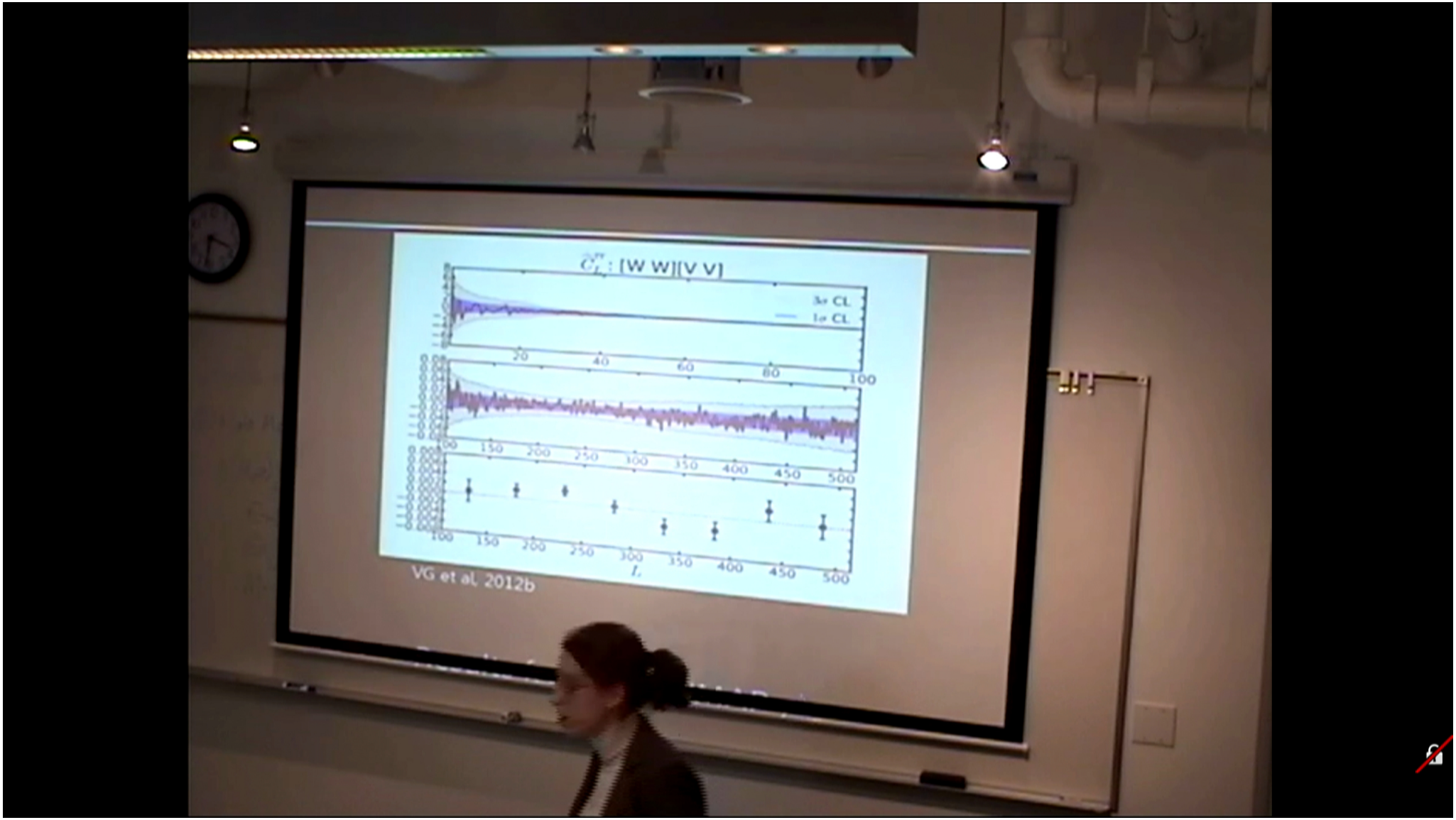
C_L^{TT} : [W W][V V]
3σ CL
1σ CL
20
40
60
80
100
100
150
200
250
300
350
400
450
500
100
150
200
250
300
350
400
450
500
l_c
VG et al. 2012b

Assume:
white noise power with rms $\Delta\tau$ below coherence scale $\theta_c \sim \pi/\Lambda_c$, smoothed on larger scales.

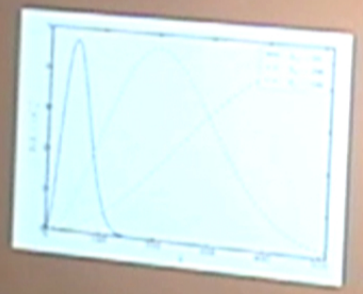

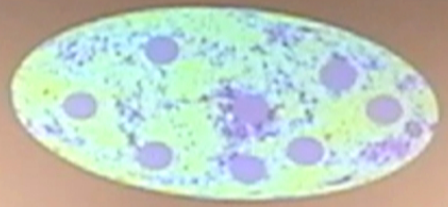

$$C_L^{\tau\tau} = \frac{4\pi}{L_c^2}(\Delta\tau)^2 e^{-L^2/L_c^2}$$

VG et al. 2012b

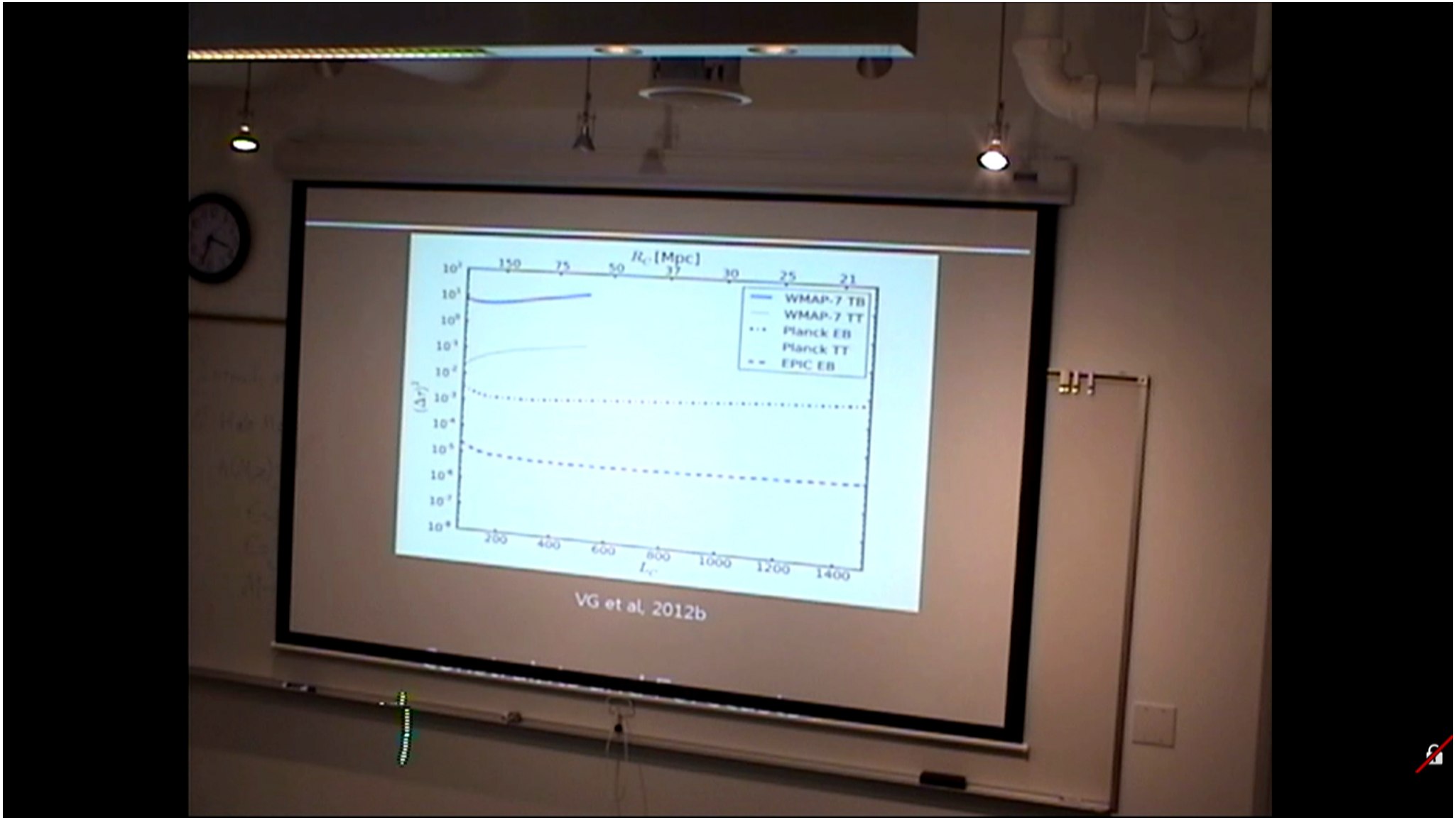
R_C [Mpc]
150
75
50
37
30
25
21
WMAP-7 TB
WMAP-7 TT
Planck EB
Planck TT
EPIC EB
$(\Delta\gamma)^2$
200
400
600
800
1000
1200
1400
l_{vc}
VG et al, 2012b

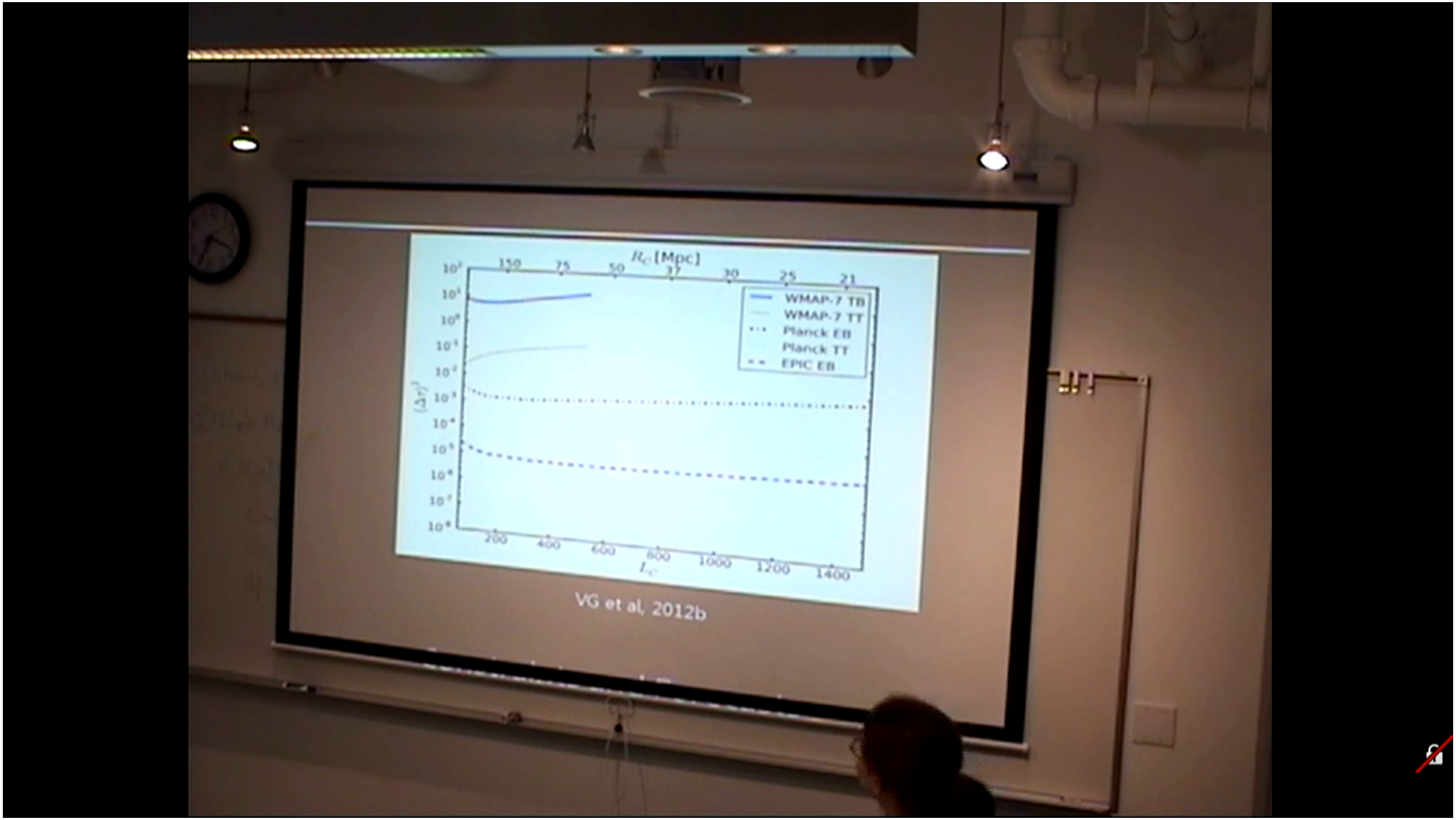
R_C [Mpc]
150
75
50
37
30
25
21
WMAP-7 TB
WMAP-7 TT
Planck EB
Planck TT
EPIC EB
$(\Delta\gamma)^2$
200
400
600
800
1000
1200
1400
l_{VC}
VG et al, 2012b

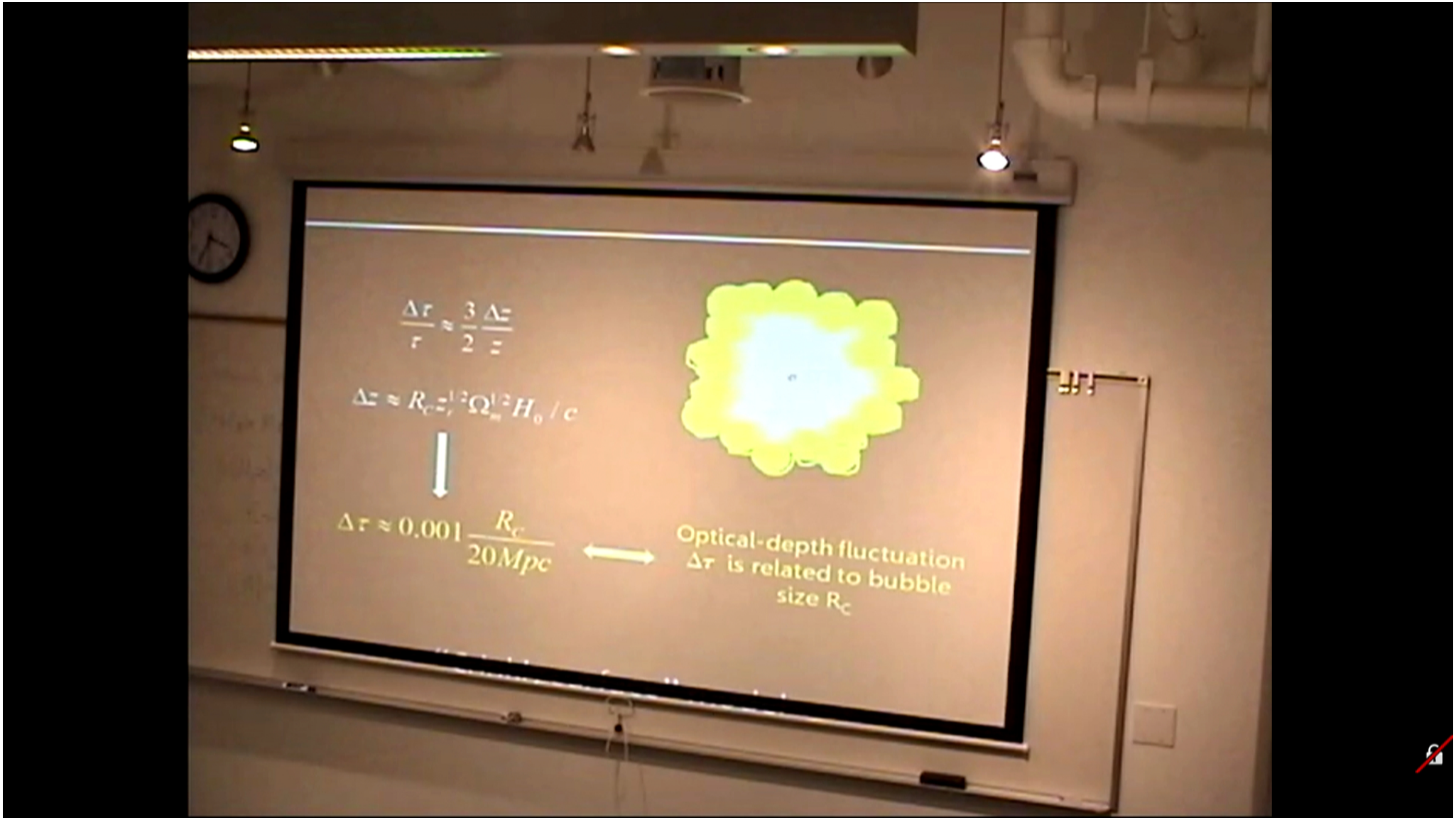
$\frac{\Delta r}{r} \approx \frac{3}{2}\frac{\Delta z}{z}$
$\Delta z \approx R_c z_r^{1/2} \Omega_m^{1/2} H_0 / c$
$\Delta\tau \approx 0.001 \frac{R_c}{20 Mpc}$
Optical-depth fluctuation $\Delta\tau$ is related to bubble size R_c

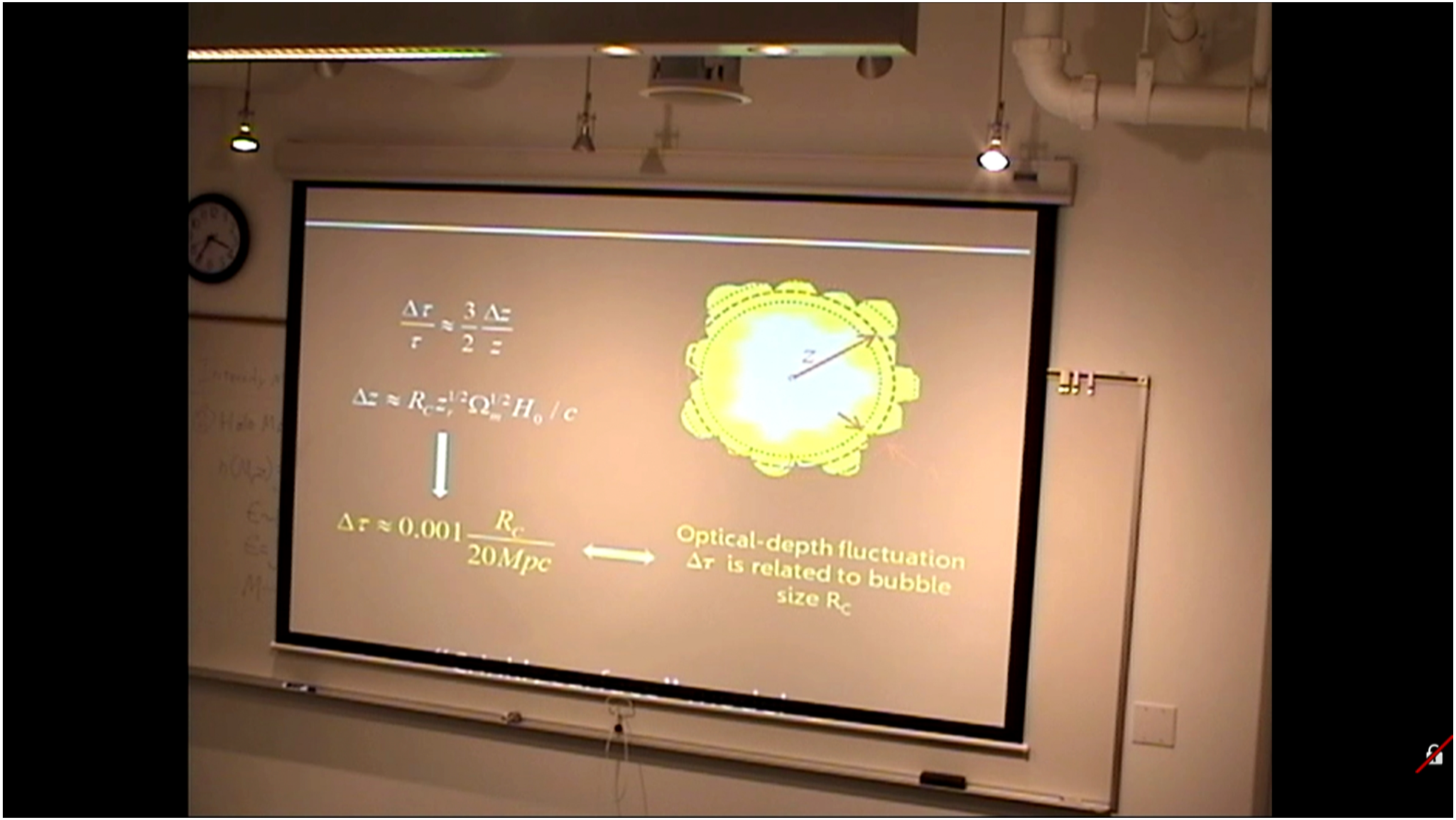
$\frac{\Delta r}{r} \approx \frac{3}{2}\frac{\Delta z}{z}$
$\Delta z \approx R_c z_r^{1/2} \Omega_m^{1/2} H_0 / c$
$\Delta\tau \approx 0.001 \frac{R_c}{20Mpc}$
Optical-depth fluctuation $\Delta\tau$ is related to bubble size R_c
z

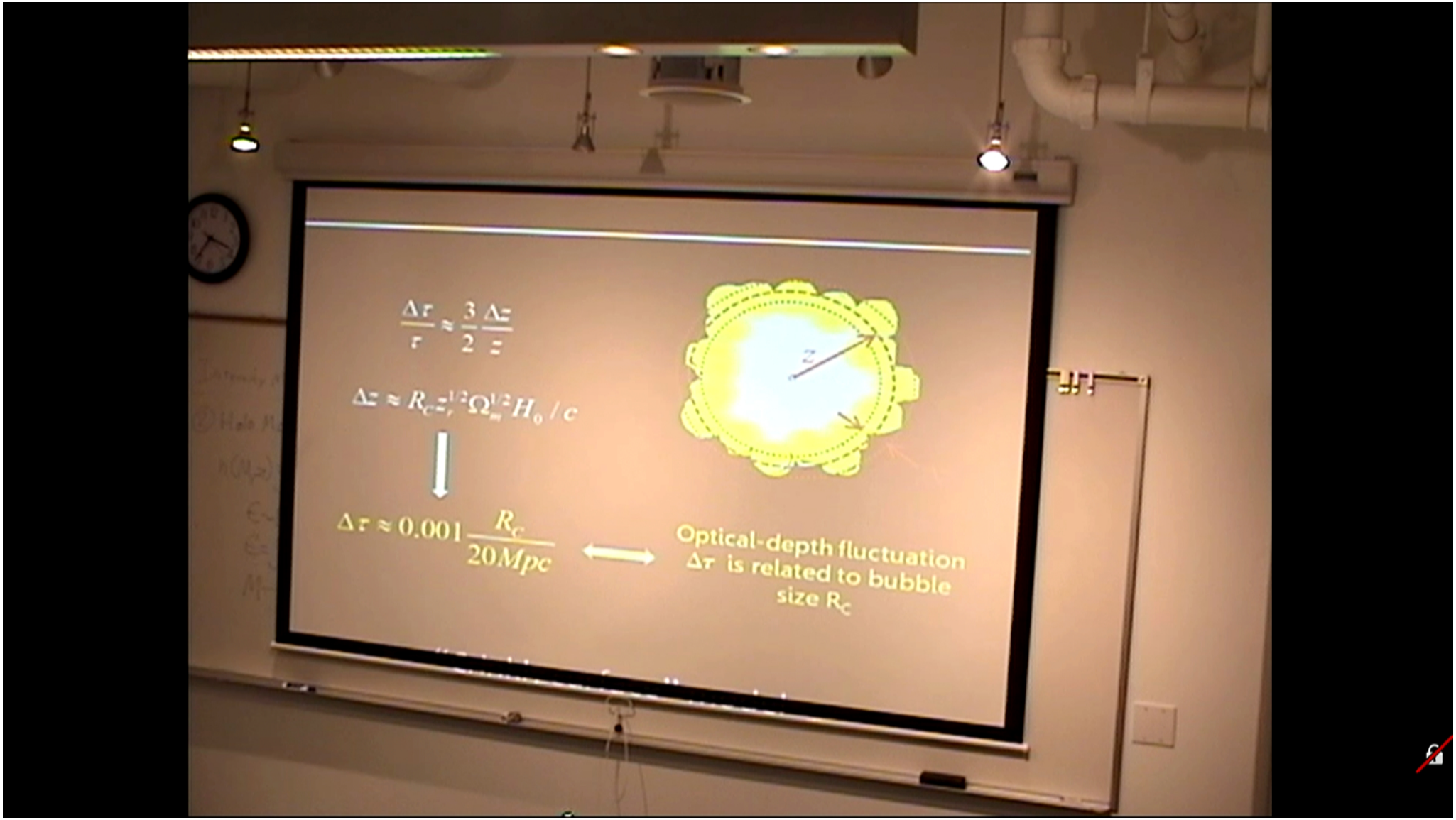
$\frac{\Delta r}{r} \approx \frac{3}{2}\frac{\Delta z}{z}$
$\Delta z \approx R_c z_r^{1/2} \Omega_m^{1/2} H_0 / c$
$\Delta\tau \approx 0.001 \frac{R_c}{20 Mpc}$
z
Optical-depth fluctuation $\Delta\tau$ is related to bubble size R_c

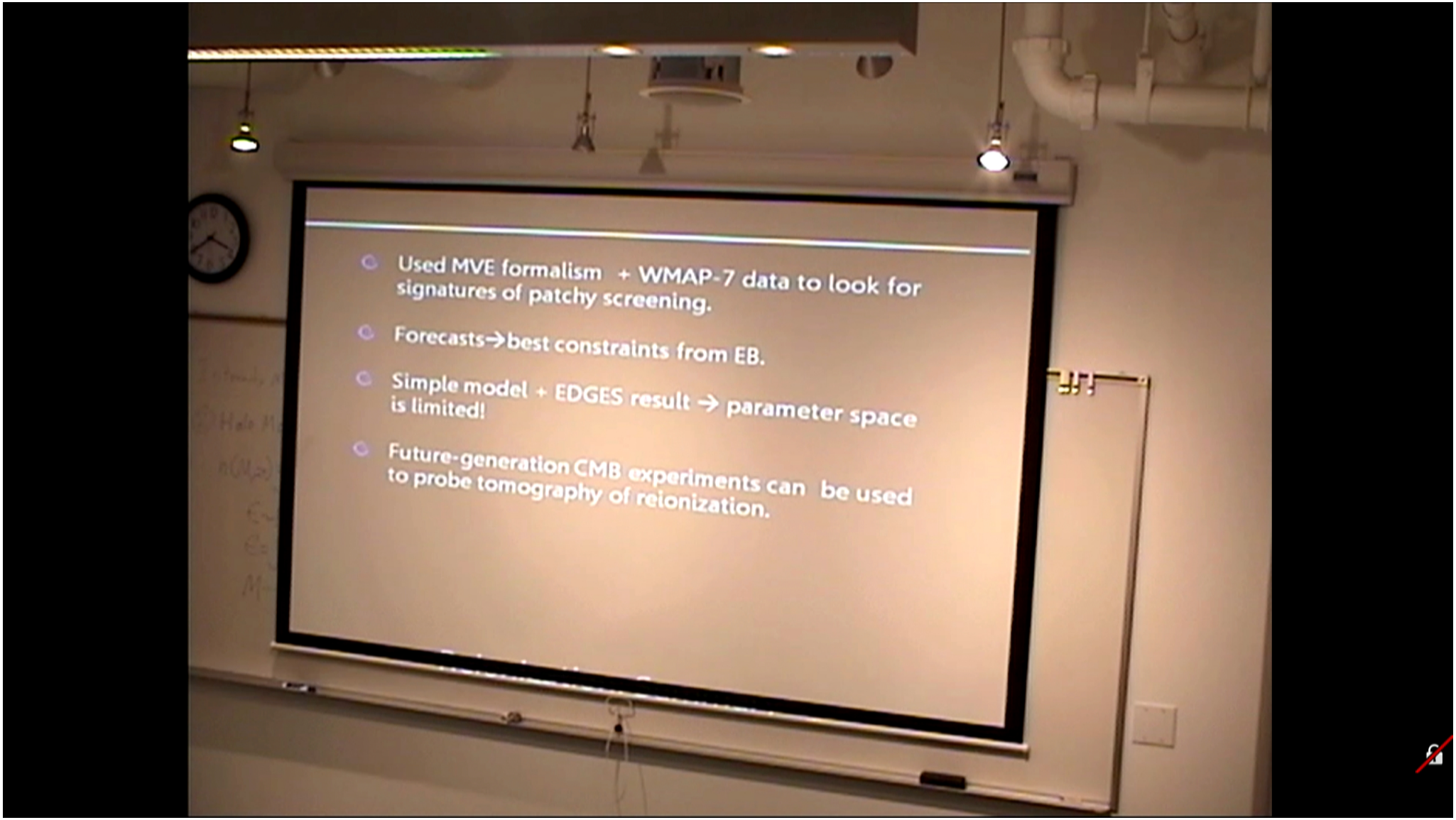
Used MVE formalism + WMAP-7 data to look for signatures of patchy screening.
Forecasts→best constraints from EB.
Simple model + EDGES result → parameter space is limited!
Future-generation CMB experiments can be used to probe tomography of reionization.

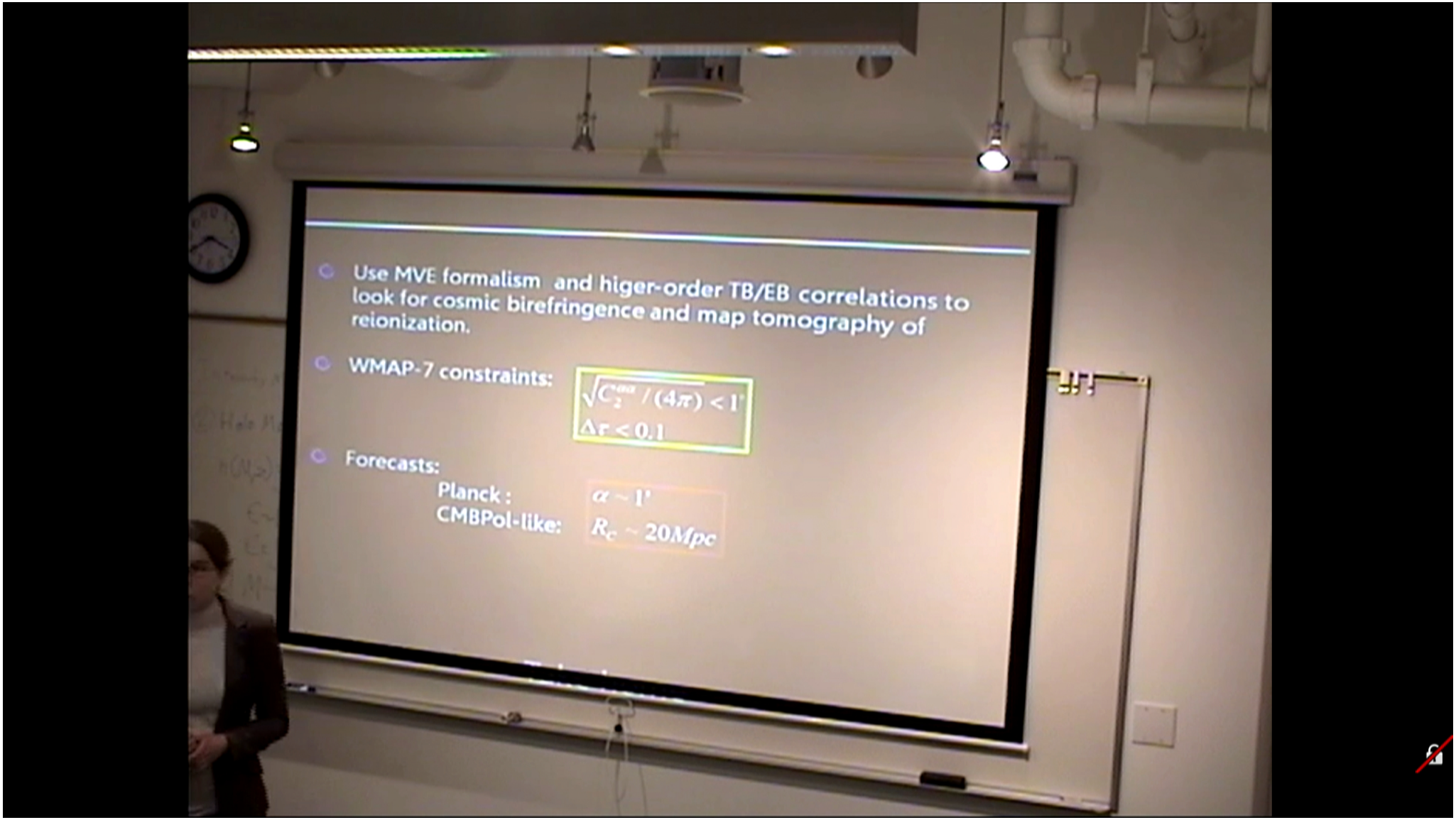
Use MVE formalism and higer-order TB/EB correlations to look for cosmic birefringence and map tomography of reionization.
WMAP-7 constraints:
$\sqrt{C_2^{\alpha\alpha}/(4\pi)} < 1^\circ$
$\Delta\tau < 0.1$
Forecasts:
Planck : $\alpha \sim 1^\circ$
CMBPol-like: $R_c \sim 20 Mpc$